CATALYTIC PYROLYSIS OF PLASTIC WASTES OVER SAPO-34 CATALYST

A THESIS SUBMITTED TO
THE GRADUATE SCHOOL OF NATURAL AND APPLIED SCIENCES
OF
MIDDLE EAST TECHNICAL UNIVERSITY

BY

TÜLAY BURSALI

IN PARTIAL FULLFILMENT OF THE REQUIREMENTS
FOR
THE DEGREE OF MASTER OF SCIENCE
IN
CHEMICAL ENGINEERING

SEPTEMBER 2014

Approval of the thesis:

CATALYTIC PYROLYSIS OF PLASTIC WASTES OVER SAPO-34 CATALYST

submitted by **TÜLAY BURSALI** in partial fullfilment of the requirements for the degree of **Master of Science in Chemical Engineering Department, Middle East Technical University** by,

Prof. Dr. Canan Özgen _____
Dean, Graduate School of **Natural and Applied Sciences**

Prof. Dr. Halil Kalıpçılar _____
Head of Department, **Chemical Engineering**

Assoc. Prof. Dr. Naime A. Sezgi _____
Supervisor, **Chemical Engineering Dept., METU**

Prof. Dr.Timur Doğu _____
Co-Supervisor, **Chemical Engineering Dept., METU**

Examining Committee Members:

Prof. Dr. Suna Balcı _____
Chemical Engineering Dept., Gazi University

Assoc. Prof. Dr. Naime A. Sezgi _____
Chemical Engineering Dept., METU

Prof. Dr. Timur Doğu _____
Chemical Engineering Dept., METU

Assoc. Prof. Dr. Nuray Oktar _____
Chemical Engineering Dept., Gazi University

Asst. Prof. Erhan Bat _____
Chemical Engineering Dept., METU

Date: 03.09.2014

I hereby declare that all information in this document has been obtained and presented in accordance with academic rules and ethical conduct. I also declare that, as required by these rules and conduct, I have fully cited and referenced all material and results that are not original to this work.

Name, Last name : TÜLAY BURSALI

Signature :

ABSTRACT

CATALYTIC PYROLYSIS OF PLASTIC WASTES OVER SAPO-34 CATALYST

Bursalı, Tülay

M. S., Department of Chemical Engineering

Supervisor : Assoc. Prof. Dr. Naime Aslı Sezgi

Co-Supervisor: Prof. Dr. Timur Doğu

September 2014, 161 pages

Thermoplastic materials have a wide variety of usage area due to their low costs and easy processing properties. However, these materials cause a serious environmental pollution because of being non-biodegradable and their long-term self-recycling. Considering energy need and clean environment, it is proper to degrade thermoplastic materials into lower moleculer weight products which are potential raw materials for petrochemical industry. In addition, it is possible to decrease the reaction temperature & time and to increase the product yield by using a proper catalyst.

In this study, SAPO-34 material was synthesized via hydrothermal route and then it was used in the catalytic thermal degradation of polypropylene and polystyrene. XRD result showed that the synthesized material was SAPO-34. BET analysis revealed that the material was microporous and exhibited *Type I* isotherm. The material formed in a cubic-like shape. DRIFTS result showed the existence of Lewis and Brønsted acid sites in the structure. Using ^{27}Al and ^{29}Si magic angle spinning nuclear magnetic resonance techniques, it was observed that ^{27}Al atoms were octahedrally and tetrahedrally; ^{29}Si atoms were tetrahedrally coordinated in the structure of the synthesized material.

The reaction orders and the activation energy values of polypropylene and polystyrene degradation reactions in the presence of SAPO-34 were determined using TGA data. Both of the reactions were determined as “first order”. The activation energy of polypropylene degradation reaction decreased from 172 kJ/mol to a value of 131±11 kJ/mol and the activation energy of polystyrene degradation reaction decreased from 357±4 kJ/mol to 262±4 kJ/mol in the presence of SAPO-34 catalyst.

In the pyrolysis system, the non-catalytic and catalytic degradation experiments of polypropylene and polystyrene over SAPO-34 material were performed and gaseous and liquid products were analyzed using GC. In the degradation reactions of PP, liquid products formed at 425 ºC and higher temperatures. Solid residue was observed only at 400 ºC and lower temperatures. The presence of SAPO-34 increased the gaseous product yield considerable at 400 °C and lower temperatures. There was a slight change in yield values of liquid products in the presence of the catalyst compared to the absence of SAPO-34. During the reaction, the catalyst was not deactivated and coke was not formed.

In the catalytic degradation reaction of PP, the gaseous products were mainly composed of ethylene and propene. In addition to these gases, the formation of methane, acetylene, propane and butane was observed at 400 ºC for 30 min reaction time in the presence of the catalyst. However they were not formed at the same temperature & reaction time in the non-catalytic degradation. The highest amount of hydrocarbon in liquid products was C_{10} in the non-catalytic and catalytic degradation of PP. In the presence of SAPO-34, heavier hydrocarbons degraded to lighter hydrocarbons with an increase in temperature. The amounts of lighter hydrocarbons produced at a reaction time of 30 min in the presence of SAPO-34 were higher than that of lighter hydrocarbons produced in the absence of catalyst.

In the degradation reactions of PS at 415 °C, only liquid and gas products were formed. The presence of SAPO-34 did not effect the yields of liquid & gas products. During the reaction, the catalyst was not deactivated and coke was not formed.

The majority of the gas products were methane and ethylene in the non-catalytic degradation of PS. In addition to these gases, butane was formed in the presence of

SAPO-34. The liquid products were mainly composed of C_8 – C_{10} hydrocarbons. The formation of C_9 hydrocarbons was observed in the presence of SAPO-34 compared to the absence of the catalyst. These results showed that the polymer degraded into its monomer & lighter hydrocarbons in the presence of SAPO-34.

The TGA and GC results revealed that SAPO-34 was active in the catalytic thermal degradation reactions of PP and PS.

Keywords: Catalytic degradation, pyrolysis, polypropylene, polystyrene, SAPO-34, silica-alumina type catalyst

ÖZ

PLASTİK ATIKLARIN SAPO-34 KATALİZÖRÜ ÜZERİNDE KATALİTİK PİROLİZİ

Bursalı, Tülay
Yüksek Lisans, Kimya Mühendisliği Bölümü
Tez Yöneticisi : Doç. Dr. Naime Aslı Sezgi
Ortak Tez Yöneticisi: Prof. Dr. Timur Doğu

Eylül 2014, 161 sayfa

Termoplastik malzemeler, düşük maliyetleri ve kolay işlenme yöntemleri ile tüm dünyada oldukça geniş bir kullanım alanına sahiptirler. Fakat bu malzemelerin kendiliğinden geri dönüşümü olmaması sebebiyle ciddi bir çevre kirliliği problemine sebep olmaktadırlar. Enerji ihtiyacı ve çevre kirliliği göz önüne alındığında, termoplastik malzemelerin petrokimya endüstrisi için ham madde olarak kullanılabilen, daha düşük molekül ağırlığına sahip hidrokarbonlara dönüştürülmesi daha uygundur. Ayrıca uygun bir katalizör kullanılarak reaksiyon sıcaklığı ile süresini düşürüp ürün verimini arttırmak mümkündür.

Bu çalışmada, SAPO-34 katalizörü hidrotermal sentez yöntemi ile sentezlenmiş olup polipropilen ile polistirenin katalitik indirgeme reaksiyonunda kullanılmıştır. XRD analizi sonucu, sentezlenen malzemenin SAPO-34 olduğuna karar verilmiştir. Malzeme mikrogözenekli olup *1. Tip* izoterm göstermiştir. Malzeme kübik yapıya benzer şekilde oluşmuştur. DRIFTS sonucu, malzemenin Lewis ve Bronsted asit yapılarından oluştuğunu ortaya çıkarmıştır. ^{27}Al ve ^{29}Si sihirli açı spini nükleer manyetik rezonans tekniği kullanılarak yapıdaki alüminyum atomlarının dört yüzlü ve sekiz yüzlü; silikon atomlarının ise dört yüzlü şeklinde yerleştiği belirlenmiştir.

TGA verileri kullanılarak polipropilen ve polistirenin katalitik ve katalitik olmayan indirgeme reaksiyonlarının reaksiyon dereceleri ile aktivasyon enerji değerleri hesaplanmıştır. Her iki reaksiyonun derecesi "1" olarak bulunmuştur. SAPO-34 kullanıldığı zaman polipropilenin indirgeme reaksiyonunun aktivasyon enerji değerinin 172 kJ/mol'den 131±11 kJ/mol değerine; polistirenin indirgeme reaksiyonunun aktivasyon enerji değerinin 357±4 kJ/mol'den 262±4 kJ/mol'e düştüğü gözlemlenmiştir.

Piroliz sisteminde polipropilen ve polistirenin SAPO-34 üzerinde katalitik indirgeme reaksiyonları yapılmış olup çıkan gaz ve sıvı ürünler, gaz kromatografi kullanılarak analiz edilmiştir. Polipropilenin indirgeme reaksiyonunda sıvı ürünler, 425 °C ve üzerindeki sıcaklıklarda gözlemlenmiştir. Katı tortu ise yalnızca 400 °C ve altındaki sıcaklıklarda görülmüştür. Ortamda SAPO-34 katalizörünün bulunması, 400 °C ve altındaki sıcaklıklarda elde edilen gaz ürün verimini oldukça arttırmıştır. SAPO-34'süz ortama göre katalizör ortamında sıvı ürün veri değerlerinde çok az bir değişim vardır. Reaksiyon süresince katalizör deaktivite olmamış ve kok oluşmamıştır.

Polipropilenin katalitik indirgeme reaksiyonunda gaz ürünler çoğunlukla etilen ve propenden oluşmuştur. Bu gazlara ek olarak, 400 °C'de, 30 dk reaksiyon süresinde, ortamda katalizör bulunduğunda metan, asetilen, propan ve bütan oluşumu gözlenmiştir. Ancak aynı sıcaklık ve reaksiyon süresinde, katalizörsüz ortamda bu ürünler oluşmamıştır. Polipropilenin katalitik ve katalitik olmayan indirgeme reaksiyonları sonucu oluşan sıvı ürünler arasında en yüksek miktara sahip hidrokarbon, C_{10} hidrokarbonudur. Ortamda SAPO-34 bulunduğu zaman, artan sıcaklık ile ağır hidrokarbonlar, daha hafif hidrokarbonlara indirgenmiştir. SAPO-34 ortamında, 30 dk reaksiyon süresinde oluşan sıvı ürün miktarı, SAPO-34'süz ortamda oluşan sıvı ürün miktarından fazladır.

Polistirenin 415 °C'de indirgeme reaksiyonları sonucu yalnızca gaz ve sıvı ürün elde edilmiştir. Ortamdaki SAPO-34 katalizörünün varlığı, sıvı ve gaz ürün verimini etkilememiştir. Reaksiyon boyunca SAPO-34 deaktivite olmamış, kok oluşumu gözlenmemiştir.

Katalizörsüz polistirenin indirgemesinde gaz ürünlerin çoğu metan ve etilendir. Ortamda SAPO-34 olduğu zaman bu gazlara ilaveten bütan oluşmuştur. Sıvı ürünler çoğunlukla C_8–C_{10} hidrokarbonlarından meydana gelmiştir. Katalizörsüz ortama göre SAPO-34 ortamında C_9 hidrokarbonlarının oluşumu görülmüştür. Bu sonuçlar, polimerin ortamda SAPO-34 bulunması ile monomerine ve düşük molekül ağırlıklı hidrokarbonlarına indirgendiğini göstermektedir.

TGA ve GC sonuçları, SAPO-34 katalizörünün, polipropilenin ve polistirenin indirgeme reaksiyonlarında aktivite gösterdiğini ortaya koymuştur.

Anahtar Kelimeler: Katalitik indirgeme, piroliz, polipropilen, polistiren, SAPO-34, silika-alümina tipi katalizör

To my mother, my grandmother and Kazim Kurdoğlu

ACKNOWLEDGEMENTS

First of all, I would like to express my deepest gratitude to my supervisor Assoc. Prof. Dr. Naime Aslı Sezgi for her guidance, advice, cricitism, encouragements and insight throughtout the research.

I would also like to thank my co-supervisor Prof. Dr. Timur Doğu for his suggestions and guidance during my experimental studies.

I would like to thank METU Chemical Engineering Department for giving me a chance to conduct my thesis studies and making it possible to complete my thesis studies properly.

I would like to thank Mihrican Açıkgöz for helping me about TGA and XRD analyses, Yavuz Güngör for his help in XRD analysis, Gülten Orakçı for helping me in gas chromatography and BET analyses. I would also like to thank Turgut Aksakal for his support in using laboratory equipment and Kerime Güney and Kemal Yıldırım for their kindness and helpfulness.

I would like to thank İsa Çağlar for his patience and Adil Demir, Süleyman Nazif Kuşhan and Ertuğrul Özdemir for their helps in my experimental system.

I would like to thank METU Central Laboratory for TGA, XRD & SEM analyses.

I would like to thank my dear friend, Miray Yaşar, who always believed in me and gave me encourage even at my hardest times. It's such a pleasure to have a friend like her.

I would also like to thank Tuğçe Kırbaş, Burçin İkizer and Erdem Balık for their helpful and enjoyable friendships throughout my study. Thanks also to my lab mates, Seval Gündüz and Arzu Arslan for their helps in my experiments.

I would specially like to thank my dear family, my mother Süreyya Sağkal and my grandmother Hüsniye Sağkal for their endless love, patience and emotional support throughout my graduate studies.

Last, but not least, special thanks to my fiance, Kazim Kurdoğlu, for his patience and great support through this time. I would like to thank him for being such a wonderful person and tolerating me for seven years.

TABLE OF CONTENTS

LIST OF TABLES

TABLES

LIST OF FIGURES

FIGURES

LIST OF SYMBOLS

A	Pre-exponential factor
A_i	Area of the peak read from gas chromatography
E_A	Activation energy of the reaction (kJ/mol)
n	Order of the reaction
n_i	Mole number of the compound i
R	Gas constant (8.314 J/kmol)
S_i	Selectivity of the compound i
w_i	Weight fraction of the compound i
x_i	Mole fraction of the liquid compound i
y_i	Mole fraction of the gas compound i

Greek Letters:

α	Fraction of polymer decomposed at time t
β_i	Calibration factor of the compound i

***Abbreviations*:**

EDS	Energy-dispersive X-ray spectroscopy
FTIR	Fourier transform infrared spectroscopy
GC	Gas chromatograph
IUPAC	International Union of Pure and Applied Chemistry
NMR	Nuclear magnetic resonance
PE	Polyethylene
PET	Polyethylene terephthalate
PP	Polypropylene
PS	Polystyrene
PVC	Polyvinyl chloride
SEM	Scanning electron microscope

TGA	Thermal gravimetric analyzer
wt	Weight
XRD	X-ray Diffraction

CHAPTER 1

INTRODUCTION

Thermoplastic materials have a wide variety of usage area like automotive, machine parts, food and beverage industries, medical equipment and packaging and storage material industries due to their low costs and easy processing properties. Thermoplastic consumption is roughly 80 % or more of the total plastic consumption in the world [1]. However, these materials cause a serious environmental pollution because of being non-biodegradable and their long-term self-recycling. Landfilling and incineration are the main treatment methods for thermoplastic materials. The majority of municipal plastic waste in Europe is still sent to landfill areas. Growth in the amount of waste brings about inadequate landfilling areas. Another option for the treatment of plastic wastes is incineration which aims to recover their thermal content and provide an alternative source of energy. However, this method is considered to be dangerous due to the probable emission of toxic chemicals, mostly aromatic chemicals, when human health is considered. Therefore, new, long-lasting and non-hazardous methods are now being searched [2].

Considering energy need and clean environment, recycling is a more proper method than the other ways. Recycling can be done as mechanical and chemical. Mechanical recycling of plastics involves a number of treatments and operations. This type of recycling can be only applied to thermoplastics. Another diffuculty of the mechanical recycling is the formation of different color-products which were made of the same resin. In addition, most polymers are exposed to undesirable degradation during their use due to the effect of a number of factors. This degradation leads to a progressive reduction in polymer chain length and to a partial oxidation of the polymer chains.

Therefore, recycled polymers usually show lower properties and performance than the pure polymer does. These type of polymers are useful only for simple applications [3].

Chemical recycling gives valuable end products and can be applied to all kind of materials regardless of their conditions. Pyrolysis, which is one of the chemical recycling methods, is widely used especially in the United States of America and Europe. It can be defined simply as breaking apart of chemical bonds by the use of thermal energy. In the pyrolysis process, plastic wastes can be converted into monomers, fuels or other valuable materials in the presence or absence of catalyst. Mixed, unwashed plastic wastes can be also treated by pyrolysis [4]. As compared with the previous techniques such as dumping, incineration etc., pyrolysis is an environment-friendly process and also more favored with its valuable end products. However, high energy consumption and a wide product distribution generate a problem for non-catalytic pyrolysis processes. To overcome these problems, catalytic degradation process would be preferred. The process time and reaction temperature can be minimized and end product efficiency can be maximized and apart from these, product distribution can be controlled by selecting a proper catalyst type. So, narrow distributed products with higher market values can be obtained [5].

Solid acid catalysts are mostly used in polymer degradation reactions. Aluminosilicates and zeolites are the main support materials which are being used in catalytic degradation of polymers [5, 6]. Previously, Y-zeolite and ZSM-5 zeolite catalysts were examined as cracking catalysts in a microreactor, pilot plant and full scale models [7]. Industrially, ZSM-5 zeolites are used to increase the octane number in gasoline production such as high-yield ethyl benzene and convert methanol to high-grade gasoline [8]. MCM-41, Al-MCM-41, Al-SBA-15, ZSM-5, and nanocrystalline ZSM-5 (nZSM-5) were investigated for polyethylene degradation reactions. Al-MCM-41 and n-ZSM-5 exhibited the strongest catalytic activities while ZSM-5 showed a very low catalytic activity [9]. ZSM-5, mordenite and ultrastable Y zeolite (US-Y) were also investigated for polyethylene degradation and it was found that the typical

production distribution was in the carbon range of 3 – 15. Alkanes were the main products over large-pore ultrastable Y. In addition to alkanes, alkenes and aromatics were also observed. Medium-pore mordenite and ZSM-5 gave significantly more olefins [10]. However, few studies related to the catalytic thermal degradation of thermoplastic materials over silicoaluminophosphate (SAPO) catalysts have been reported, even though the SAPO has a high potential in the plastic recycling reactions [11].

SAPO-34, one of the main catalysts in the family of silicoaluminophosphate materials, has been studied in a diverse range of catalytic applications. The most outstanding performance was observed in the catalytic conversion of methanol into olefins, which is known as the methanol to olefin (MTO) process [12]. There are some studies about SAPO-34 being used in the catalytic thermal decomposition of HDPE (high density polyethylene) and catalytic cracking of hexene [6, 11].

In this study, catalytic performance of SAPO-34 was investigated in polymer degradation reaction. First, SAPO-34 was synthesized via hydrothermal route and its properties were investigated using different characterization techniques. Then, the non-catalytic and catalytic degradation experiments of PP and PS were carried out. Gaseous and liquid products obtained from both reactions were analyzed using a gas chromatography. So the effect of the catalyst on product distributions was investigated.

CHAPTER 2

DEGRADATION OF POLYMERS

2.1. Polymer

A polymeric substance is conventionally described in terms of its structural units which are connected one another by covalent bonds. In many cases, a single type of structural unit suffices for the representation of the entire polymer molecule. The generation of the entire structure through repetition of one or few elementary units, is the basic typical property of polymeric material, as is implied by the etymology of the term *polymer*. In the linear polymers, the structural units are connected one to another in *linear* sequence. As an alternative, the structural units of the polymer may be connected together in such a manner as to form *nonlinear, or branced*. Linear and nonlinear polymer structures are given in Figure 1.

In the figure, principal structure unit is represented by A, and x is the degree of polymerization, or number of structural units and Y represents the branching units in the molecule [13].

There are three main groups of polymer and they are specified in Table 1. Thermoplastics are the most general group of polymers among the others. They are usually called as *plastics*. Linear or branched thermoplastics can be melted reversibly or can be dissolved in a proper solvent. To obtain a rigid structure, thermosets are heated, and once they are set, they don't melt upon prolonged heating. Thermosets usually have short chains between crosslinks and show glassy fragile behavior. Rubbers, or elastomers have long, flexible chains between the crosslinks in the structure. In other words, elastomers are the thermosets which can't be melted [14].

$$A' - A - A - A - \ldots - A'' \qquad \text{or} \qquad A' (- A -)_{x-2} - A''$$

(a)

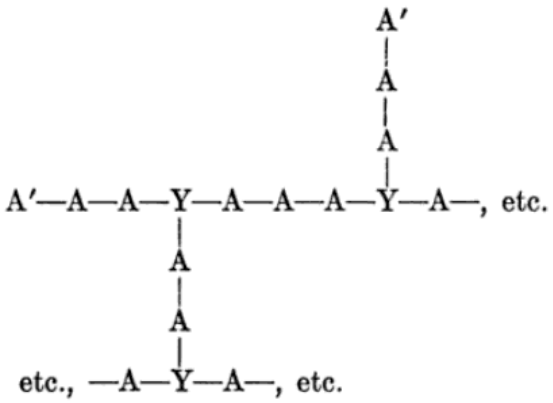

(b)

Figure 1. Linear (a) and nonlinear (b) polymer structures

Table 1. Major groups of polymers [15]

Polymer groups	Examples
Crystallizable thermoplastics	Polyacetal, Polyamide, Polycarbonate, Poly (ethylene terephthalate) (PET), Polyethylene (PE), Polypropylene (PP)
Glassy thermoplastics	Polystyrene (PS), Poly (methyl methacrylate), Poly (vinyl chloride) (PVC), Poly (vinyl acetate)
Thermosets	Epoxy, Phenolic, Polyester
Elastomers	Polybutadiene, Ethylene-propylene copolymers, Styrene-butadiene rubber, Ethylene-vinyl acetate, Styrene-butadiene copolymers

2.1.1. Application Areas of Polymers

Polymers are widely used in many important industries througout the world. Petroleum, coal, and natural gas are the feedstocks of synthetic polymers. These feedstocks are also the sources of ethylene, methane, aromatics and alkenes. Polymers are used widely in daily applications such as communication, clothing, appliances, medical applications, aerospace parts, housing materials, and automotive [14].

Polymers have advantages compared to the other types of materials (metals, ceramics etc.) due to their low weight, low processing costs, and properties such as toughness and transparency. The functional common properties such as tensile strength, impact strength, modulus, and elongation make these materials more cost effective. Plastics and engineering resins are processed into a wide range of fabricated forms such as membranes and filters, films, fibers, extrudates, and moldings [14].

Polypropylene (PP), polyethylene (PE), polystyrene (PS), polyethylene terephthalate (PET) and polyvinyl chloride (PVC) are the most common polymers among the others. PP is used mostly in fibers, films, membranes, and packaging industry and PS is used in engineering resins while PE has application areas such as fibers, films, biomedical and packaging industries. PVC is used mostly in pipes, doors and windows, cards, bottles, and other non-food packaging. PET has many application areas such as beverage, food and other liquid containers, thermoforming applications, synthetic fibers, and engineering resins [14].

The application areas of polymers are specified in Table 2.

Table 2. Some application areas of polymers [14]

Fibers	Polyethylene (PE), polyester, polyamide (PA), acetate, polyacrylonitrile (PAN), polybenzobisthiazole, polypropylene (PP), acrylic, aramid
Films, packaging	Polyethylene (PE), polyester, polypropylene (PP), polycarbonate (PC), polyisoprene (PI), fluoropolymers, polyurethanes, polyvinyl chloride (PVC)
Membranes	Cellulose acetate, polysulfone (PSU), polyamide (PA), polypropylene (PP), polycarbonate (PC), polyisoprene (PI), polyacrylonitrile, fluoropolymers
Engineering resins	Polyoxymethylene (POM), polyester, polyamide (PA), polyethersulfone, polyphenylene sulfide (PPS), acrylonitrile-butadiene-styrene (ABS), polystyrene (PS)
Biomedical uses	Acrylics, polyethylene (PE), ultrahigh molecular weight polyethylene (UHMWPE), polyester, silicone, polyamide (PA)
Adhesives	Polyvinyl acetate (PVA), epoxies, polyisoprene (PI)
Emulsions	Styrene-butadiene-styrene (SBS), polyvinyl acetate (PVA)
Coatings	Epoxies, polyisoprene (PI), Polyvinyl acetate (PVA)
Elastomers	Styrene-butadiene rubber (SBR), urethanes, polyisobutylene (PIB), ethylene-propylene rubber (EPR)

2.1.1.1. Polypropylene

Polypropylene is prepared by polymerizing propylene which is a gaseous byproduct of petroleum refining, The polymerizing reaction takes place in the presence of a proper catalyst at a temperature range of 340-360 K and pressure range of 30-40 atm. Propylene is an unsaturated hydrocarbon which contains only carbon and hydrogen atoms. By polymerization reaction, many propylene molecules are joined together and one large molecule of polypropylene is formed [15].

There are different ways to connect the monomers. Commercial PP is produced using crystallizable polymer chains over catalysts. This method gives rise to PP production with a semi-crystalline solid with good physical, mechanical, and thermal properties. This type of material is referred to as "isotactic" polypropylene (i-PP). Also there is another form of PP which is produced as a byproduct from semi-crystalline PP production in lower volumes. It has very poor mechanical and thermal properties. It is tacky, but soft, and generally used in sealants, caulk products, and adhesives. This type of material is referred to "atactic" (noncrystallizable, a-PP) polypropylene.

In the melt state, the average length of the polymer chain and the breadth of the polymer chain length distribution in a polymer are the main characteristic properties of polypropylene. However, in the solid state, the type of crystalline structure and the amount of amorphous phases which polymer chains form are related to the the main properties of the PP material. The relative amount of each phase depends on the stereochemical & structural characteristics of the polymer chains and the conditions under which the conversion of the resin to the products like films, fibers, and various other geometric shapes during fabrication by thermoforming, molding, or extrusion.

PP is proper in room-temperature applications due to its physical, mechanical, and thermal characteristic properties. It is rather solid with a low density, high melting point, and has a high impact resistance. Different characteristic properties of PP can be obtained using several methods. For example; altering the chain regularity or the

(average) chain lengths, incorporation of a comonomer or an impact modifier into the polymer chain [16].

The molecular formula of PP is $(C_3H_6)_n$. The structure of PP is given in Figure 2.

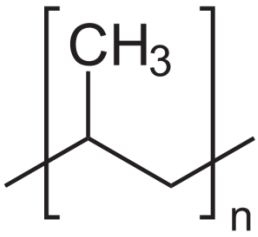

Figure 2. The structure of polypropylene [17]

2.1.1.2. Polystyrene

Polystyrene, also known as *polyvinyl benzene*, is a glasslike solid which shows mechanical strength below 100 °C. PS is aromatic, nonpolar, chemically inert, resistant to water, and easy to process [18].

In 1839, the German chemist Eduard Simon found a colorless, mobile liquid from distilling liquid storax and he gave a name "*Styrol*" which is now known as "*Styrene*". It was a medical balsam which was found in some tree species [19]. In 1851, French chemist Berthelot produced styrene monomers by passing benzene and ethylene through a red-hot tube. Today's commercial methods are based basically on this method [19]. A considerable amount of styrene is still produced by the catalytic dehydrogenation of ethylbenzene which is converted to styrene in a reversible gas-phase endothermic reaction.

The most general-purpose PS is produced by solution polymerization in a continuos process with the aid of peroxide initiation and is used commonly in wall tile, optical, medical, automotive and electrical parts, blister packages, lenses, bottle caps, small

jars, vacuum-formed refrigerator liners, containers of all kinds, and transparent display boxes. The forms of thin films and sheet stock are used in packaging foods and other items [19, 20].

The chemical formula of polystyrene is $(C_8H_8)_n$ and the structure of polystyrene is given in Figure 3.

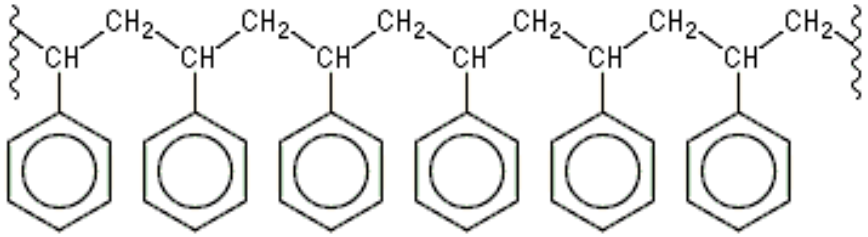

Figure 3. The structure of polystyrene [22]

2.1.1.3. Polyethylene

Polyethylene (also known as *polythene*) has the largest volume in production of synthetic polymer. About 80 million metric tons are produced annually and the growth rate is expected to be continued at about 5 % per year [23].

In its simplest form, a polyethylene molecule is composed of mainly a long backbone which is covalently linked to C atoms, and each C atom is linked to two H atoms. There are methyl groups at the end of the chains [24]. The structure of pure PE is given in Figure 4.

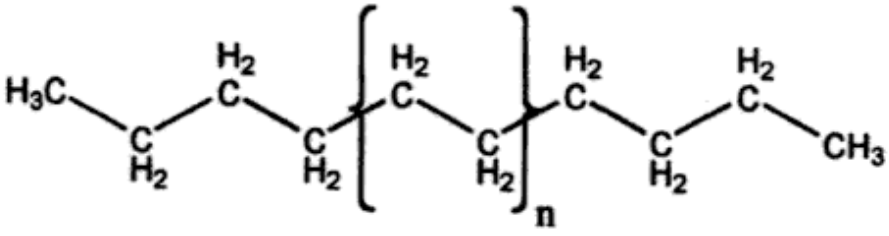

Figure 4. Chemical structure of pure polyethylene [24]

Polyethylene is very a promising material since it was discovered by Gibson and Fawcett in 1933 at “Imperial Chemical Industries”. The production of PE occurs at high pressures & temperatures. The selection of the catalyst to be used in the reaction depends on the properties of the product. Several PE structures like long or short branches may be present, depending on the procedure used in the synthesis [25].

There are 7 main classes of PE which are given below [24]:

High density polyethylene

Low density polyethylene

Linear low density polyethylene

Very low density polyethylene

Ethylene-vinyl ester copolymers

Ionomers

Cross-linked polyethylene

Polyethylene has the highest amount in the plastic consumption throughout the world. It is a multifaceted plastic due to its high performance when compared to other materials such as glass, paper or metal. Polyethylene is mostly used in packaging and the other application areas of polyethylene include construction, transport, electronics, recreational [25].

2.1.1.4. Polyvinyl chloride

Vinyl chloride was synthesized by Regnault in 1835. Three years later, its polymerisation to polyvinylidene chloride by exposuring to sunlight was reported. First, polyvinyl bromide was produced by Hoffmann in 1860 and in 1872, Baumann

synthesized successfully PVC by carrying out polymerisation reactions of vinyl compounds in sealed tubes. He obtained white, powdery/flaky solids [26]. It was started the industrial PVC production using several technologies in Germany, the USA, and the UK by the start of World War II.

PVC is very low in cost when compared to other plastic materials. It can also be applied to a wide range of areas due to its versatility in application areas and processing possibilities. It is also durable, easily maintained, and can be produced in a large range of colors. PVC can be used as food contacting materials and in medical applications. It is also suitable to be used in outdoor weathering. PVC has a very low thermal stability and it quickly degrades at processing temperatures. By combining various additives, it can be used to make different products [26].

Its repeating unit and its usage area are given in Figure 5 and Figure 6, respectively [27]. PVC is commonly used in cables, tubes, flooring and walls as it is seen in the figure.

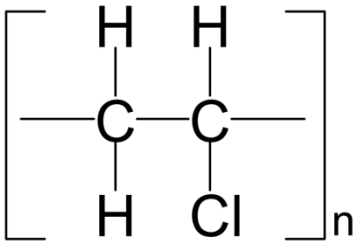

Figure 5. The repeating unit of polyvinyl chloride [28]

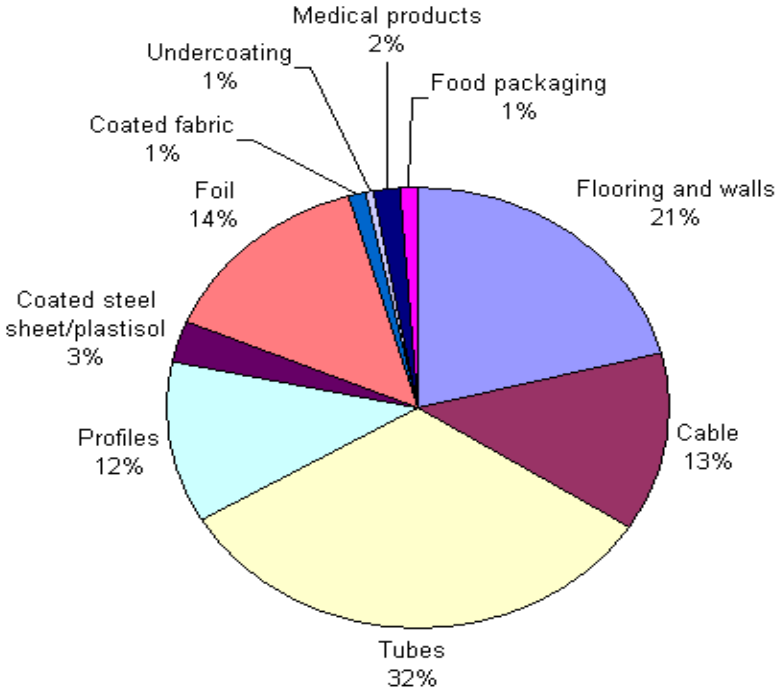

Figure 6. Average worldwide consumption patterns of PVC [29]

2.1.1.5. Polyethylene terephthalate

The potential of polyethylene terephthalate as a fiber-forming polymer was recognized by Whinfield and Dickson in England, 1941. Although the properties of PET were proper for fiber production, it couldn't be commercialized during World War II. However, some manufacture companies started its production in the 50s. After the expiration of the original patents, other countries started its polyester fiber production. The first commercial engineering PET resins for injection molding were introduced by Akzo Chemie in Europe and Teijin in Japan, and then DuPont Company introduced the *Rynite* product [30].

PET can be obtained by the direct esterification of ethylene glycol with terephthalic acid, but lately different processes using dimethyl terephthalate were developed. These processes have advantages such as being easy to purify, notably indissoluble due to its

latter undergoing sublimination at 300 °C. Ester has a higher solubility which allows a greater handling convenience and faster reaction rates in the early stages of the transesterification processes.

PET is a though material similar to other thermoplastic materials. The unfilled PET materials show no breaks in the unnotched impact strength test at low temperatures such as – 40 °C. But the filled ones are notch-sensitive. The surface of molded PET is glassy, hard, and abrasion-resistant, with low coefficients of friction. PET is very durable to high temperatures & humidity due to its properties such as low-moisture absorption [30]. Engineering PET has wide application areas such as electronic, automotive, housewares, lighting, power tools, materials handling, sporting goods, and plumbing [30].

The repeating unit of polyethylene terephthalate is given in Figure 7.

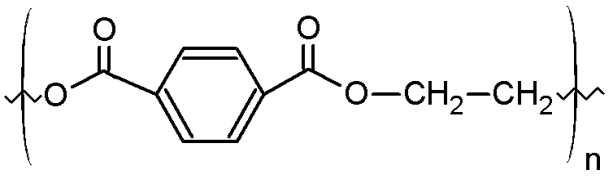

Figure 7. The repeating unit of PET [31]

2.2. Degradation of Polymers

It is inevitable to use plastic materials in our daily life due to their contribution to the new scientefic technologies and numerous applications. With an increase in the use of various types of plastics, the release of their waste into the environment also increased. The growing amount of the plastic wastes became dangerous in recent years [32]. Polymer wastes are regarded as a potential cheap source for energy need & chemical industry [33]. In Europe, the plastic consumption (growing annualy by 4-8 %) was 45 Mt while the amount of waste from plastics was nearly 30 Mt in 2000. The amount of plastic consumption is increasing continually. So it can be said that the plastic waste

amount is also increasing day by day [34]. The plastics wastes are estimated about 10 % (by weight) of total municipal solid wastes. The percentage is nearly 20 % in volume. Plastics cause a serious environmental problem because of their low biodegradability. Therefore, new radical solutions which are based on source reduction, recycling, and re-using are being searched nowadays [35].

One way to dispose the plastic wastes is landfilling which is not recommended because of economical and environmental reasons. Besides, the landfilling areas have became inadequate lately. One of the other treatment options for plastic wastes is incineration which is hazardous to the environment because of the toxic gases & soot particles which are released during the incineration process. There is the Kyoto Protocol which considers of reducing CO_2 emission by 20% [32]. Apart from these, another alternative for treating industrial & municipal polymer wastes is recycling. This method is considered as promising solution to the problem of increasing plastic waste amount in the world [34]. The recycling can be done both mechanical and chemical. Mechanical recycling is the conversion of used polymeric materials into new, utilizable products. This method is a popular recovery path for manufacturers. The recycling process takes place on single-polymer waste streams which is considered as a market for recycled products. But the quality of the products might not be close to the original ones. Moreover, these products are often higher priced than the virgin ones [33].

The other recycling method is chemical recycling. This method has attracted much interest in recent years. The aim of this method is to convert polymer wastes into basic petrochemicals which can be used as hydrocarbon feedstock or fuel oil for a variety of downstream processes [36]. There are three main approaches in chemical recycling: partial oxidation, depolymerisation, and cracking (non-catalytic thermal degradation, catalytic thermal degradation and hydrocracking degradation) [33].

- ***Depolymerisation***

Materials such as nylon, polyester, PA, and PET are depolymerised to initial diacids and diols or diamines following reversible synthesis reactions. On the other hand, some materials (polyolefins etc.) cannot be depolymerised into the original monomers easily and these materials compose roughly 65 % of municipal solid plastic wastes [33].

- ***Partial Oxidation***

As a result of the direct combustion of polymer wastes, harmful gases and substances such as sulfur oxides, light hydrocarbons, NO_x release to the environment. However, with partial oxidation, synthesis gas & hydrocarbons could be obtained. The amount & the quality of the products are dependent on the polymer type which degrades. The recent studies have shown that co-gasification of biomass with polymer waste increases the H_2 production while reduces the CO content. The formation of bulk chemicals (e.g. acetic acid) from polyolefins by oxidation in the presence of NO and/or O_2, is also possible with this method [33].

- ***Cracking***

Cracking process is the breaking down of the polymer chains. At the end of this reaction, useful lower molecular weight compounds are obtained. There are three cracking reactions which are hydrocracking, thermal and catalytic thermal degradation [33].

2.2.1. Hydrocracking

Hydrocracking of polymers is the reaction of polymers using H_2 over a catalyst in an autoclave at moderate pressures & temperatures. The most important purpose of this method is to produce a high quality gasoline using a wide range of feeds. Polyolefins, PET, PS, PVC and mixed polymers can be regarded as the typical feeds for hydrocracking [33].

2.2.2. Non-Catalytic Thermal Degradation

The non-catalytic thermal degradation is the process which produces a broad product range. However, it requires high operating temperature & long reaction time [33]. The non-catalytic thermal decomposition of polymers refers to the case where polymers at elevated temperatures start to undergo chemical changes without the involvement of another compound. The thermal degradation reaction is carried out at an inert atmosphere [37].

The thermal decomposition of plastics progress through a radical mechanism which involves 3 different decomposition routes [3] that are listed below:

i. Random scission at any point in the polymer backbone leads to the formation of monomers. These monomers in turn may be subjected to additional random cracking reactions.
ii. With end-chain scission, a small molecule and a long-chain polymeric section are formed.
iii. The polymer chain may retain its length or the release of the small molecule might be accompanied by the breaking of the polymeric chain. At the end of the reaction, small molecules form.

2.2.3. Catalytic Thermal Degradation

The catalytic thermal decomposition of plastic waste offers considerable advantages such as lower temperatures and upgraded product quality when compared to the non-catalytic thermal decomposition. Catalytic degradation takes place at considerably lower temperatures & reaction times. Hydrocarbons which can be used as motor engine fuel are produced by this method, eliminating the necessity of further processes [38].

Compared to the simple cleavage of the non-catalytical thermal degradation, the catalytic thermal degradation has the advantages which are given below:

- In the presence of catalyst, the polymer molecules start breaking down at lower temperatures compared to the non-catalytic thermal degradation. A notable catalytic conversion of polyolefins into volatile end products has been detected at low temperatures even at 200 °C. On the other hand, in the non-catalytic thermal degradation of polyethylene and polypropylene, to observe the formation of gases, the reaction temperature should be high, more than 400 °C.

- In the same reaction temperature, the catalytic thermal degradation of polymers is faster than the non-catalytic thermal degradation. At the temperature of about 400 °C, the first volatile products are observed just after a few minutes of contact of polymer with the catalyst.

- The end products of catalytic degradation of polymers have higher quality than that of the products of thermal degradation. Produced oils have similar properties to commercial gasolines with the presence of high proportion of branched, cyclic and aromatic structures [3].

2.2.3.1. Catalysts Used for Catalytic Degradation

A wide variety of catalysts such as, acidic & basic solids, Friedel-Crafts catalysts, bifunctional solids has been studied in the degradation reaction. They were effective in promoting the decomposition of plastic materials. The mostly used catalysts in plastic degradation reactions are acidic solids which are mainly, zeolites, amorphous silica-alumina and alumina. These type of materials are usually used in petroleum processing and petrochemical industries. Their catalytic activity and product selectivity depend on their textural and acid properties. Because the performance of the catalyst in the degradation reaction is mainly related to the type of the acid sites in the material, the acidity of the catalyst is an important factor. The acid sites are closely related to the Lewis & Bronsted acid sites. Also the presence of acid sites in the

catalysts accounts for their capability to produce carbocations on their surface, which facilitate degradation of the polymeric materials [39][40].

Zeolites are microporous crystalline silicoaluminates. They have a perfectly defined crystalline structure based on the linkage between SiO_4 and AlO_4^- tetrahedra through oxygen bridges. The pore sizes which are below 1 nm allow different molecules to enter, diffuse and react within them. Zeolites are classified according to their pore size (small, medium and large), the number of channel systems, and aluminum content.

Alumina and amorphous silica-alumina are usually mesoporous materials. The pore size, pore volume, and surface area of alumina and amorphous silica-alumina depend mainly on the synthesis method. Also their textural properties can be controlled to a certain extent by changing the synthesis conditions. These parameters are also highly relevant in determining the catalytic properties of these materials [3].

CHAPTER 3

SILICOALUMINOPHOSPHATE (SAPO)

Molecular sieves are one of the major groups of crystalline microporous inorganic materials and these sieves have been used widely in industry as catalysts, adsorbents, and ion exchangers. The developments in the synthesis of molecular sieves have enlarged their framework types and compositions. In the past years, more than 200 zeotype structures have been identified. It is pleasing to explore novel synthetic methodologies and new zeotype materials since molecular sieves have the potential to promote innovative applications and some new industrial processes [41].

Aluminophosphates (AlPO) and silicoaluminophosphates (SAPO) are two of the most popular molecular sieves. They were identified by Union Carbide in 1980s. The structures of aluminophosphates and silicoaluminophosphates contain various structure types. Some are analogical to certain types of zeolites such as SAPO-34 chabazite (CHA) structure, but most of them has unique structure without analogous zeolite. Generally AlPO molecular sieves don't have any actual catalytic capabilities because of their neutral framework. The acidity of AlPOs, and SAPOs occurs by substitutioning of silicon into the framework. The acidity of the material determines its catalytic applications. Among SAPOs, microporous SAPO-34 has received great attention in recent years due to its high selectivity in the methanol to olefin (MTO) reactions. There are many studies in the literature related to the synthesis and crystallization mechanisms of SAPO-34, its catalytic properties in MTO reactions, and reaction mechanisms. The number "34" indicates the structure of chabazite in the SAPO-34 material. Although the composition is different, the materials which have the same structure take same number. For instance, $AlPO_4$-34 and SAPO-34 have the same chabazite structure. Structural properties of aluminophosphate based structures

are tabulated in Table 3. The structure types of aluminophosphate based materials are listed in Table 4 [34][35][44].

Table 3. Properties of AlPO based structures [43]

Pore size	Number of tetrahedral atoms in largest ring	Structure Type
Very large	18	VPI-5
Large	12	5, 36, 37, 40, 46, 50
Medium	10	11, 31, 41
Small	8	14, 17, 18, 22, 26, 33, 34, 35, 39, 42, 43, 44, 47, 52
Very small	6	16, 20

Table 4. The structure types of AlPO based materials [44]

Structure Number	Structure Type	Pore size, nm	Saturation H_2O pore volume, cm^3/g
8	Novel	0.90	0.24
5	Novel	0.80	0.31
41	Novel	0.60	0.22
34	Chabazite	0.43	0.30
20	Sodalite	0.30	0.24

Table 4 revealed that some species have similar structures to the zeolite type structures. However, some have new structure types. The table shows that, for instance, SAPO-20 has different pore size and pore volume from SAPO-34 with different structure type. SAPO-34 material has also chabazite structure type and has an average pore size

of 0.43 nm. The idealized chemical formula of CHA is expressed as $Ca_2(Al_4Si_8)O_{24}.12H_2O$. The structure of aluminosilicate framework in chabazite is built up of double 6-rings ($[4^66^2]$-rings), and consequently one $[4^{12}6^28^6]$-cavity per unit cell is formed. Each cavity is connected to six neighboring $[4^{12}6^28^6]$-cavities by sharing 8-ring windows and filled with H_2O molecules and exchangeable cations such as Ca^{2+} and Na^+. The chabazite structure of SAPO-34 is illustrated in Figure 8 [45]. The framework structure in the figure is drawn by linking (Si, Al) positions which are shown with black circles. Shaded quadrilaterals in the figure represent the 4-rings attaching the [4662]-rings. Al, Si or P atoms are denoted with dots. These atoms are connected to each other by oxygen atoms [45].

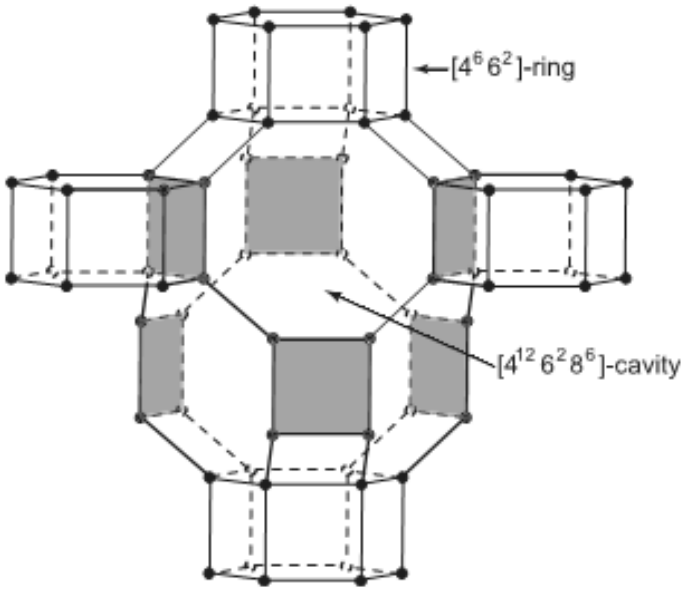

Figure 8. Chabazite structure of SAPO-34 [45]

There are many studies about the synthesis SAPO-34 material and its applications in the literature. Wang *et al.* [41] synthesized SAPO-34 aminothermally with alkanolamines as novel templates and its uses for CO_2 separation. SAPO molecular

sieves were synthesized using eight types of alkanolamines which were triethanolamine, diethanolamine, diisopropanolamine, triisopropanolamine, N,N-dimethylethanolamine, N,Ndiethylethanolamine, N-methyldiethanolamine, and diglycolamine. Silica sol, pseudoboehmite and H_3PO_4 were used as inorganic reactants. CO_2 was obtained from CO_2/N_2 and CO_2/CH_4 mixtures. In order to synthesize the material, alkanolamine, pseudoboehmite, silica sol, and water were mixed in a glass beaker. After stirring and adding H_3PO_4, the mixture was placed in an oven. After rotating for a while, it was heated at 473 K for 48 hours. The solution was washed after the crystallization. Finally, they were dried. As-synthesized materials were calcined to obtain the template-free samples. Characterization results of the synthesized materials showed typical rhombohedral morphology. For all SAPO-34 samples, micrometer crystal size was observed. All synthesized materials except the one synthesized using DGA have high pore volume and high surface area. As a result of the seperation experiments, the catalysts showed an excellent adsorption ability for CO_2 from both CO_2/N_2 and CO_2/CH_4 mixtures. These results demonstrated that SAPO-34-DGA could be a promising adsorbent for the CO_2 capture.

Najafi *et al.* [46] studied the hydrothermal synthesis of nanosized SAPO-34 molecular sieves using different combinations of multi templates in the material. The templates were tetraethyl ammoniumhydroxide (TEAOH), morpholine, diethylamine (DEA) and triethylamine (TEA). Firstly, the mixture of aluminum isopropoxide, deionized water and the structure-directing agents (SDAs) were stirred until a homogeneous solution was obtained. After adding the source of silica (TEOS) and phosphoric acid, the mixture was kept stirring for an hour. The initial gel was sealed in a stainless steel autoclave and then heated in an oven for crystallization. After taken the material out of the oven, it was centrifuged, washed and dried. At the end, calcination was carried out in the air to remove organic template(s) molecules. Using two or more SDAs as templates led to an increase in crystallinity, the crystallite size reduction and the morphology change to spherical aggregates of several cubic nanosized crystals compared to the results obtained using single template synthesized. Furthermore, decreasing molar ratio of TEAOH in initial gel from 2 to 0.4 didn’t change the purity

of SAPO-34, but affected its crystallinity and particle size. Microporous SAPO-34 particles and high BET surface area were obtained when three or four templates are used.

Singh *et al.* [47] studied the synthesis of mesoporous silicoaluminophosphate (MESO SAPO- 34) from the preformed microporous SAPO-34 precursors. Firstly, two different solutions (solution A and B) were prepared to obtain microporous SAPO-34. Solution A was obtained by mixing a known quantity of phosphoric acid and pseudoboehmite in distilled water, then it was stirred to get a uniform mixture. Solution B was obtained by mixing fumed silica and morpholine in distilled water with continuous stirring. This solution was added drop by drop to solution A with continuous stirring and the final mixture was aged. Synthesis of mesoporous SAPO-34 (MESO-SAPO-34) was carried out using preformed microporous SAPO-34 precursors by the following procedure with different surfactants, TMAOH concentrations, at various temperatures and durations. The surfactant solution was prepared by mixing an appropriate concentration of the surfactant in distilled water under constant stirring. Microporous SAPO-34 was obtained with a crystallization time of 5 hours. The resultant preformed microporous SAPO-34 and calculated amount of 25 wt %. TMAOH solution was added to the surfactant solution. The final gel was crystallized at different temperatures & durations. The synthesized samples were washed with water and ethanol and then, they were dried and finally calcined. According to BET analysis, the material showed *Type 3* isotherm. SEM images of both materials are poised of elongated hexagonal platelets of 2–3 μm length. The FTIR pyridine adsorption studies on MESO-SAPO-34 revealed the presence of strong Bronsted acid sites and thus proved it to be a promising catalyst for liquid-phase synthesis of phenoxy propanol using phenol and propylene oxide.

Wang *et al.* [48] synthesized small and tunable crystallite size SAPO-34 using two-step hydrothermal crystallization method and studied its catalytic performance in the MTO reaction. First of all, boehmite, TEAOH, and silicasol were mixed homogenously. Then, aqueous H_3PO_4 solution was added. After stirring, the mixture

was transferred into an autoclave. After aging, it was hydrothermally treated at 4 different temperatures and durations. The final solid products were recovered with centrifugation and then washed. Finally, H_2O_2 aqueous solution was added to remove template. The template-free SAPO-34 particles were centrifuged and washed one more time. The first SAPO-34 sample (I) was prepared by traditional one-step hydrothermal crystallization and had a chabazite (CHA) structure. The second sample (II) was prepared by a two-step hydrothermal crystallization and had a cubic-like rhombohedra morphology. The sample (II) had larger surface area, smaller crystallite, and more acid sites than the first sample (I). It was found that the sample (II) was a promising catalyst for MTO process with its small crystallite size.

Kim *et al.* [49] studied the synthesis of mesoporous SAPO-34 with amine-grafting to be used in CO_2 capture. In order to synthesize the catalyst, firstly pseudoboehmite and distilled water were added slowly to the phosphoric acid solution and stirred for a while. Another solution involving fumed silica was added to the first solution. After heating, drying, and calcination, the resulting synthesis gel was obtained. Finally, $C_9H_{23}NO_3Si$ was introduced to the mixture of the gel and toluene. According to XRD patterns, the catalysts exhibited the characteristic peaks which belong to the chabazite structure. The synthesized materials also exhibited Type I isotherm. The BET surface areas were in a range of 703 – 739 m^2/g. The mesoporous catalyst was an effective adsorbent for CO_2/N_2 separation from power station flue gases in a fixed bed operation in terms of both the CO_2 adsorption capacity and CO_2/N_2 selectivity.

Demir [50] synthesized both microporous and mesoporous SAPO-34 materials through hyrdothermal synthesis route in his study. In order to sytnhesize the microporous one, firstly tetraethylammonium hydroxide (TEAOH) was mixed with aluminum isopropoxide. While stirring the solution, fumed silica and phosphoric acid were added to the mixture. After adjusting pH value with NaOH, the solution was placed in oven and hydrothermal synthesis was performed. After cooling and aging, it was centrifuged and dried. Finally it was calcinated under dry air. In order to synthesize mesoporous SAPO-34, cetyltrimethylammonium bromide was mixed with

deionized water. After stirring the solution, aluminum isopropoxide and phosphoric acid were added. The pH value of the mixture was adjusted to 7.60. The synthesis mixture was taken into an autoclave. Hydrothermal synthesis was carried out under autogenous pressure without agitation. After cooling and aging, it was centrifuged and dried. Finally it was calcinated under dry air. BET surface areas of mesoporous catalysts were in a range of 117-133 m^2/g. The activities of these materials were tested in methanol dehydration reaction. The highest methanol conversion was obtained using mesoporous SAPO-34 like materials at 550 °C, and it was 48 %. DME selectivity and yield values were 1 and 0.49, respectively. Microporous SAPO-34 catalyst gave higher methanol conversion, 67 %, at lower temperature.

CHAPTER 4

LITERATURE SURVEY

With an increase of plastic usage in our daily life lately, plastic wastes have become a major problem. Aside the present methods like incineration and landfilling, recycling of these wastes is more eco-friendly. Polymer wastes can be catalytically or non-catalytically degraded into valuable petroleum products. The catalytic thermal degradation reaction is more advantageous than the non-catalytic one due to lower reaction temperatures and better quality end products. Acidic catalysts are commonly used in the catalytic pyrolysis of plastic wastes. Typical catalysts used for polymer degradation are zeolites, activated carbon and mesoporous materials. Studies about the thermal and catalytic thermal degradation of polymeric materials are presented below.

Park *et al*. [11] studied catalytic degradation of high density polyethylene (HDPE) over SAPO-34. The catalyst was synthesized using different templates which are tetramethylammonium hydroxide (TEAOH), diethylamine (DEA), and their mixture. It was observed that the acidity of SAPO-34 synthesized using TEAOH was higher than the others, but the number of strong acid sites of SAPO-34 synthesized using their mixture was greater than SAPO-34 synthesized using TEAOH. TGA results revealed that the catalyst synthesized using the mixture of TEAOH and DEA showed the highest catalytic activity for the degradation reaction of the polymer due to its acidity, external surface area, and crystal size. The product distribution for all catalysts was almost similar. The carbon number range for liquid products was mostly between 5 and 13.

Obalı *et al.* [51] studied the catalytic degradation of PP over aluminum containing ordered mesoporous MCM-41 & SBA-15 based materials. The catalysts were

synthesized using different aluminum sources. Degradation reactions were performed at atmospheric pressure under N_2 gas at different reaction temperatures. The catalyst/polymer ratio in the reactor was 1/2. The activation energy (E_A) of the degradation reaction decreased from 172 kJ/mol to a range of 68 - 126 kJ/mole in the presence of MCM-type catalysts. SBA-type catalysts decreased E_A value to a range of 50 – 89 kJ/mole from 172 kJ/mol. Both gaseous & liquid products were analyzed using a GC. The amount of the gaseous products remained almost constant when the reaction time increased at a reaction temperature range of 400 – 410 °C. However, the yield of the liquid products increased when the temperature increased. Nearly the same amount of product was observed for gaseous & liquid products in the presence of SBA-type catalysts. Similar behavior was also observed for most of MCM type catalysts. GC results revealed that in the presence of MCM-41 or SBA-15 based catalysts, ethylene had the highest mole fraction and selectivity compared to the products which were obtained from the degradation reactions in the presence of different catalysts (zeolite, mesoporous silica). In the presence of MCM-type catalysts which were synthesized with aluminum isopropoxide, C_5 and C_7 formation increased and the amount of heavier hydrocarbons decreased considerably with an increase in aluminum loading. SBA-type catalysts showed higher selectivity to lighter hydrocarbons (the carbon number of 14 or smaller). The selectivity of C_7 hydrocarbons among the other products was high when aluminum isopropoxide was used as the aluminum source in the catalysts. The selectivity of C_{18} hydrocarbons increased considerably when aluminum nitrate was used as the aluminum source.

Obalı et al. [52] investigated the performance of pure and Al containing SBA-type catalysts in the degradation of polypropylene. These catalysts were synthesized using different aluminum sources and different Al/Si ratios. Characterization results showed that the synthesized catalysts had high surface areas. EDS results showed that the Al was incorporated into the structures of the catalysts effectively. The materials exhibited *Type IV* isotherms. The existence of both Bronsted and Lewis acid sites in the catalysts was observed. The degradation tempeature decreased in the presence of aluminum containing SBA-type catalysts. The activation energy of the reaction

decreased to about 51 kJ/mole from 172 kJ/mole in the presence of the catalysts which contain aluminum sulphate. However, when aluminum isopropoxide was used in the synthesis, the activation energy of the reaction decreased to 82 kJ/mole. The activation energy was decreased most in the presence of the material contained aluminum sulphate with a Al/Si ratio of 0.2.

Obalı et al. [53] studied the performance of MCM-like aluminosilicate catalysts in catalytic thermal degradation of PP using a thermogravimetric analyzer (TGA). First, mesoporous aluminosilicate catalysts with various Al/Si ratios were synthesized via hydrothermal synthesis route. Two kinds of aluminum sources were used in the synthesis. The synthesized materials exhibited *Type IV* isotherms and had high surface areas. Aluminum was incorporated more effectively into the structure of the materials which were synthesized using aluminum nitrate as the aluminum source. The activities of these catalysts in the PP degradation reaction were tested and TGA results revealed that the degradation temperature decreased in the presence of aluminosilicate catalysts. When the material which was synthesized using aluminum nitrate was used, the activation energy value of the degradation reaction decreased to a range of about 72 – 118 kJ/mole from 172 kJ/mole. The material which was synthesized with a Al/Si molar ratio of 0.5 and using aluminum isopropoxide as the aluminum source gave the lowest activation energy which was 67.5 kJ/mole.

Aydemir *et al.* [54] investigated the performance of TPA impregnated SBA-15 catalysts in PE degradation reaction. TPA impregnated SBA-15 materials were synthesized by impregnation of TPA into hydrothermally synthesized SBA-15. The polyethylene degradation reactions were first order. In the presence of TPA loaded SBA-15 catalyst, the activation energy decreased from 136 kJ/mol to 74 kJ/mol. With an increase in TPA amount in the catalyst, the activation energy value decreased to 62 kJ/mol. GC analysis indicated that in the catalytic decomposition reaction, gaseous products were composed of ethylene, propene, ethane, and butane. In the liquid products, hydrocarbons were observed in a carbon number range of C_8–C_{14}.

Lee *et al.* [12] studied the catalytic decomposition of PS over natural clinoptilolite zeolite (HNZ). The performance of HNZ was tested and the results were compared with the ones obtained from the non-catalytic and catalytic degradation reaction over HZSM-5 and silica-alumina. The synthesized HNZ was microporous. The degradation experiment of PS took place in a semi-batch, under N_2 atmosphere with a constant flow rate of 30 ml/min. A mixture of 3.0 g of PS and 0.3 g of the catalyst was put inside the reactor. All the experiments were carried out at 400 °C for 2 hours. Both liquid and gas products were analyzed in a gas chromatography. Liquid oils were the main products for all catalysts. In the presence of HNZ, the yield of liquid products was almost same with the one obtained from the non-catalytic pyrolysis reaction. However, the yield was lower in the presence of HZSM-5 and it was higher in the presence of silica-alumina. The main liquid products were C_7, C_8 and C_9 hydrocarbons.

Kim *et al.* [55] investigated the performance of differently treated clinoptilolite zeolites in the degradation of PP. First of all, clinoptilolite (Na-SCLZ4.4) was synthesized using the hydrothermal route and then it was mixed with 1 M aqueous solution of NH_4Cl. The proton-exchanged clinoptilolite form (H-SCLZ4.4) was obtained. In order to modify the acidity of H-SCLZ4.4, it was refluxed with 1M aqueous HCl solution (H-SCLZ12.0 and HSCLZ20.3, 12.0 and 20.3 values represent Si/Al ratios). The pyrolysis experiments took place in a semi-batch Pyrex reactor, under nitrogen. A mixture of 3.0 g of PP and 0.3 g of the catalyst was put inside the reactor and all the experiments were performed at 400 °C for 2 hours. At the end of the non-catalytic thermal degradation and catalytic degradation of polypropylene over Na-SCLZ4.4, a high amount of residue was obtained. However, in the presence of H-SCLZ materials, no formation of residue was observed. While H-SCLZ4.4 was giving the highest yield for liquid products, the highest yield for gaseous products were obtained in the presence of H-SCLZ20.3. H-SCLZ4.4 effected the degradation of PP positively. The yield of liquid products containing C_5–C_{12} hydrocarbon groups in the presence of the catalyst was higher than 99 %. Olefins, aromatics, and iso-paraffins which were produced in the presence of H-SCLZ4.4 were mainly in the carbon number

ranges of $C_8 - C_{11}$, $C_6 - C_{10}$, and C_8 - C_{11}, respectively. For all the HSCL catalysts, the amount of ethyl toluene was the highest. In the presence of H-SCLZ4.4, the amount of naphthenes and iso-paraffins decreased as temperature increased. However, the amount of olefins increased with the temperature.

Murata *et al.* [56] studied the effect of silica–alumina catalysts on degradation of polypropylene, polystyrene and polyethylene. The degradation was performed in a continuous flow reactor which operated steadily at atmospheric pressure. Two types of silica-alumina catalysts were choosen and the mole ratios of Si/Al were 5.0 (SA-1) and 0.42 (SA-4). The reaction temperatures of PP, PS, and PE were choosen as 420, 380, and 360 °C, respectively. Silica–alumina significantly increased the formation of gases. For example, SA-1 doubled the amount of gaseous products and showed a stronger effect in the degradation of PP. In PE degradation, SA-4 gave less gaseous products compared to the ones obtained in the presence of SA-1. Silica–alumina changed the distribution of gases and affected their average molecular weights in the degradation of the polymers. Both SA-1 and SA-4 have similar effect on gas product distribution for PP degradation. These materials decreased the amount of CH_4 and C_1–C_3 compounds while increasing that of C_4 and C_5. SA-4 led higher average molecular weight of gaseous products compared to SA-1 for PE degradation. In the presence of both catalysts, less hydrogen was produced in PS degradation, but more C_2–C_4 compounds were formed. Silica–alumina catalysts showed good activity on all the polymers which were studied

Neves *et al.* [34] studied the effect of acidity behaviour of Y zeolites on the catalytic pyrolysis of high density polyethylene (HDPE). Two Y zeolites with similar Si/Al ratios were treated using $NaNO_3$ to form H-form (HY) and NH_4NO_3 for Na-form (NaY) for ion-exchange to modify the acidity behaviour of the zeolites. Two types of experiments were performed: (i) dynamic experiments where the polymer and the catalyst were heated with a constant heating rate and (ii) isothermic experiments was carried out at 473 K during 8 hours. It was observed that the degradation temperature range slightly decreased in the presence of the zeolite materials, being more apparent

in the case of the HY zeolites because of higher acidity. The lowest activation energy value was found when Na(H)Y was used.

Chiu *et al.* [57] studied the non-catalytic and catalytic thermal degradations of polybutylene terephthalate (PBT) over metal oxide, metal chloride, metal copper, metal acetate, and powder catalysts. The pyrolysis reactions took place in a quartz reactor at atmospheric pressure, and different reaction temperatures (320 °C, 340 °C, 360 °C, 380 °C, and 400 °C). These results revealed that the copper (II) chloride ($CuCl_2$) was the most active catalyst for increasing the PBT weight loss more than 100 % while it was less than 100 % in the non-catalytic thermal degradation at 360 °C for 30 min. The $CuCl_2$/ PBT weight ratio was tested between 0 and 0.2 and the optimal ratio was found to be 0.1. The major products obtained from the non-catalytic and catalytic pyrolysis reactions were ethane, carbonmonoxide, carbondioxide, 1-butene, 1,3-butadiene, 2-butene, and butadiene dimmer. In the degradation of PBT over copper (II) chloride, the amount of 1,3-butadiene increased while butadiene dimer decreased. It can be concluded that the copper (II) chloride catalyst was effective in the degradation of PBT but not effective on the distribution of the gases. The major liquid products obtained from the non-catalytic and catalytic PBT degradation reactions were composed of benzoic acid, butadiene dimer, methyl terephthalate 1-methyl-2-propenyl benzoate, and 4-heptylacetophenone. The compound with the highest mole fraction was 4-heptylacetophenone among the liquid products. The formation of this compound reduced significantly upon adding copper (II) chloride catalyst to the PBT. When $CuCl_2$ was used, three new liquid products (ethyl benzoate, benzene, 1,4-dichlorobutane) were observed.

Chaianansutcharit *et al.* [58] studied catalytic pyrolysis of polypropylene and polyethylene over hexagonal mesoporous silica catalyst. Aluminum containing hexagonal mesoporous silica (Al-HMS) catalysts with the Si/Al mole ratios of 20, 40, 60, and 200 were synthesized. Catalytic degradation experiments took place in a glass-type fixed bed reactor under atmospheric pressure at 380 °C and 430 °C. Pure N_2 gas with a constant flow rate of 20 ml/min was passed through both reactors during the

experiment. During heating, polyolefins started melting and were in contact with the catalyst in the reactor. In PP degradation, the yield of liquid products increased with a decrease in the Si/Al mole ratio. However, the yields of liquids remained constant while the yield of gaseous products slightly increased when the Si/Al mole ratio in the catalyst was lower than 30. When the catalyst was used, propane, propene, ethane, ethene, butene, pentane, and methane were formed and the main gas products were propene and butene. In the PE degradation, the liquid products were distributed in a carbon number range of $C_5 - C_{25}$ when the pure HSM catalyst was used. In the presence of Al-HMS, the distribution of liquids was in a wide range as in the non-catalytic degradation, but a high portion of light hydrocarbons was in the range of $C_5 - C_9$. Gas products were mainly composed of propylene & ethylene.

4.1. Objective of This Study

There are many studies about the catalytic degradation of polymers in the literature. But there isn't any study related to the thermal degradation of polypropylene and polystyrene in the presence of SAPO-34. The aim of this study is:

- To synthesize and characterize SAPO-34 material,
- To determine kinetic parameters of polypropylene and polystyrene degradation reactions using thermogravimetric analyses,
- To investigate the effect of temperature and SAPO-34 material on the gas and liquid product distributions.

CHAPTER 5

EXPERIMENTAL METHOD

In this study, SAPO-34 material was firstly synthesized via hydrothermal route and then characterized using characterization techniques (XRD, FTIR, SEM, N_2 physisorption, NMR). Secondly, kinetic parameters of the polypropylene and polystyrene degradation reactions were determined using thermogravimetric data. Product distribution in the presence of the catalyst was investigated in a pyrolysis system using a gas chromatography. The experimental studies are explained below in detail.

5.1. Synthesis of SAPO-34 Material

The SAPO-34 material was synthesized via hydrothermal route using the synthesis procedure described by Demir, 2011 [50]. The composition of the synthesized material was Al_2O_3 / P_2O_5 / 0.30 SiO_2 / 2.0 TEAOH / 50 H_2O. In the synthesis of SAPO-34, the following materials were used: Tetraethylammonium hydroxide (TEAOH, 20 wt % aqueous solution, Merck) as surfactant source, fumed silica (Sigma-Aldrich, S5505) as silica source, aluminum isopropoxide (Merck) as aluminum source, ortho-phosphoric acid (Merck, 85 wt %) as phosphorus source, sodium hydroxide (Merck, 1 N) as base source and deionized water as solvent source.

The synthesis procedure is composed of six parts.

- The first part is the preparation of the solution. 15.1 grams of aluminum isopropoxide was weighed and dissolved in 54 mL of tetraethylammonium hydroxide. The mixture was kept stirring at 350 rpm and 40 °C for 1.5 h. Then, 0.66 grams of fumed silica was added to the mixture and 10 minutes later, 5 mL phosphoric acid diluted in 12.2 grams of water was added drop by drop to the mixture while being stirred. Then, the pH value of the mixture was measured and adjusted to 7.60 by adding NaOH. The temperature and stirring speed of the solution were kept constant during preparation of the solution mixture.

- The second part is the hydrothermal synthesis. The solution was taken into a teflon bottle which was placed in an autoclave made of stainless steel. For hydrothermal synthesis, the autoclave was kept at 200 °C under autogenous pressure for 48 h.

- The third part is aging. After taking the autoclave from the oven, it was left for cooling for 24 h. Then, the mixture in the bottle was taken outside and 300 mL of deionized water was added to the mixture. The solution was aged for 24 h at room temperature.

- The fourth part is filtering. The final solution was filtered to apart the solid part from liquid part. For that purpose, the solution was taken on a filter paper which was placed in a Buchner funnel connected to a vacuum pump. The pump was started and liquid part passed from the paper gathered in the bottle, under the Buchner funnel. Filtration was proceeded until the pH of the liquid part became around 7.00.

- The fifth part is drying. The solid material recovered from the solution was put in an oven in a teflon bottle and was dried at 110 °C for 24 h.

- The final part is calcination. After drying, the material was calcined in a quartz tubular reactor which was placed in a tubular furnace. The furnace was heated from room temperature to 550 °C with a heating rate of 1 °C/min and kept at 550 °C for 8 hours. During the calcination, dry air was passed through the reactor with a rate of 1 dm^3/min so the surfactant and impurities in the pores were removed and the pores of the material were opened.

SAPO-34 material was synthesized 5 times to use in the catalytic pyrolysis experiments. The samples were designated as SAPO-34#1, SAPO-34#2, SAPO-34#3, SAPO-34#4, SAPO-34#5. The synthesis procedure of SAPO-34 is given schematically in Figure 9.

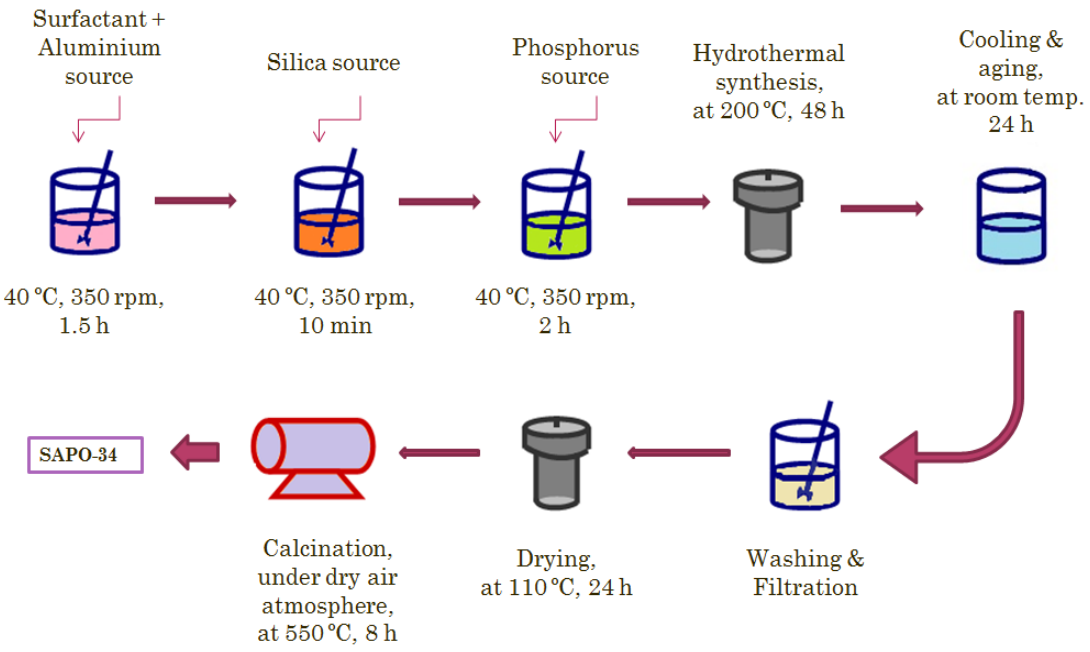

Figure 9. Schematic diagram of hydrothermal SAPO-34 synthesis route

5.2. Characterization of SAPO-34

Synthesized SAPO-34 material was characterized using several characterization techniques to determine its physical and structural properties such as pore diameter, pore volume, geometric shape. Detailed explanations of these techniques are given below.

5.2.1. X-Ray Diffraction (XRD)

X-ray diffraction analysis is an experimental technique which is used in revealing the crystal structure of material [59]. When crystals diffract X-rays, the atoms or ions act as secondary point sources and scatter the X-rays; but in the optical grating, it is the lines that scratched or ruled on the glass surface which cause scattering. *Bragg's Law* was used to treat diffraction by crystals. Bragg's Law is represented by the equation of $n\lambda=2dsin\theta$, where λ is the wavelength, n is the order of reflection, d is the lattice plane spacing and θ is the angle of incidence/reflection to the planes [60].

X-ray diffraction of the synthesized material was carried out by Rigaku Ultima-IV Diffractometer with nickel filtered CuK radiation which has a characteristic wavelength (λ) of 1.5406 Å to obtain information about its crystal structure. The Bragg angle range was 1-70° and the scanning rate was 2°/min. The analysis was performed at 40 kV and 40 mA.

5.2.2. Scanning Electron microscopy (SEM) & Energy-Dispersive X-ray Spectroscopy (EDS)

Electron detectors are used to gather various kinds of signals which are generated from the primary beam/specimen interaction [61].

Scanning electron microscopy analysis was performed using QUANTA 400F Field Emission Scanning Electron Microscope to get information about morphology of the material. Before the analysis, the samples were coated with Au-Pd to increase the surface conductivity of the synthesized material and to prevent surface charging [62].

Energy-dispersive X-ray spectroscopy (EDS) analysis was carried out using Jem Jeol 2100F 200kV HRTEM to get information about the elements in the synthesized material.

5.2.3. Diffuse Reflectance Infrared Fourier Transform Spectroscopy (DRIFTS)

DRIFTS analysis of the synthesized material was performed using Perkin Elmer-Spectrum One spectrometer at the wavelength between 400-4000 cm^{-1}. To get information about the acid sites in the material, two samples were analyzed. One of the samples was pyridine free and the other one was with pyridine. First, the sample was dried at 110 °C overnight under vacuum. Then, 0.0025 gr sample was combined with 2 ml of pyridine and the mixture was kept under the hood for 2 h to allow pyridine to evaporate. Potassium bromide (KBr) was used to obtain a background. The difference between the spectrum of pyridine adsorbed sample and the spectrum of pyridine free sample was taken to obtain information about the acid sites of the synthesized material.

5.2.4. Nitrogen physisorption

Nitrogen adsorption analysis for multipoint measurements were carried out using a Quantachrome Autosorb-6 equipment. The samples were dried at 120 °C for 16 h before the surface area measurmenet. The analyses were performed at a relative pressure range of 0.05 to 0.99 at liquid nitrogen temperature (77 K).

5.2.5. Nuclear magnetic resonance (NMR)

Coordination environments of Al and Si atoms were analyzed using ^{27}Al & ^{29}Si magic angle spinning (MAS) NMR spectrometer. Bruker AVANCE 300 MHz with a magnetic field of 7 Tesla was used in the analysis. The sample was spinned at a rate of 8500 Hz in a 4 mm MAS rotor. Spectra were recorded at room temperature.

5.3. Thermogravimetric Analysis (TGA)

Thermogravimetric analyses were performed using Perkin Elmer Pyris 1 Thermogravimetric Analyzer to determine kinetic parameters of PP and PS degradation reactions.

Before starting the analysis, TGA device and Gas Control Unit (TAGS) were started and then, the valve of nitrogen gas was opened. The flow of the gas was adjusted to 60 cc/min. The gas was passed through the system for 5 min. Sample cup made of platinum was placed on the device to determine the tare of the cup. The sample was weighted and placed into the cup. Temperature programming was started and a thermogram was obtained using the software of *Pyris 1 TGA*. At the end of the analysis, TAGS, valves, and ventilating system were closed down one by one.

The experiments were carried out under nitrogen atmosphere in a temperature range of 25 – 550 °C with a constant heating rate of 5 °C/min. The nitrogen flow rate was 60 cc/min. Catalyst/Polymer ratio of the prepared sample was 1/2. The samples prepared with PP and PS were analyzed 3 times.

5.4. Polymer Degradation System

5.4.1. Experimental Setup

A schematic diagram for the experimental set-up is given in Figure 10. The degradation reaction took place in a reactor made of quartz. The reactor was comprised of two parts: lower and upper. The lower part was in the form of spiral and filled with tiny glass particles on the purpose of increasing the surface area to make sure the flowing gas to reach the reaction temperature before entering the reacting part. Between the upper and lower parts, there was a porous glass where both the polymer and the catalyst were put together. Therefore, while the carrier gas was passing through the porous glass, the polymer and the catalyst didn’t flow into the spiral part. It also provided good mixing.

The carrier gas which was selected as nitrogen, came from a nitrogen tank and entered the reactor from the lower part. The flow rate of the gas was adjusted using a rotameter which connected to the tank. The reactor was placed in a tubular furnace. The furnace was covered with an insulating material to prevent the heat loss through the furnace during the reaction.

The inside temperature of the reactor was measured using a thermocouple which was inserted into the reactor. So it was possible to measure the exact reaction temperature. The upper part was tubular glass connected to a steel pipe which was covered with heating tape and isolating material. There was also one more thermocouple attached to the pipe. It was connected to the temperature controller. Therefore, the temperature of the heating tape was controlled and heated to the reaction temperature to prevent early condensation of the products when they were passing through the pipe.

At the end of the steel pipe, there were a spiral condenser and collecting bottles. Cold water coming from the water bath cooled down the gas. Therefore, some of the gaseous products leaving the pipe were condensed in the condenser and liquid products were collected in the collecting bottles. The non-condensed gas products were collected in a gas balloon. A soap bubblemeter was connected to the end of the gas balloon to check the gas flow rate of N_2. The gas leaving the bubblemeter was sent to the vent.

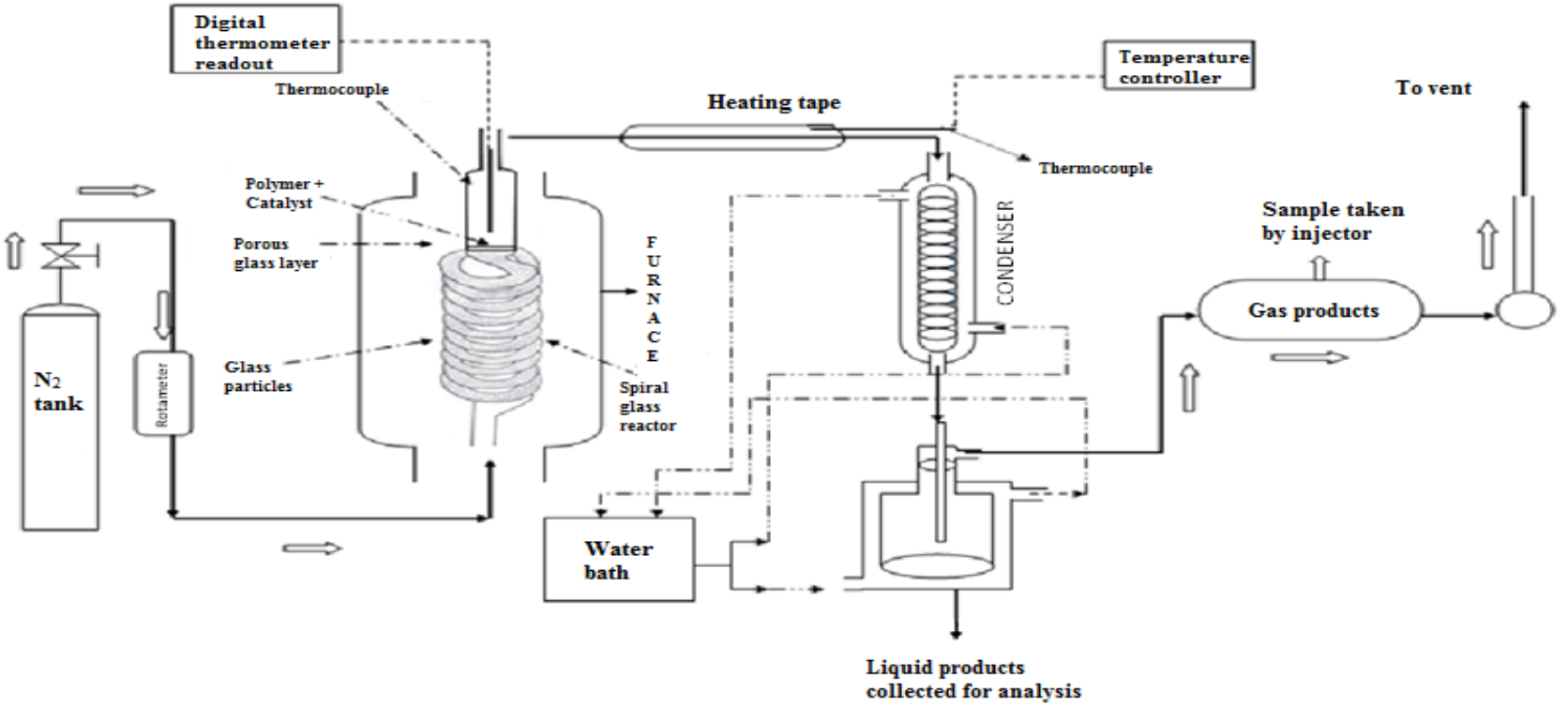

Figure 10. Experimental set-up for catalytic degradation of polypropylene and polystyrene [74]

5.4.2. Experimental Procedure

For the non-catalytic thermal degradation reaction, 1 gr of polymer and for the catalytic one, a mixture of 1 gr polymer and 0.5 gr catalyst were placed in the reactor. After inserting the thermocouple, all the fitting were tightened. The nitrogen gas was fed to the reactor with a flow rate of 60 cc/min and pressure of 2 bars. After controlling the possible gas leakage, the furnace temperature was adjusted to the desired reaction temperature. The settled heating rate of the furnace was 5 °C/min. The temperature of the water bath was also set to about -5 °C to ensure the sufficient cooling for the condensation of products. The temperature of the heating tape around the steel pipe was set to the temperature of the reactor and kept at the reaction temperature during the reaction.

After the reaction completed, gaseous products were taken from the collecting balloon with an injector to analyze in the gas chromatograph. The system was cooled down to room temperature. Liquid products and solid residue/catalyst were collected. To collect the solid residue and the catalyst, the reactor was turned upside down and then heated until the remaining material melted. The melting solid residue was collected from the reactor and then solid residue and liquid products were weighted using a precision scales and recorded. Liquid products were analyzed using the gas chromatograph.

During the experiment, the furnace temperature, reactor temperature, gas flow rate and water bath temperature were recorded in every 15 minutes. Experimental conditions are listed in Tables Table 5 & Table 6.

Table 5. Experimental conditions for the non-catalytic and catalytic thermal degradation reactions of PP

Sample	Reaction Temperature, °C	Reaction Time, min
PP	315	15
		30
	400	15
		30
	425	15
		30
	440	15
		30
PP+SAPO-34	315	15
		30
	400	15
		30
	425	15
		30
	440	15
		30

Table 6. Experimental conditions for the non-catalytic and catalytic thermal degradation reactions of PS

Sample	Reaction Temperature, °C	Reaction Time, min
PS	415	15
		30
PS+ SAPO-34	415	15
		30

5.4.3. Product analysis procedure

Analyses of both gaseous and liquid products were carried out using *Varian Star 3400 Gas Chromatograph (GC).* During the reaction, gas samples were collected by a gas tight syringe every 5 minutes and were injected in the gas chromatograph using the program *"Varian Star Chromatography Workstation version 6.2".* A packed column (Propac Q) with the sizes of 6' and 1/8" was used to analyze the gas products. Every single sample was analyzed twice and the average values of calculation results were considered. The conditions for gas analysis are given in Table 7.

Table 7. Analysis conditions for gas products [63]

Oven Temperature, °C	80 (Isothermal)
Injection Temperature, °C	110
Detector Type	TCD
Detector Temperature, °C	120
Column Pressure, psi	30
Analysis Time, min	35
Carrier Gas	He
Carrier Gas Rate, ml/min	30

Liquid samples were recovered when the furnace and the reactor had cooled down to room temperature and then injected to the GC using a microliter liquid syringe. HP-5 capillary column with an inside diameter of 0.32 mm and a length of 30 meters was used to analyze the liquid products. Every single sample was analyzed twice and the average area values were used in the calculation. The conditions for liquid analysis are given in Table 8.

Table 8. Analysis conditions for liquid products [63]

Oven Temperature	40 °C (for 10 min.) to 150 °C (for 15 min.) with a heating rate of 5 °C/min and then to 200 °C (for 70 min.) with heating rate of 1 °C/min
Injection Temperature (°C)	210
Injection amount (µL)	0.1
Detector Type	FID
Detector Temperature (°C)	225
Column Pressure (psi)	5
Analysis Time (min)	167
Carrier Gas	He
Carrier Gas Rate (mL/min)	1.5
Split Ratio	100:1

CHAPTER 6

RESULTS AND DISCUSSION

In this study, the SAPO-34 catalyst was synthesized hydrothermally and characterized using XRD, BET, SEM, NMR, and FTIR. Kinetic parameters of the polypropylene & polystyrene degradation reactions were determined using TGA data. Then, the performance of SAPO-34 was tested in the degradation reaction of polypropylene and polystyrene and gas & liquid products were analyzed using GC.

6.1. Characterization Results of SAPO-34

6.1.1. XRD Results

XRD pattern of the synthesized SAPO-34#1 is given in Figure 11. The peaks of the synthesized material were observed at the Bragg Angle values of 9.63º, 13.04º, 14.2º, 16.24º, 18.1º, 19.26º, 20.88º, 22.08º, 23.18º, 25.18º, 26.09º, 27.83º, 28.41º, 29.78º, 30.73º, 31.11º, 32.57º, 33.59º, 34.75º, 36.2º, 38.91º, 39.87º, 43.18º, 47.74º, 49.17º, 49.87º, 50.86º, 53.4º, 54.56º and 55.62º. Those peaks belong to SAPO-34 which were consistent with the XRD pattern of SAPO-34 material given in the literature [42][50][64].

The peaks at 22.01º, 31.22º, 36.13º and 28.44º were attributed to SiO_2 and the peaks around 27.9º, 33.1º, 47.09º and 56.33º were assigned to SiO. The peaks around 21.73º, 28.13º, 31.21º and 35.81º were due to $AlPO_4$ and peaks at 2θ values of 43.42º, 35.35º, 57.48º, 25.36º, 68.18º, 52.58º, 37.98º and 66.52º belong to α-Al_2O_3. The peaks around 20.54º, 26.05º, 24.13º, 30.82º, 28.96º and 33.17º correspond to $Al(PO_3)_3$. XRD results showed that the synthesized material was SAPO-34. All the synthesized SAPO-34

materials showed the same XRD patterns (Appendix A). XRD data of SAPO-34, SiO, SiO_2, $AlPO_4$, α-Al_2O_3, and $Al(PO_3)_3$ are given in Appendix A [65][66].

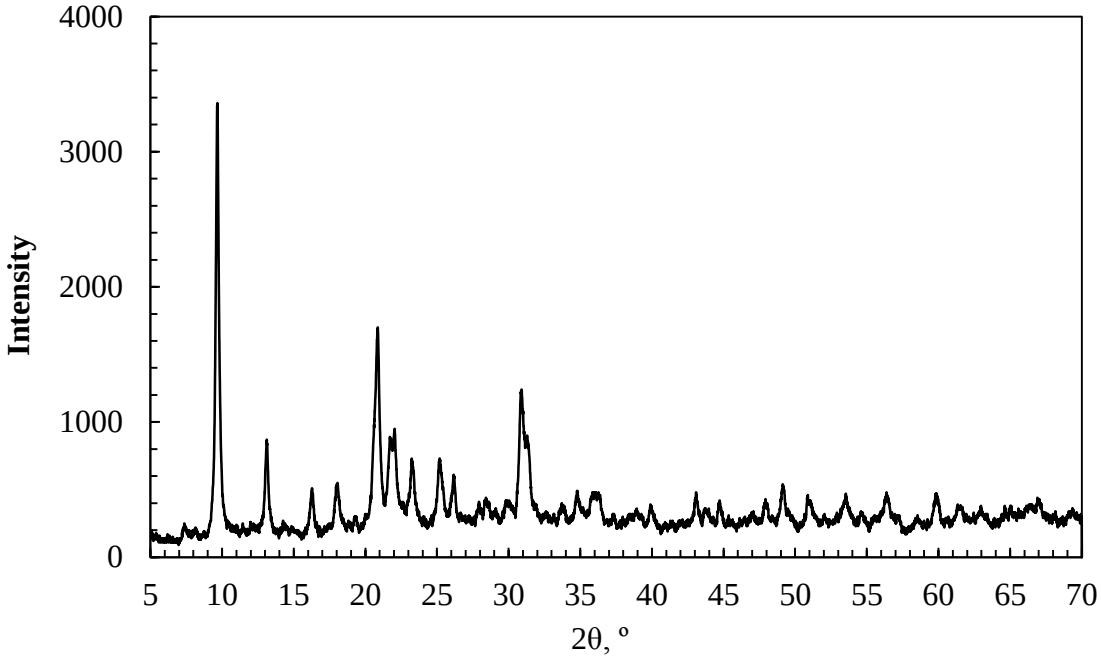

Figure 11. XRD pattern of synthesized SAPO-34#1 material

XRD patterns of SAPO-34 material after being used in the degradation reactions of polypropylene (at 440 ºC) and polystyrene (at 415 ºC) are given in Appendix A. The figures revealed that the crystal structure of the material didn't change due to the degradation reaction of both polymers.

6.1.2. SEM & EDS Results

SEM images of the synthesized sample are given in Figure 12. SEM result showed that the synthesized material was formed in cubic-like structure which was similar to the structure of SAPO-34 material [64][42].

The approximate dimensions of cubic-like particles were 2.18 x 2.52 μm (Figure 12.b) and 2.14 x 2.64 μm (Figure 12.c). The average particle size of the material was 2.5 x

2.5 μm. SEM images revealed that the particle size of the synthesized material was not uniform.

EDS spectrum of the synthesized material (SAPO-34#1) is given in Figure 13. The material contains C, O, Al, Na, Si, P, and Pd elements. Al, Si, O, P elements belong to SAPO-34 material. Pd comes from the coating of the samples with Au-Pd and C comes from the tape which was used in the preparation of the analysis. Na is due to NaOH solution which was used in the preparation of the solution part. The Al and Si elements which were found in the material by EDS analysis and their weight ratio are given in Table 9. The Al/Si ratio in material was calculated from the composition of the SAPO-34 material, which was given in Chaper 5, and was found to be 6.66. The Al/Si ratio was also calculated using EDS spectrum results and was found to be 5.80.
EDS spectra of the synthesized SAPO-34 samples are given in Appendix B.

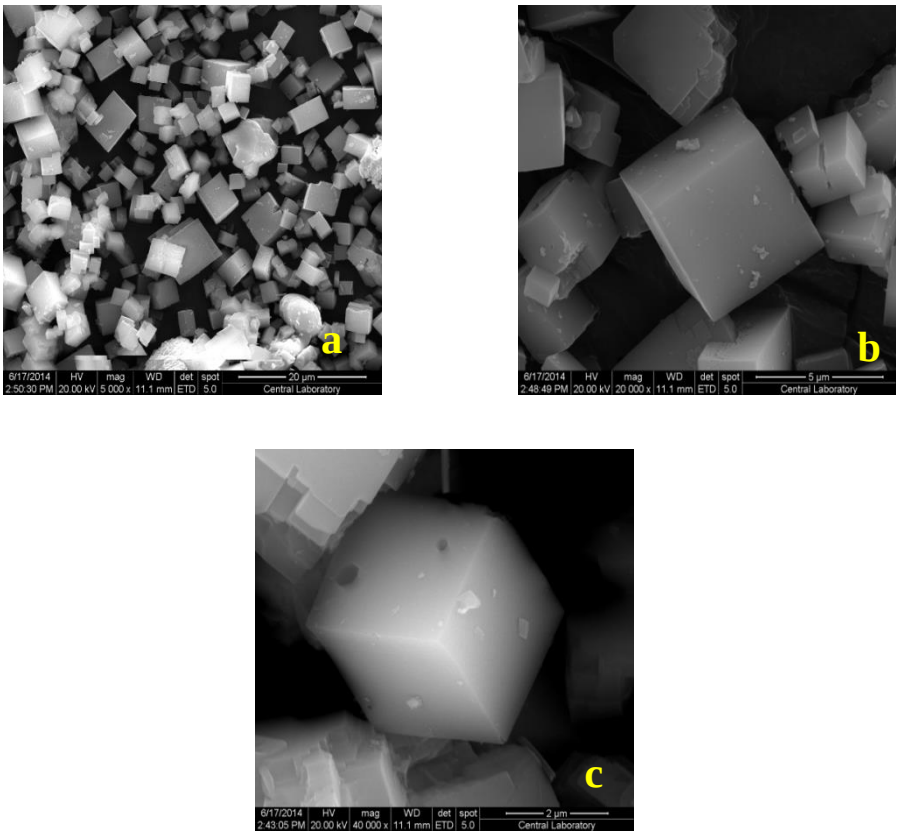

Figure 12. The SEM images of the synthesized SAPO-34#1 material (a) 5000 (b) 20000, and (c) 40000 magnifications

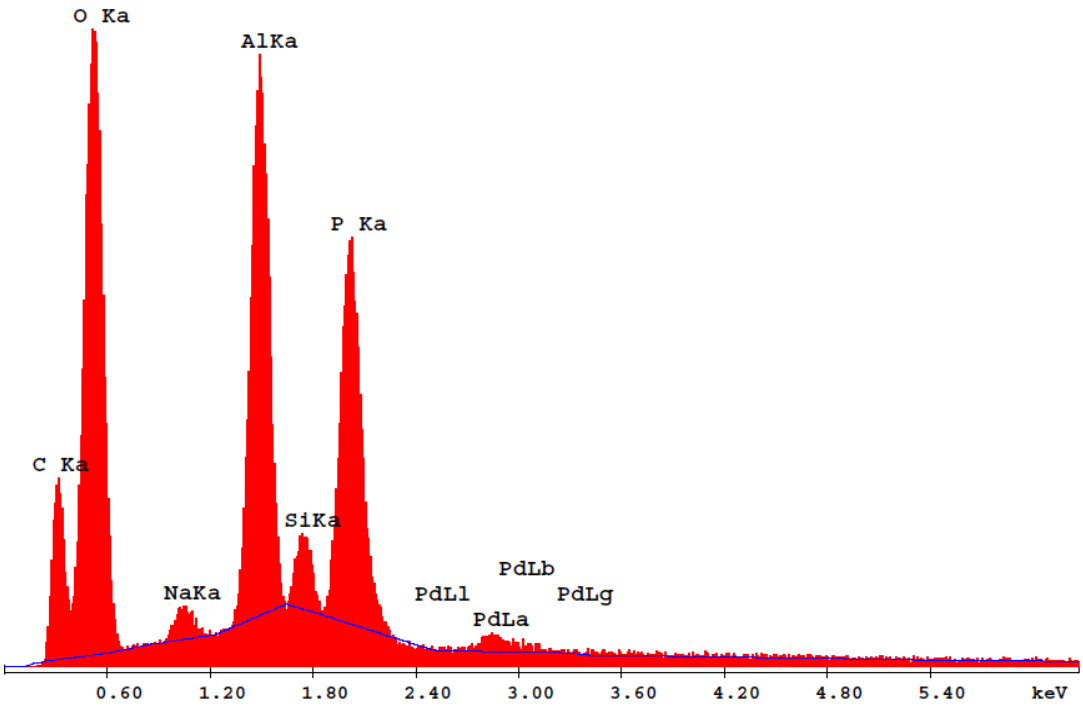

Figure 13. EDS spectrum of the synthesized SAPO-34#1 material

Table 9. Weight percent of the Al and Si elements in the materials

Element ID	wt. (%)
Al	12.33
Si	2.13
Al/Si	5.80

6.1.3. Nitrogen Physisorption Results

Nitrogen adsorption isotherm of the synthesized material is given in Figure 14. The material exhibited *Type I* isotherm which shows that the synthesized material is microporous according to the Brunauer classification [67]. Brunauer–Emmett–Teller (BET) surface area was found to be 308.5 m^2/g and pore volume and average pore diameter values of the synthesized SAPO-34 were calculated using Saito-Foley (SF)

method and were found to be 0.2 cc/g, and 1.35 nm, respectively. The pore diameter value also demonstrated that the material was microporous which was consistent with the isotherm type.

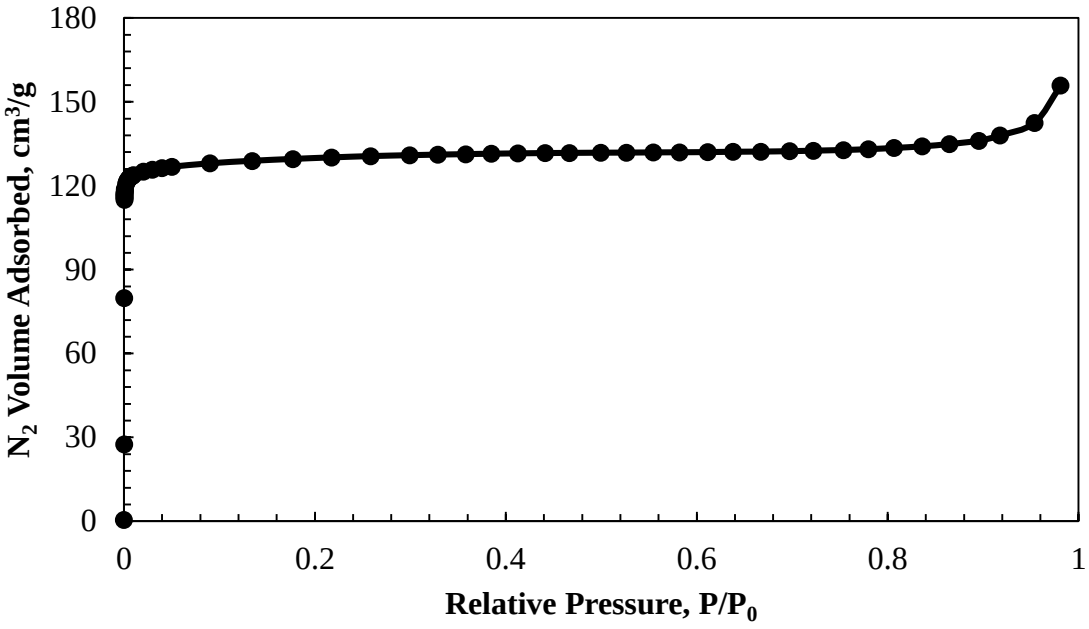

Figure 14. Nitrogen adsorption isotherm of the synthesized SAPO-34#1

6.1.4. NMR Results

Both ^{27}Al and ^{29}Si MAS NMR techniques were applied to the synthesized SAPO-34 material to find out the coordinational environments of Al and Si. The ^{27}Al & ^{29}Si NMR spectra of the synthesized material are shown in Figure 15. A sharp Al peak was observed at around 30 ppm which is due to tetrahedrally coordinated framework aluminum atom. The broad peak around 6 ppm was observed due to the presence of pentacoordinated aluminum atoms. The peak at around -20 ppm was attributed to octahedrally coordinated aluminum atoms due to the extra linkages of tetrahedral Al to –OH groups which were derived from the template or the hydrolysis of water [68][69].

Si peaks were observed at around -95, -100, -105, and -110 ppm which are due to tetrahedrally coordinated framework silicon atoms indicating that the Si atoms were incorporated into the framework [69][70][71].

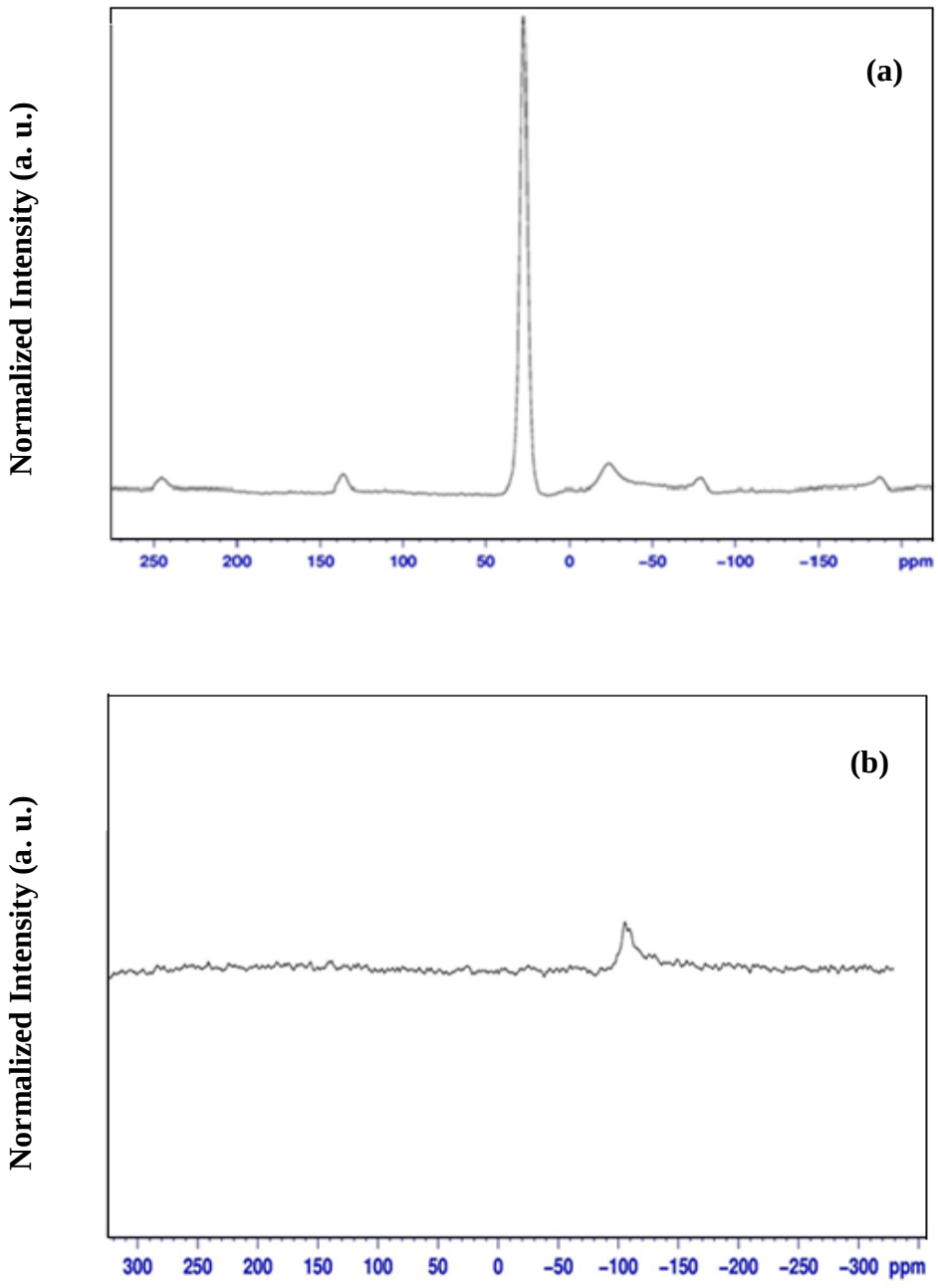

Figure 15. ^{27}Al (a) and ^{29}Si (b) MAS NMR spectra of SAPO-34#1

6.1.5. DRIFTS Result

The difference of DRIFTS spectra which were obtained from pyridine adsorbed and fresh catalyst sample is shown in Figure 16. The peak at 1490 cm^{-1} corresponds to the Lewis acid site and the peak at 1550 cm^{-1} was attributed to the Bronsted acid sites [72].

DRIFTS spectrum revealed that the material had both Lewis and Bronsted acid sites which are consistent with the literature [47][73].

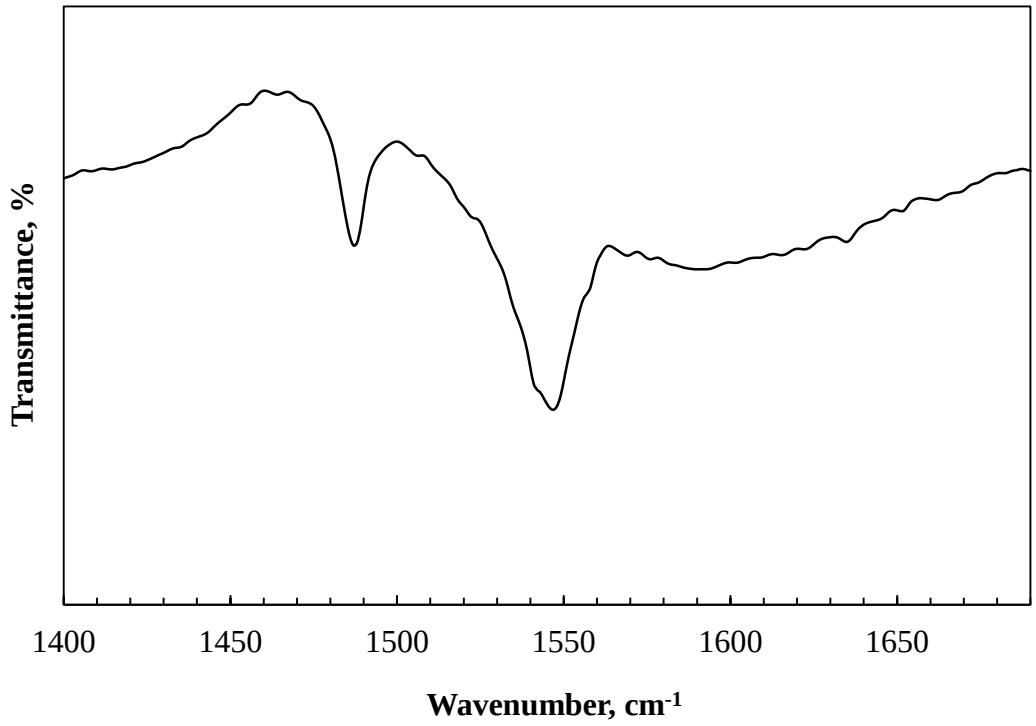

Figure 16. DRIFTS spectrum of the synthesized SAPO-34#1 material

6.2. TGA Results

Thermogravimetric analyses were carried out to obtain the kinetic parameters of the thermal degradation reactions of polypropylene and polystyrene. The experiments were carried out under non-isothermal conditions using catalyst/polymer weight ratio of 1/2. TGA plots of polypropylene-SAPO-34 and polystyrene-SAPO-34 mixtures with the SAPO-34 to polymer weight ratio of 1/2 are given in Figure 17.

A sudden decrease in the weight loss of the mixture was observed in the temperature range of 360–480 ºC for PP mixture and 360–440 ºC for PS mixture. This behavior might be due to the breaking of the carbon bonds. The catalytic thermal degradation of polypropylene started at 380 °C and ended at 460 °C while the degradation of pure polypropylene started at 411 °C and ended at 474 °C (Figure 17.a). TGA results of polypropylene-SAPO-34 revealed that the decomposition temperature shifted to lower temperature in the presence of SAPO-34.

A similar sudden decrease was also observed in the catalytic pyrolysis of polystyrene. The degradation temperature of pure PS started at 366 °C and ended at 427 °C, and in the presence of SAPO-34, it started at 358 °C and ended at 444 °C (Figure 17.b). There was not any difference between the degradation temperatures of pure PS and PS+SAPO-34 mixture. In other words, the degradation temperature range was approximately same.

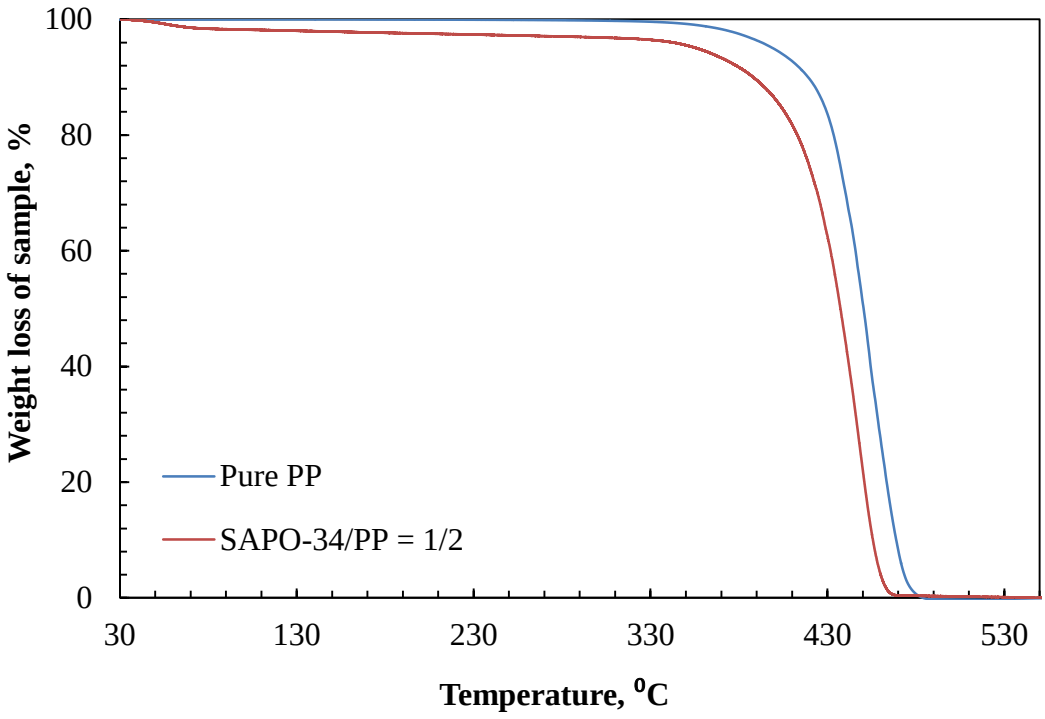

(a)

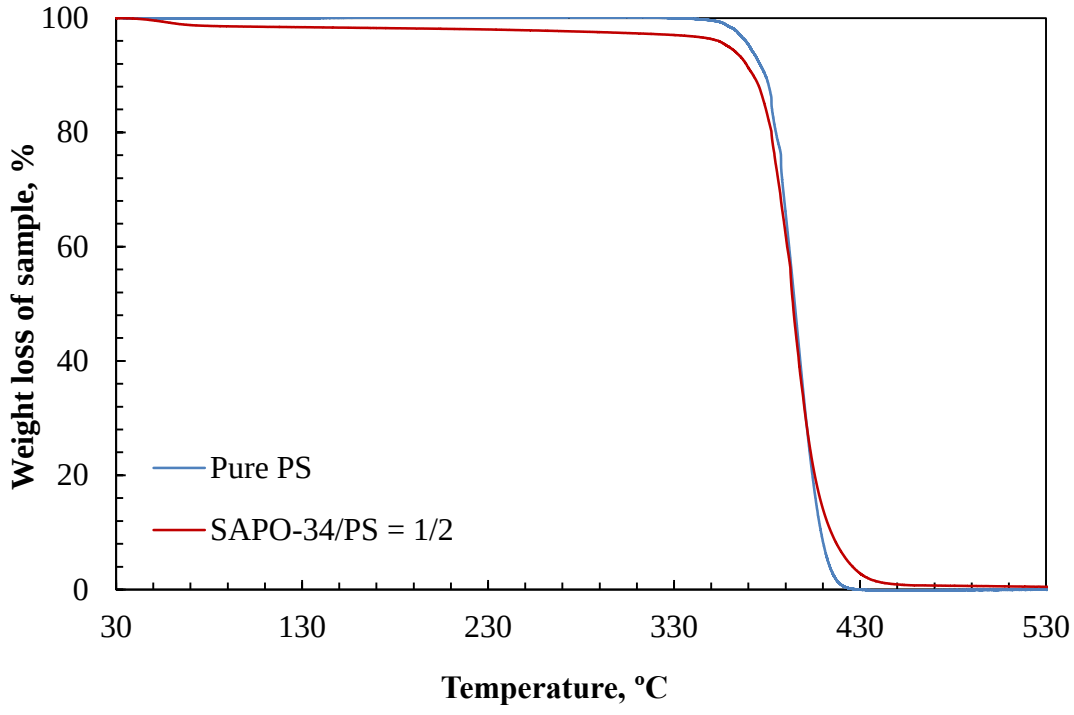

(b)

Figure 17. TGA plots for PP+SAPO-34 (a) and PS+SAPO-34 (b) mixtures

6.2.1. Determination of Kinetic Parameters for Polypropylene and Polystyrene Degradation Reactions

Kinetic parameters of both polypropylene and polystyrene degradation reactions were determined using the TGA data following a similar procedure as reported in the literature [74][75]. The activation energies were calculated in the presence of the catalyst. Sample calculations of activation energy, standard deviation and reaction order are given in Appendix C. Thermogravimetric analyses for the catalytic degradation were performed 3 times for each polymer. All TGA plots are given in Appendix D. The activation energies of both polypropylene and polystyrene degradation reactions are given in Table 10.

Table 10. Activation energies for PP & PS degradation reactions (SAPO-34/Polymer = 1/2)

Sample ID	Activation Energy, E_A (kJ/mol)
Pure PP	172 [52]
PP+SAPO-34	131±11
Pure PS	357±4
PS+SAPO-34	262±4

The activation energy value of pure PP decomposition reaction was found to be 172 kJ/mol [52]. When SAPO-34 catalyst was used in the PP degradation reaction, the activation energy value of PP pyrolysis reaction decreased to 131±11 kJ/mol. In the literature, the activation energy values of PP decomposition reactions were found to be in a range of 67.5 – 125.7 kJ/mol and 50.7 – 89.2 kJ/mol in the presence of MCM-type and SBA-type catalysts, respectively [52][53]. Because MCM and SBA-type catalysts had higher surface area and pore diameter than SAPO-34 had, they decreased the activation energy more than SAPO-34 did. In the presence of ZSM-12, the activation energy decreased to 100 kJ/mol [76].

The activation energy value of catalytic PS degradation reaction decreased from 357 kJ/mol to 260 kJ/mol. It was observed that SAPO-34 material decreased the activation

energy value. In the literature, the activation energies of PS degradation reactions were 92 kJ/mol and 138 kJ/mol in the presence of *p*-toluene sulfonic acid and Fe-K/Al_2O_3 catalysts, respectively [77][78].

The overall reaction orders of both polypropylene and polystyrene degradation reactions were found to be "1" for SAPO-34 material.

6.3. Polymer Degradation Reaction System

Both the non-catalytic and catalytic thermal decomposition experiments of PP & PS were performed isothermally in the polymer pyrolysis system under N_2 atmosphere with a constant flow rate and a constant heating rate of 60 cc/min and 5 °C/min, respectively.

6.3.1. Results of Polypropylene Degradation Experiments

In order to carry out the non-catalytic thermal degradation reactions, 1 g of PP was placed inside the reactor while for the catalytic thermal degradation reaction, 1 g of PP and 0.5 g of SAPO-34 were loaded to the reactor before each experiment. The reaction temperatures were 315 °C, 400 °C, 425 °C, and 440 °C and the reaction times were 15 and 30 minutes for all the experiments. In addition to solid residue, liquid and gaseous products were observed. Solid residue and liquid products were weighted at the end of the experiments and the amount of gaseous products were calculated by taking the difference between the initial polymer loading and the total amount of solid residue and liquid products. Product yield of polymer degradation reaction was calculated from the following equation:

$$Yield\ (wt\ \%) = \left(\frac{weight\ of\ liquid\ or\ gas\ product}{initial\ weight\ of\ polymer}\right) * 100$$

The amounts of solid residue, gaseous & liquid products of the non-catalytic and catalytic pyrolysis experiments are given in Appendix D. The liquid & gas product yields in the polypropylene degradation reaction are given in Table 11.

In both the non-catalytic and catalytic thermal decomposition experiments, solid residue was observed while no liquid formed at temperatures 400 °C and lower.

Table 11. Product and solid residue yields in the PP degradation reaction

Sample	Reaction Temperature, °C	Reaction Time, min	Yield (wt %)		
			Gas	Liquid	Solid residue
PP	315	15	24	0	76
		30	24	0	76
	400	15	42	0	58
		30	98	0	2
	425	15	86	14	0
		30	77	23	0
	440	15	86	14	0
		30	87	13	0
PP+SAPO-34	315	15	46	0	54
		30	80	0	20
	400	15	63	0	37
		30	100	0	0
	425	15	63	37	0
		30	78	22	0
	440	15	85	15	0
		30	76	24	0

However, at 425 ℃ and higher temperatures, liquid products were obtained while no solid residue was observed. Gas products formed at every reaction temperatures (315 ℃, 400 ℃, 425 ℃, and 440 ℃). The amount of gaseous products increased significantly due to the presence of SAPO-34 at 315 ℃. At 400 ℃, the gas product yield increased for 15 min reaction time while it didn't change for 30 min reaction time in the presence of the catalyst. When the temperature increased to 425 ℃, liquid products formed in addition to the gaseous ones. At both 425 ℃ & 440 ℃, the yield of liquid products increased due to the presence of SAPO-34. However, it didn't change significantly due to the increasing reaction temperature from 425 ℃ to 440 ℃. These results showed that the catalytic degradation of polypropylene over SAPO-34 favored the production of gaseous products.

Obalı et al. [51] also observed the same increasing trend in liquid product yields with increasing reaction temperature in PP thermal degradation reaction. In the presence of MCM-type catalysts, the liquid product yield was in a range of 18 – 32 % at a temperature range of 275 – 360 ℃ while it was around 23 % between 300 – 345 ℃ in the presence of SBA-type catalysts. Chaianansutcharit et al. [58] observed that the increase in the liquid product yield in the presence of silica-alumina containing catalyst at 380 ºC. The liquid product yields in the presence of HMS catalyst and Al loaded HMS catalyst were around 65 % and 80 %, respectively.

During the degradation reaction period, the catalyst was not deactivated. However, a little color change in the catalyst used in the high temperature pyrolysis experiments was observed. Therefore, TGA analyses of used catalysts in the degradation reactions of PP &PS were performed in order to obtain information about coke formation on the catalyst.

TGA plots of the catalysts which were used in the degradation reactions of PP at 440 ℃ and PS at 415 ℃ for the reaction time of 30 min are given in Appendix D (Figures D.3 & D.4). In both TGA plots, roughly 16 % weight loss at around 100 ℃ was observed. This weight loss might be due to the removal of water from the material. It might be concluded that the coke didn't form on the catalyst after the reaction.

XRD patterns of the used catalysts in PP and PS degradation reactions are also given in Appendix A (Figures A.5 & A.6). The figures revealed that the crystal structure of the catalyst didn't change after being used in the degradation reactions of both polymers.

6.3.1.1. Gas Analysis of Polypropylene Non-Catalytic Thermal Degradation

Gas products were analyzed using GC. Then, the calibration factor for each gas product was determined by performing calibration experiments. A sample calculation of calibration factor for gaseous products is shown in Appendix E. The mole & weight fractions and selectivities of gas products were calculated using these calibration factors. Sample calculations for the mole & weight fractions and selectivities of gaseous products are shown in Appendix F. The mole and weight fractions and selectivities for gaseous products obtained from the non-catalytic thermal degradation of polypropylene are given in Appendix G.

The variation of mole fractions & selectivities of gaseous products obtained from the non-catalytic thermal decomposition of polypropylene at different reaction & times are given in Figure 18 & 19, respectively.

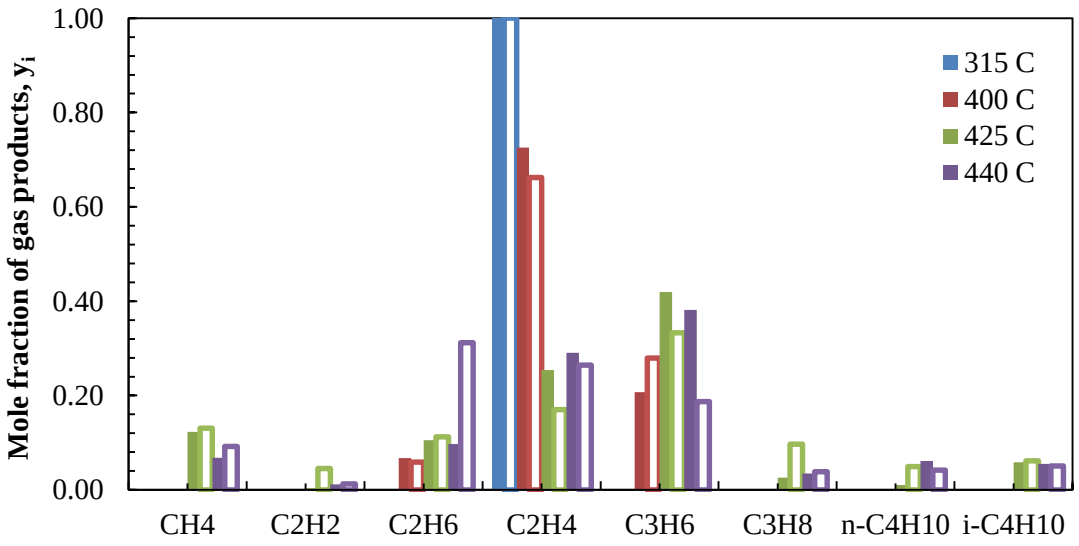

Figure 18. The variation of gas product mole fractions for the non-catalytic thermal degradation of PP at different reaction temperatures & times (Filled: 15 min; Blank: 30 min)

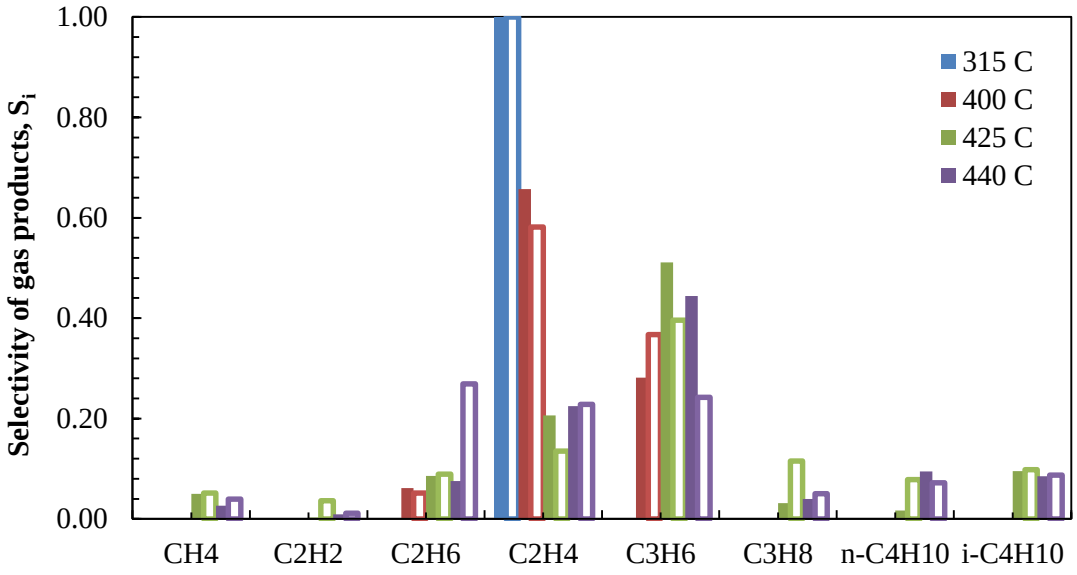

Figure 19. The variation of gas product selectivities for the non-catalytic thermal degradation of PP at different reaction temperatures & times (Filled: 15 min; Blank: 30 min)

Ethylene was the only component which was formed at 315 °C for both reaction times. With an increase in reaction temperature, the mole fraction and selectivity of ethylene decreased while ethane (C_2H_6) and propene (C_3H_6) formed in addition to ethylene for both reaction times. This is due to breaking carbon bonds with increasing temperature. At 425 °C, the formation of methane (CH_4), propane (C_3H_8) and butane (C_4H_{10}) was observed together with the previous gases (ethane, ethylene and propene) for 15 min reaction time. When the reaction time increased to 30 min from 15 min, acetylene formation was also observed in addition to the other gases at 425 °C. All the gaseous products (methane, acetylene, ethane, ethylene, propene, propane and butane) were observed at 440 °C for both reaction times. These results revealed that polypropylene decomposed into lighter gas products with increasing reaction temperature & time and this was an expected result.

Similar gas product distributions were also obtained in the studies of Obalı *et al.* [51] and Murata *et al.* [56]. The major gas products were ethylene and propene in the study of Obalı et al. at a temperature range of 400 – 425 °C [51]. Murata et al. [56] observed

mostly $C_1 - C_4$ hydrocarbons including methane, ethane, propane, ethylene, butane at 380 °C.

6.3.1.2. Gas Analysis of Catalytic Thermal Degradation Experiments

The gas products obtained from the catalytic thermal degradation of polypropylene were analyzed to show the effect of SAPO-34 on product distribution. The mole and weight fraction and selectivity values of gaseous products obtained from the catalytic decomposition reaction of PP are tabulated in Appendix G.

The variation of mole fractions and selectivities of gaseous products obtained from catalytic thermal decomposition of polypropylene at different reaction temperatures and times are given in Figure 20 &Figure 21, respectively.

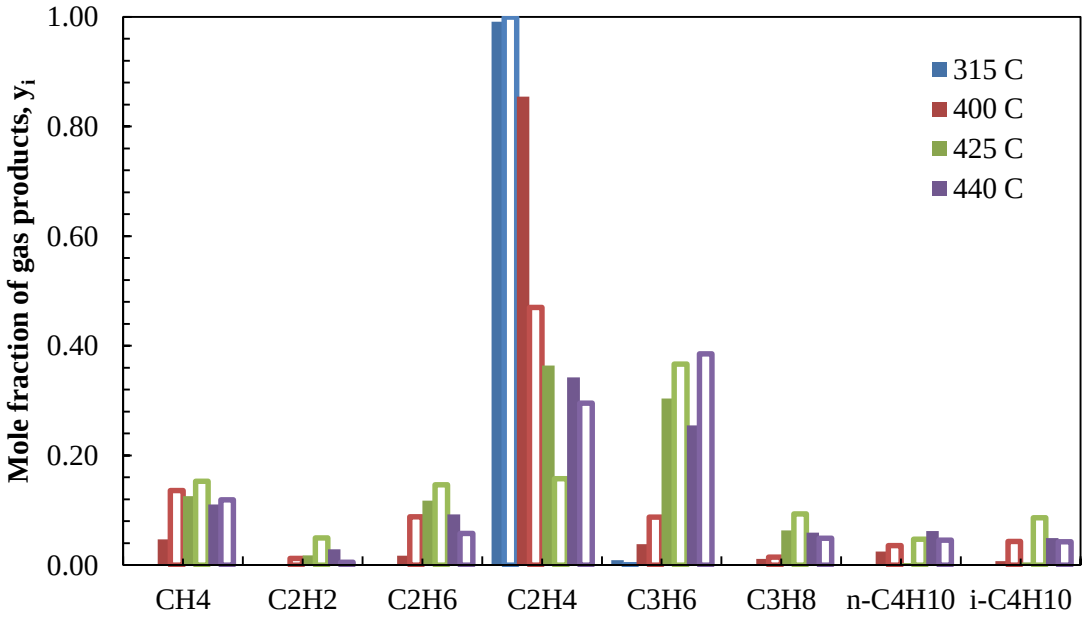

Figure 20. The variation of gas product mole fractions for the catalytic thermal degradation of PP at different reaction temperatures & times (Filled: 15 min; Blank: 30 min)

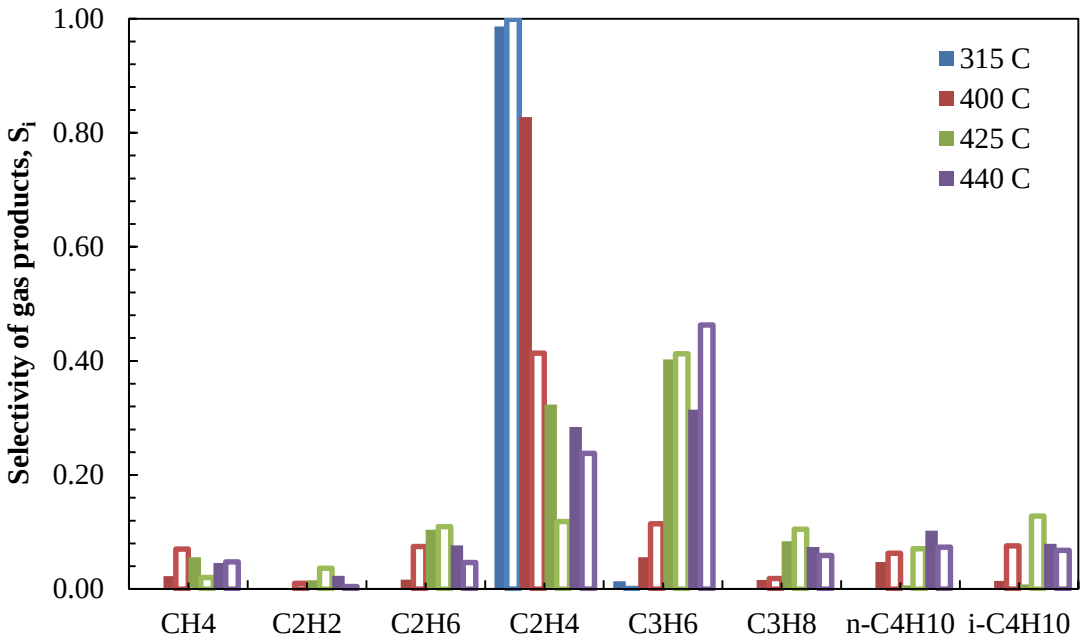

Figure 21. The variation of gas product selectivities for the catalytic thermal degradation of PP at different reaction temperatures & times (Filled: 15 min; Blank: 30 min)

It was observed that the gas products were mainly composed of ethylene and propene for the catalytic thermal degradation of polypropylene. The mole fraction and selectivity of ethylene was extremely high at lower temperatures (315 & 400 °C) when compared to other gas products in the presence of SAPO-34. At 315 °C, ethylene and a little bit propene were observed at both reaction times. Methane, propane, acetylene, ethane, and butane formed in addition to ethylene and propene at 400 °C and higher temperatures. This might be due to the effective decomposition of polypropylene to lighter gas products at high reaction temperatures. With an increase in reaction temperature from 400 °C to 425 °C, the mole fractions and selectivities of acetylene, ethane, propene and propane increased while the fraction of ethylene decreased which might be due to the effective decomposition of PP with increasing reaction temperature. With an increase in reaction temperature from 425 °C to 440 °C, the mole fractions and selectivities of propene and ethylene increased while the fractions of acetylene, ethane, propane decreased.

Obalı [51] obtained a high amount of ethylene in addition to propene, butane while no formation of methane, ethane and acetylene gases was observed in the pyrolysis experiments of PP over MCM-type & SBA-type mesoporous catalysts at 315 °C. Murata et al. [56] observed that the amounts of C_4 - C_5 hydrocarbons increased due to the presence of commercial silica-alumina catalyst at 380 °C.

The comparison of mole fractions & selectivities of the gas products which were obtained from the non-catalytic and catalytic thermal degradation reactions of PP at different temperatures are given in Figure 22 & Figure 23 for 15 min reaction time and Figure 24 & Figure 25 for 30 min reaction time, respectively.

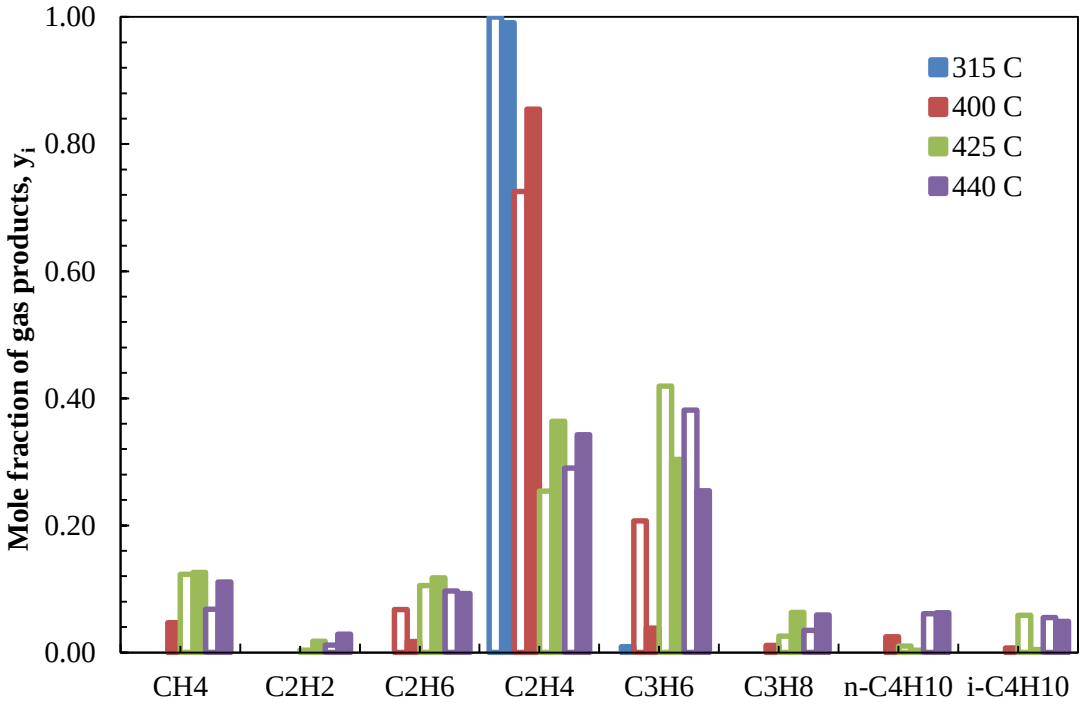

Figure 22. The comparison of gas product mole fractions for the degradation of PP in the presence and absence of catalyst at different reaction temperatures for 15 min reaction time (Blank: Pure PP; Filled: PP + SAPO-34)

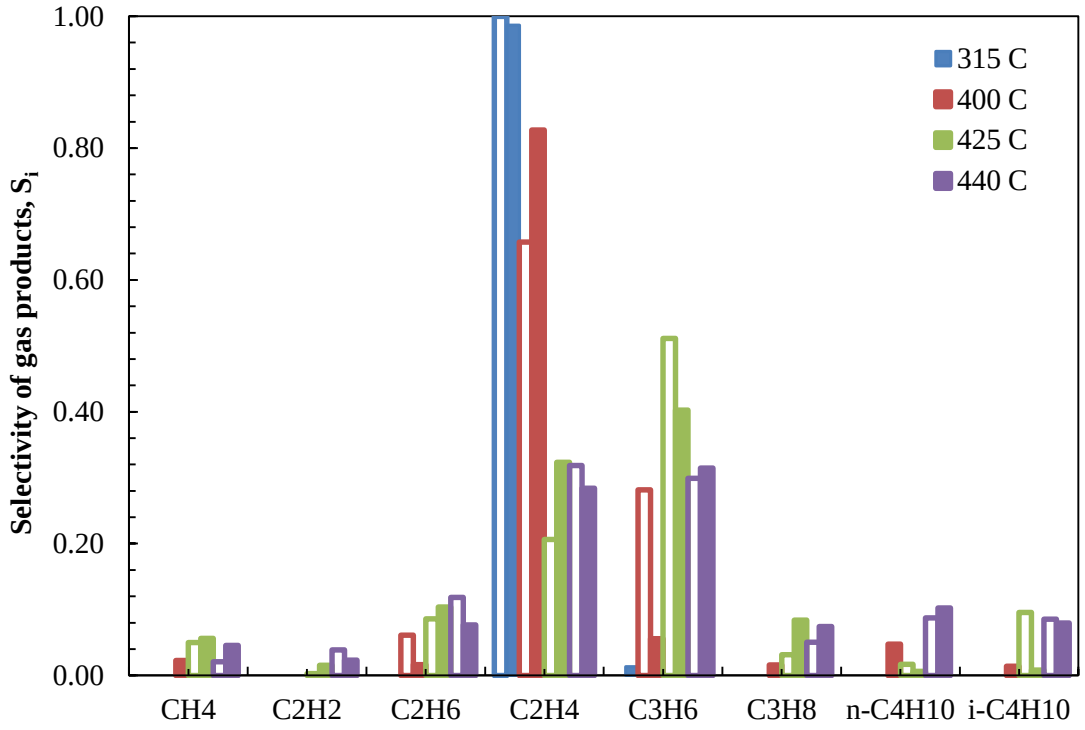

Figure 23. The comparison of gas product selectivities for the degradation of PP in the presence and absence of catalyst at different reaction temperatures for 15 min reaction time (Blank: Pure PP; Filled: PP + SAPO-34)

Figures 22 & 23 revealed that the gas product was composed of ethylene at temperatures lower than 400 °C for 15 min reaction time. However, the formation of propene was also observed in addition to ethylene in the presence of SAPO-34 at 315 ºC. At 400 °C, methane, propane and butane were formed in addition to ethane, ethylene and propene in the presence of the catalyst while they weren't observed in the absence of SAPO-34. This might be due to the promoting effect of SAPO-34 on the degradation of polypropylene. At 440 °C, the presence of SAPO-34 didn't significantly effect the gaseous product distribution. SAPO-34 material showed a stronger effect in the reaction temperatures of 400 °C & 425 °C at different reaction times.

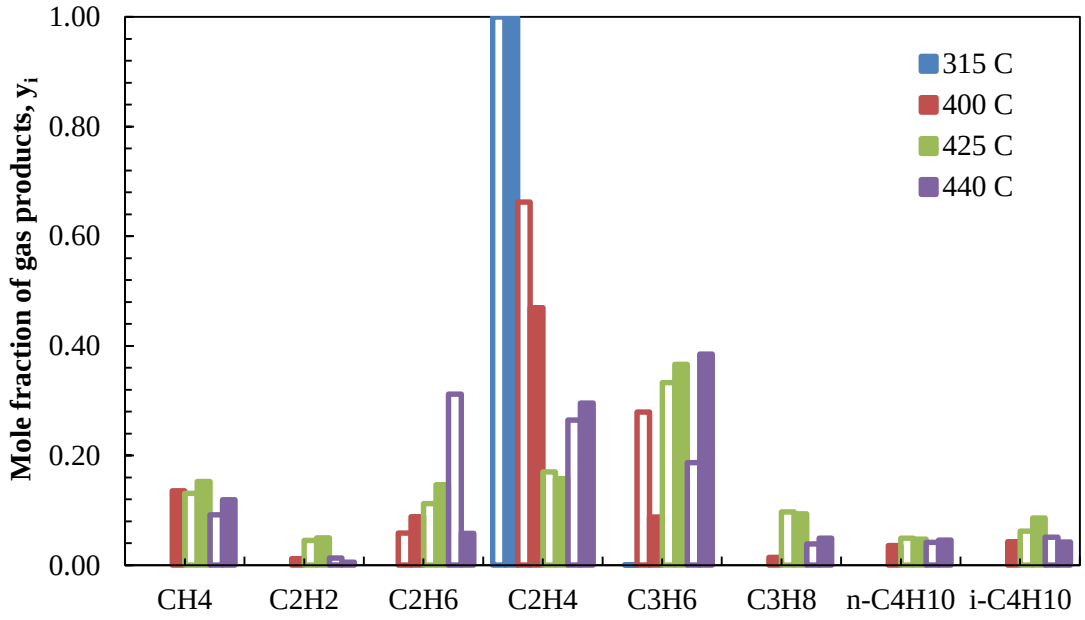

Figure 24. The comparison of gas product mole fractions from the degradation of PP in the presence and absence of catalyst at different reaction temperatures for 30 min reaction time (Blank: Pure PP; Filled: PP + SAPO-34)

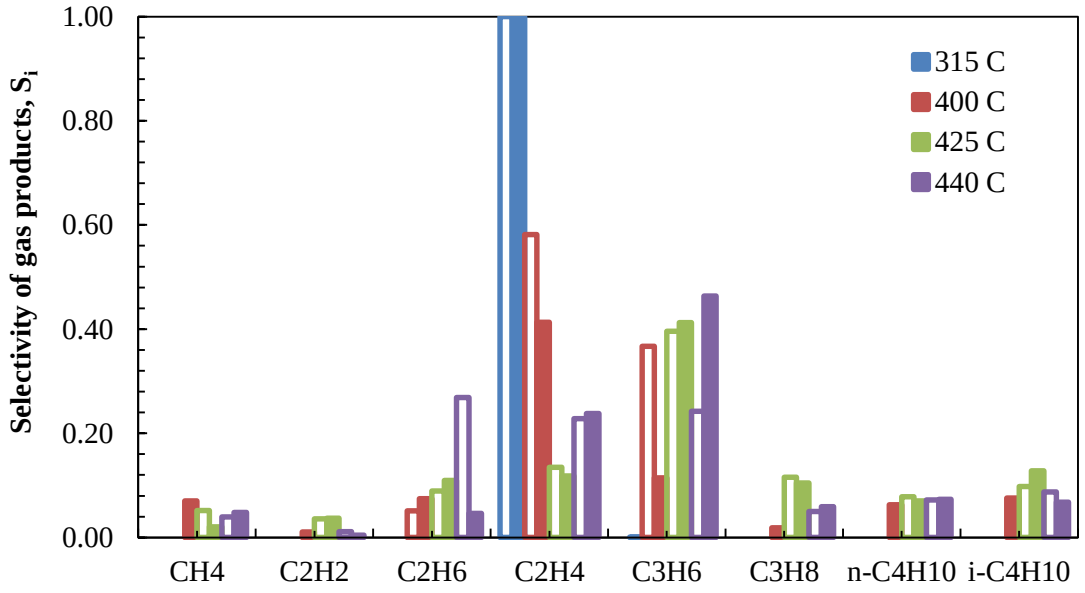

Figure 25. The comparison of gas product selectivities from the degradation of PP in the presence and absence of catalyst at different reaction temperatures for 30 min reaction time (Blank: Pure PP; Filled: PP + SAPO-34)

It was observed from Figures 24 & 25 that the formation of propene was observed in addition to ethylene in the presence of SAPO-34 at 315 °C while it didn't form in the absence of the material. When the temperature increased to 400 °C from 315 °C, methane, acetylene, propane and butane formed in the presence of SAPO-34 while they weren't observed in the thermal degradation of PP. The formation of low molecular weight hydrocarbons showed that SAPO-34 material promoted the degradation of polypropylene at 400 °C. At a temperature of 425 °C, the gaseous product distribution didn't change significantly in the presence of SAPO-34. At 440 °C, the gas amounts didn't change except for ethane and propene; the amount of ethane decreased while propene increased in the presence of the catalyst.

These results revealed that the SAPO-34 material was highly ethylene selective. Ethylene is used to produce various petrochemical products such as polyethylene, ethylene oxide, vinyl acetate, ethylene glycol, ethanol which are used in automative, textile, plastic and detergent industries [79].

6.3.1.3. Liquid Analysis of Non-Catalytic Thermal Degradation of Polypropylene

Liquid products obtained from the decomposition reactions of PP were analyzed in GC. Calibration factors for each liquid product were determined by several calibration experiments. The calculation method of the calibration factors is shown in Appendix H. The calculated mole fraction & selectivity values of liquid products obtained from the thermal decomposition reaction of polypropylene are tabulated in Appendix I.

The variations of selectivity & mole fraction results of liquid products obtained from the non-catalytic thermal decomposition reaction of polypropylene at different reaction temperatures & times are given in Figures 26 & 27, respectively.

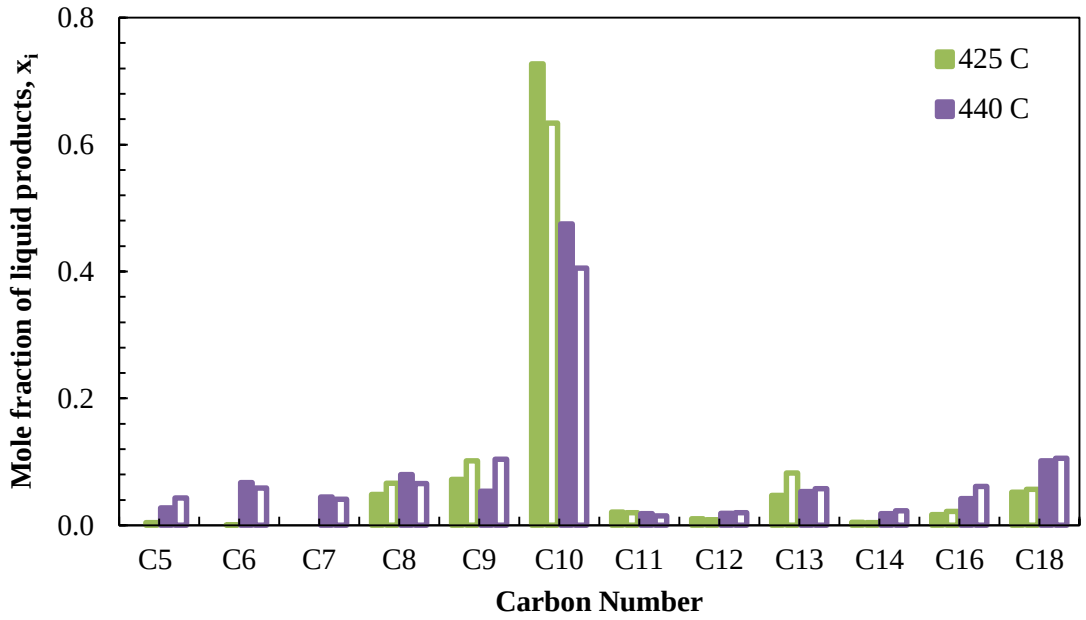

Figure 26. The variation of liquid product mole fractions for the non-catalytic thermal degradation of PP at different reaction temperatures & times (Filled: 15 min; Blank: 30 min)

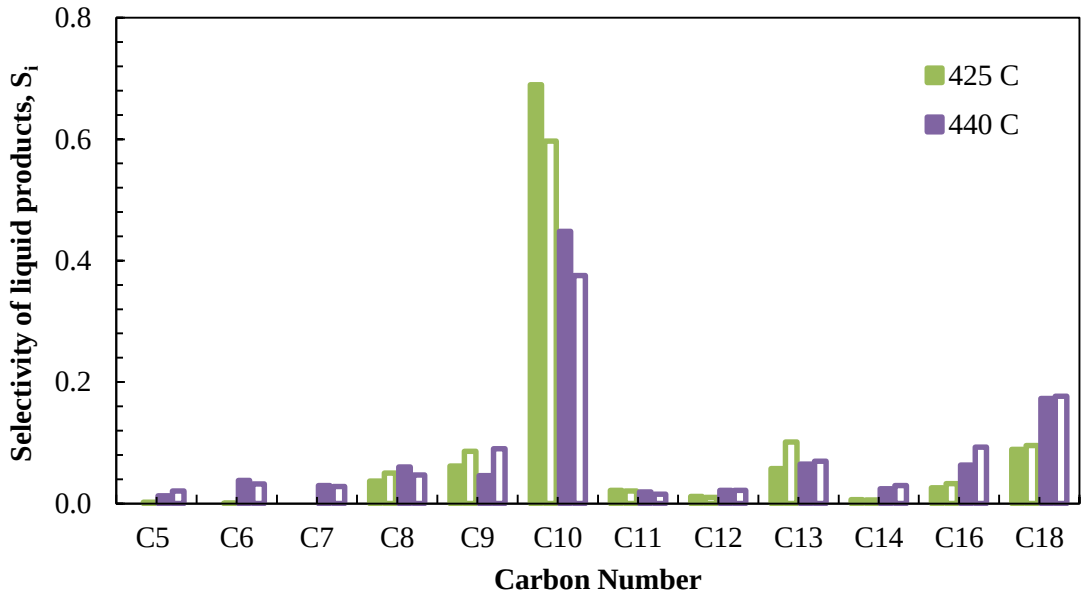

Figure 27. The variation of liquid product selectivities for the non-catalytic thermal degradation of PP at different reaction temperatures & times (Filled: 15 min; Blank: 30 min)

Figures 26 & 27 revealed that the majority of the liquid products was composed of C_{10} hydrocarbons including tert-butyl benzene ($C_{10}H_{14}$), n-decane ($C_{10}H_{22}$), sec-butyl benzene ($C_{10}H_{14}$), 4-isopropyl toluene ($C_{10}H_{14}$), n-butyl benzene ($C_{10}H_{14}$), and naphthalene ($C_{10}H_8$) at both temperatures (425 ºC & 440 ºC). At 425 °C, the fractions of C_8, C_9, C_{13} hydrocarbons increased while the amount of C_{10} decreased when the reaction time increased to 30 min from 15 min. A slight increase in the mole fractions of C_{16} & C_{18} was also observed wtih an increase in the reaction time. With an increase in reaction temperature from 425 °C to 440 °C, the fractions of $C_5 - C_7$ & $C_{14} - C_{18}$ hydrocarbon ranges also increased while the mole fractions and selectivities of C_{10} hydrocarbons decreased. This might be due to conversion of higher molecular weight hydrocarbons to lower molecular weight hydrocarbons.

6.3.1.4. Liquid Analysis of Catalytic Thermal Degradation of Polypropylene

Catalytic thermal decomposition reaction of polypropylene was carried out to observe the effect of the catalyst on product distribution. The experiments were carried out at different reaction temperature & times. The mole fraction and selectivity results of liquid products obtained from the catalytic thermal decomposition reaction of polypropylene are tabulated in Appendix I.

The variation of the mole fractions and selectivities of the liquid products obtained from the catalytic thermal decomposition reaction of polypropylene are given in Figures 28 & 29, respectively.

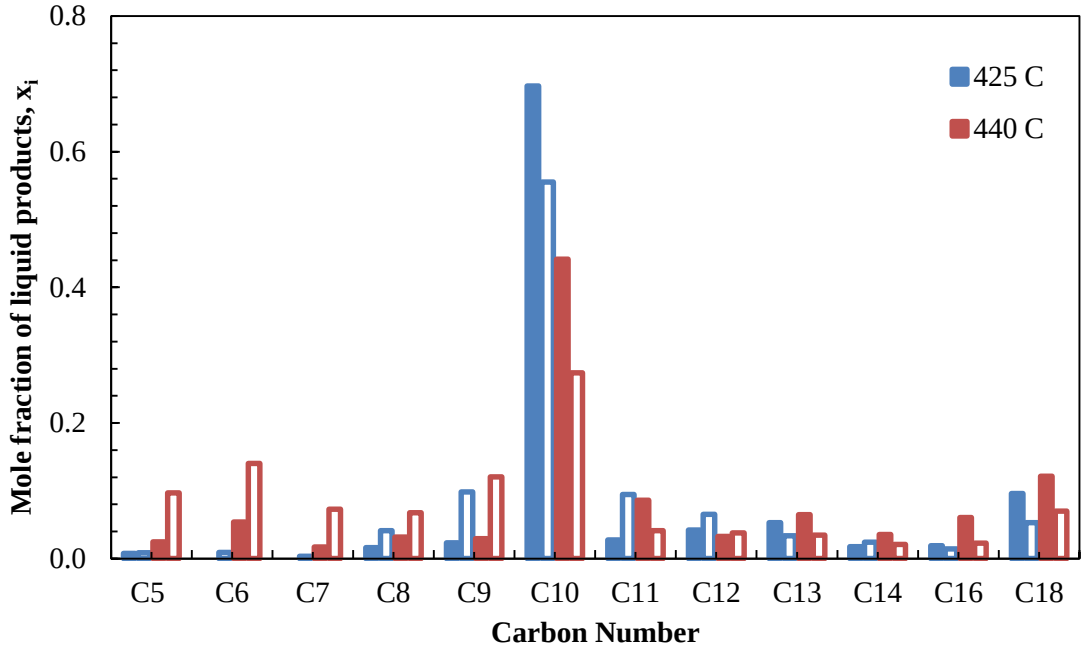

Figure 28. The variation of liquid product mole fractions from the catalytic thermal degradation of PP at different reaction temperatures & times (Filled: 15 min; Blank: 30 min)

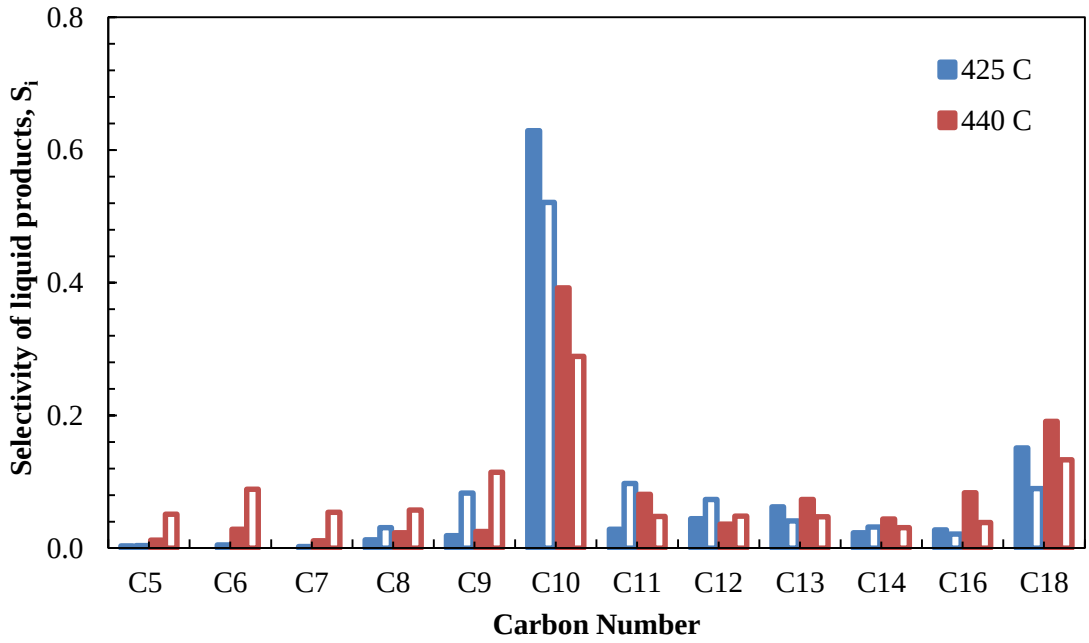

Figure 29. The variation of liquid product selectivities from the catalytic thermal degradation of PP at different reaction temperatures & times (Filled: 15 min; Blank: 30 min)

Figures 28 & 29 revelaed that in the presence of SAPO-34, C_{10} hydrocarbons including tert-butyl benzene ($C_{10}H_{14}$), n-decane ($C_{10}H_{22}$), sec-butyl benzene ($C_{10}H_{14}$), 4-isopropyl toluene ($C_{10}H_{14}$), n-butyl benzene ($C_{10}H_{14}$), and naphthalene ($C_{10}H_8$) had the highest mole fractions and selectivities among other liquid products at both reaction temperatures. With an increase in reaction time from 15 min to 30 min, the formation of C_6, C_7 hydrocarbons in addition to the hydrocarbon range of $C_8 - C_{18}$ was observed at 425 ºC. With an increase in temperature, the fractions of C_5 - C_9 hydrocarbons increased while the amounts of C_{10} & C_{12} hydrocarbons decreased which is might be due to the promoting effect of SAPO-34 at higher temperatures than 425 ºC. In the literature, liquid product distribution at 315 °C was in a carbon range between $C_7 - C_{13}$ in the presence of MCM-type catalyst. But in the presence of SBA-type catalyst, mainly C_7 hydrocarbons were observed [51]. In the other study, the amounts of C_7, C_8 and C_{10} hydrocarbons increased while the amount of heavier hydrocarbons decreased at 380 ºC in the presence of silica-alumina type catalyst [56]. In the catalyic degradation of PP over Na-SCLZ material (clinoptilolite), the liquid products were in a carbon range of $C_8 - C_{11}$ at 400 ºC. In the presence of H-SCLZ (proton form clinoptilolite) material, mainly $C_5 - C_{12}$ hydrocarbons were observed at the same temperature [55]. In the presence of the HMS (Hexagonal mesoporous silica) catalyst at 380 ºC, the liquid products were mainly composed of C_9, C_{11} and C_{14} [58].

The comparison of mole fraction and selectivity values of the liquid products which were obtained from the non-catalytic and catalytic thermal decomposition reactions of polypropylene at different reaction temperatures for 15 min are given in Figures 30 & 31, respectively.

The comparison of mole fractions and selectivity values of the liquid products which were obtained from the non-catalytic and catalytic thermal decomposition reactions of polypropylene at different reaction temperatures for 30 min are given in Figures 32 & 33, respectively.

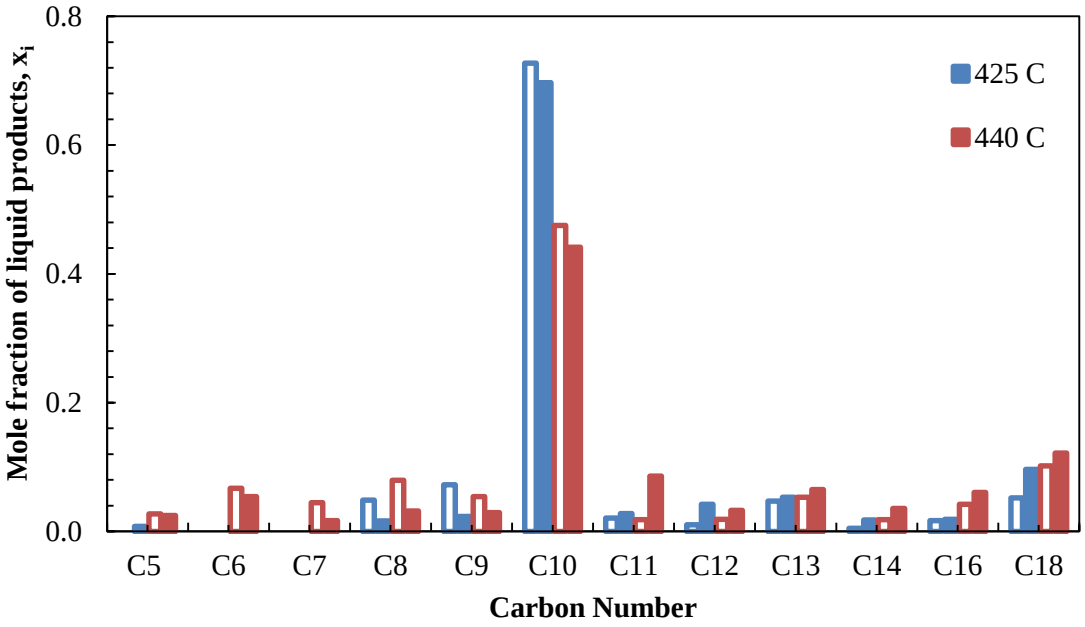

Figure 30. The comparison of liquid product mole fractions from the non-catalytic and catalytic thermal degradation of PP at different reaction temperatures for 15 min reaction time (Blank: Pure PP; Filled: PP + SAPO-34)

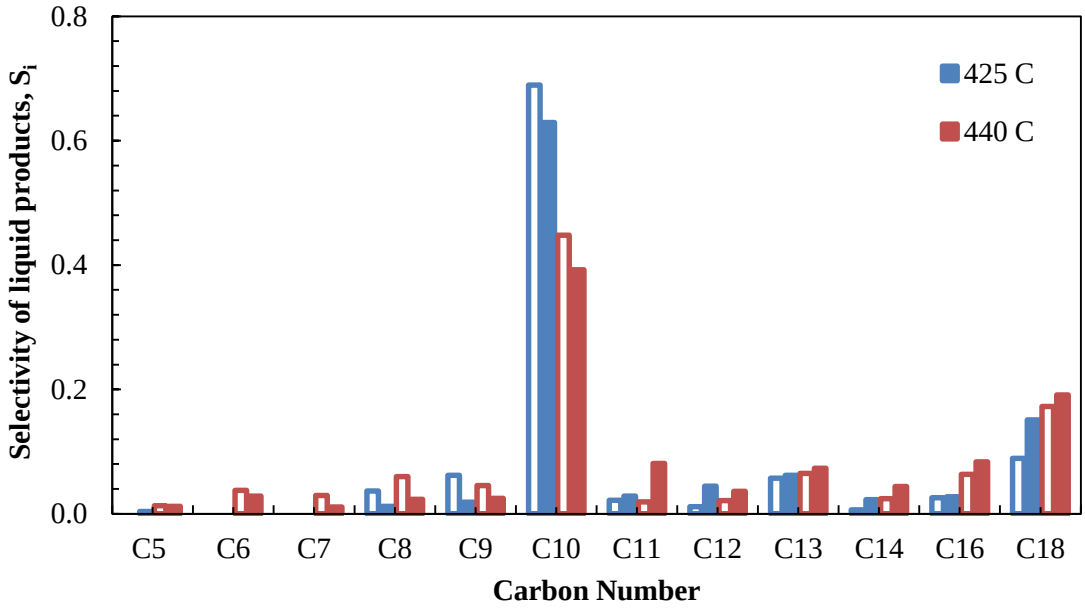

Figure 31. The comparison of liquid product selectivities from the non-catalytic and catalytic thermal degradation of PP at different reaction temperatures for 15 min reaction time (Blank: Pure PP; Filled: PP + SAPO-34)

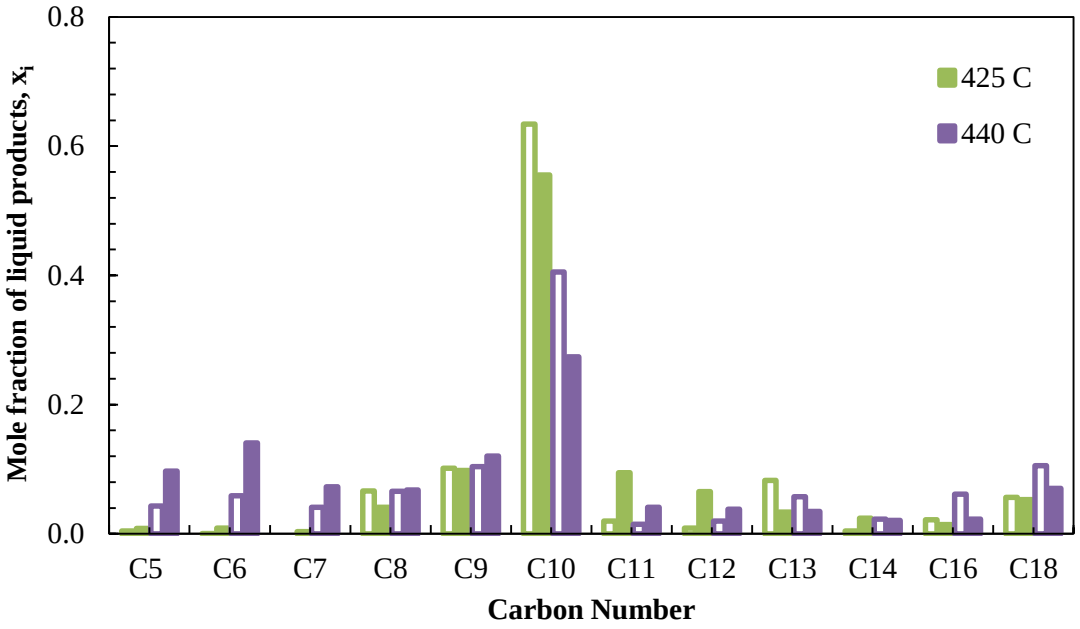

Figure 32. The comparison of liquid product mole fractions from the non-catalytic and catalytic thermal degradation of PP at different reaction temperatures for 30 min reaction time (Blank: Pure PP; Filled: PP + SAPO-34)

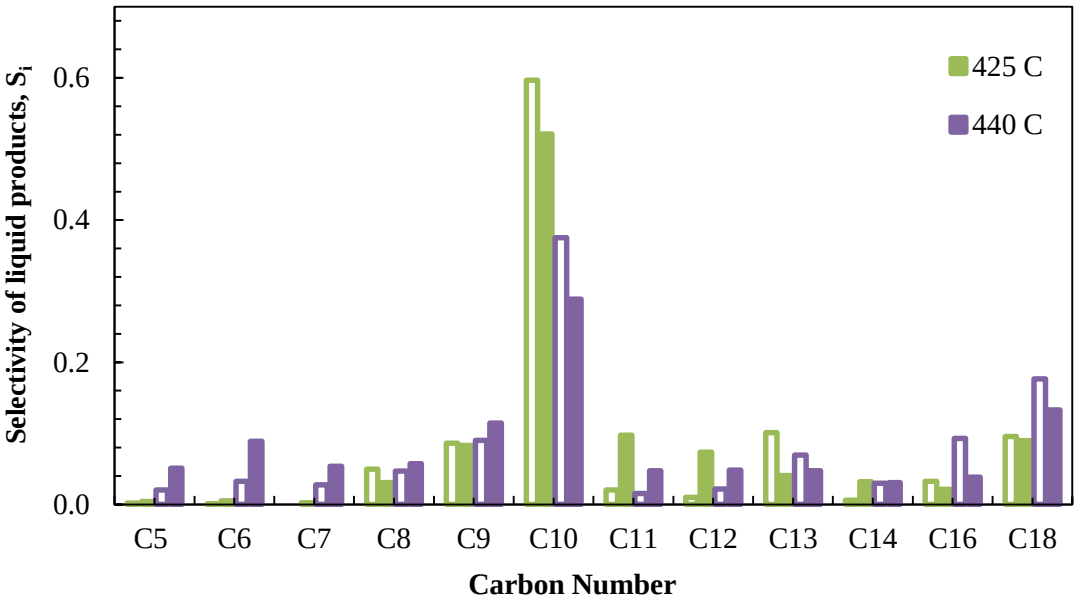

Figure 33. The comparison of liquid product selectivities of obtained from the non-catalytic and catalytic thermal degradation of PP at different reaction temperatures for 30 min reaction time (Blank: Pure PP; Filled: PP + SAPO-34)

Figures 30 - 33 revealed that the majority of the liquid products obtained from the non-catalytic and catalytic thermal degradation reactions of PP was mainly composed of C_{10} hydrocarbons. In the presence of the catalyst, although heavier hydrocarbons degraded to lighter hydrocarbons with an increase in temperature, the amounts of lighter hydrocarbons for 15 min were less than that of lighter hydrocarbons in the absence of the catalyst for 15 min (Figure 30). However, the amounts of lighter hydrocarbons for 30 min were higher than that of lighter ones for 30 min. This might be due to the fact that polymer degraded to lower molecular weight hydrocarbons and these lighter hydrocarbons could easily penetrate into the pore of the catalyst within 30 min.

6.3.2. Results of Polystyrene Degradation Experiments

In order to carry out the non-catalytic thermal degradation reactions, 1 g of polystyrene was placed inside the reactor. For the catalytic thermal degradation reaction, 1 g of polystyrene and 0.5 g of SAPO-34 were loaded to the reactor before each run. The reaction temperature was decided to be 415 °C, for 15 and 30 minutes. The calculation of the amount of gas products was similar to the calculation of gas products which were obtained from the degradation of polypropylene. The product yields in the polystyrene degradation reaction are given in Table 12. The amounts of solid residue, liquid and gas products of the non-catalytic and catalytic experiments are given in Appendix D.

In both the non-catalytic and catalytic thermal degradation experiments, no solid residue was observed while gas and liquid products formed at 415 °C. In the non-catalytic thermal degradation reactions, the amount of liquid products increased with an increase in reaction time. Similarly, when the reaction time increased to 30 min from 15 min, the amount of liquid products increased in the catalytic thermal degradation reaction of polystyrene. However, the amounts of liquid products didn't change due to the presence of the catalyst. These results revealed that SAPO-34 material wasn't effective on the products yield for the degradation reaction of

polystyrene. However, they also indicated that the reaction time was important to product quantity.

In the literature, the liquid product yield of PS degradation reaction was around 80 wt. %, and it increased to 98 wt. % in the presence of AIT100s catalyst (a novel catalyst composed of Al_2O_3 and Pt) at 410 °C [80].

Catalyst deactivation was not observed in the catalytic thermal degradation reaction of PS (Figure D.4 in Appendix D). The color of the catalyst which was used in the catalytic degradation reaction of PS was not changed during the reaction.

Table 12. Product & solid residue yields for the non-catalytic and catalytic thermal degradation reactions of PS at 415 ℃, for different reaction times

Sample	Temperature,°C	Time, min	Yield (wt %)		
			Gas	Liquid	Solid residue
PS	415	15	76	24	0
		30	69	31	0
PS+SAPO-34	415	15	77	23	0
		30	66	34	0

6.3.2.1. Gas Analysis of Polystyrene Non-Catalytic Thermal Degradation

Gas products obtained from the degradation of polystyrene were analyzed qualitatively and quantitively using a GC. The mole & weight fraction and selectivity values of gas products were calculated using gas calibration factors (Appendix E). The mole &

weight fraction and selectivity results of the gas products which were obtained from the non-catalytic thermal decomposition of polypropylene are given in Appendix F.

The mole fractions and selectivities of gas products obtained from the non-catalytic thermal decomposition of polystyrene at 415 °C are given in Figures 34 & 35, respectively.

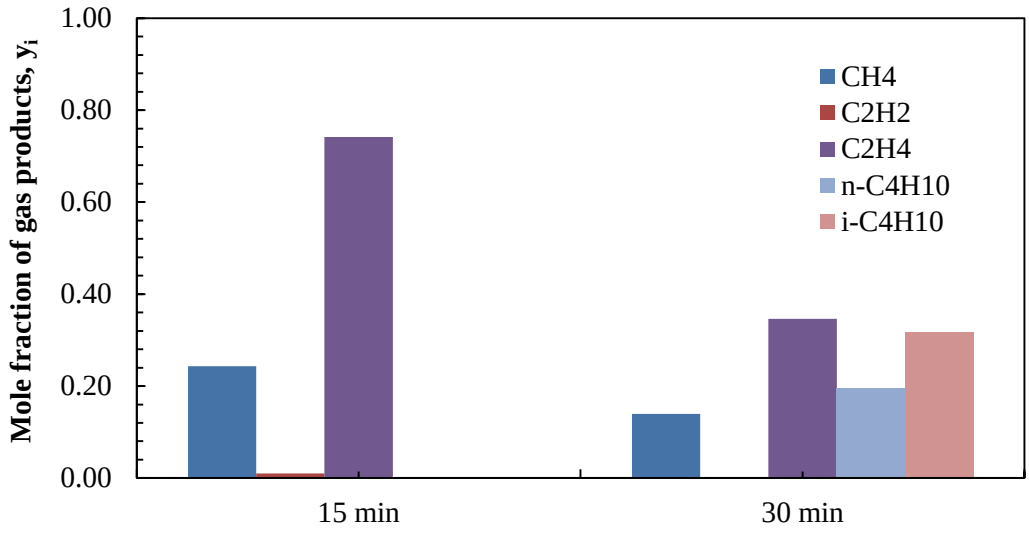

Figure 34. Mole fractions of gas products obtained from the non-catalytic thermal degradation of PS at 415 °C and different reaction times

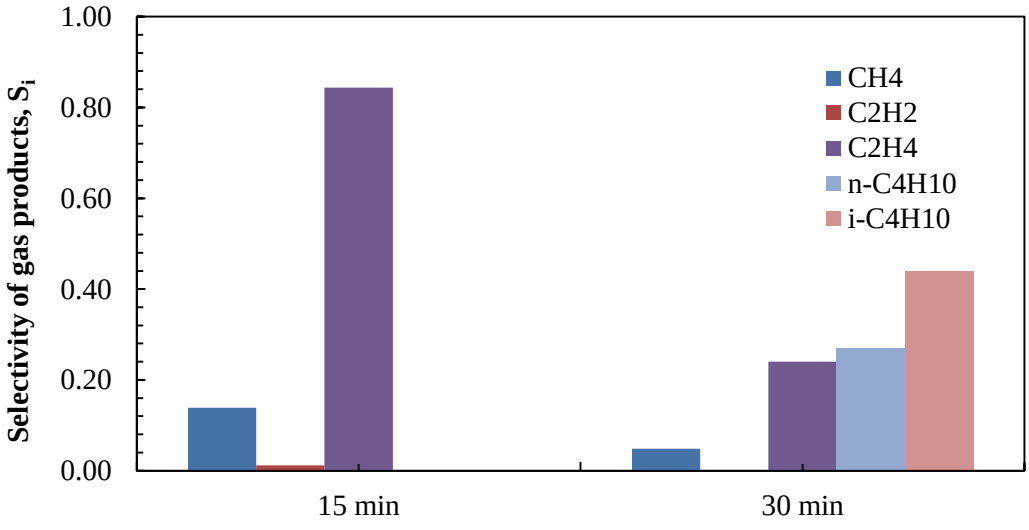

Figure 35. Selectivities of gas products obtained from the non-catalytic thermal degradation of PS at 415 °C and different reaction times

Figures 34 & 35 revealed that the mole fraction and selectivity of ethylene (C_2H_4) were relatively high compared to other products when the reaction time 15 min. With an increase in reaction time, the mole fraction and selectivity of ethylene decreased while butane formation in addition to methane was observed. Acetylene did not form when the reaction time increased to 30 min. In a study, polystyrene was degraded at 400 °C and methane, C_2, C_3, and C_4 hydrocarbons formed [81].

6.3.2.2. Gas Analysis of Catalytic Thermal Degradation of Polystyrene

The gas products obtained from the catalytic thermal degradation of polystyrene were analyzed to show the effect of SAPO-34 on product distribution. The mole fraction and selectivity results of gas products obtained in the presence of SAPO-34 catalyst are given in Appendix G.

The distribution of mole fractions and selectivities of gas products obtained from the catalytic thermal decomposition reaction of polystyrene at 415 °C, different reaction times are given in Figures 36 & 37, respectively.

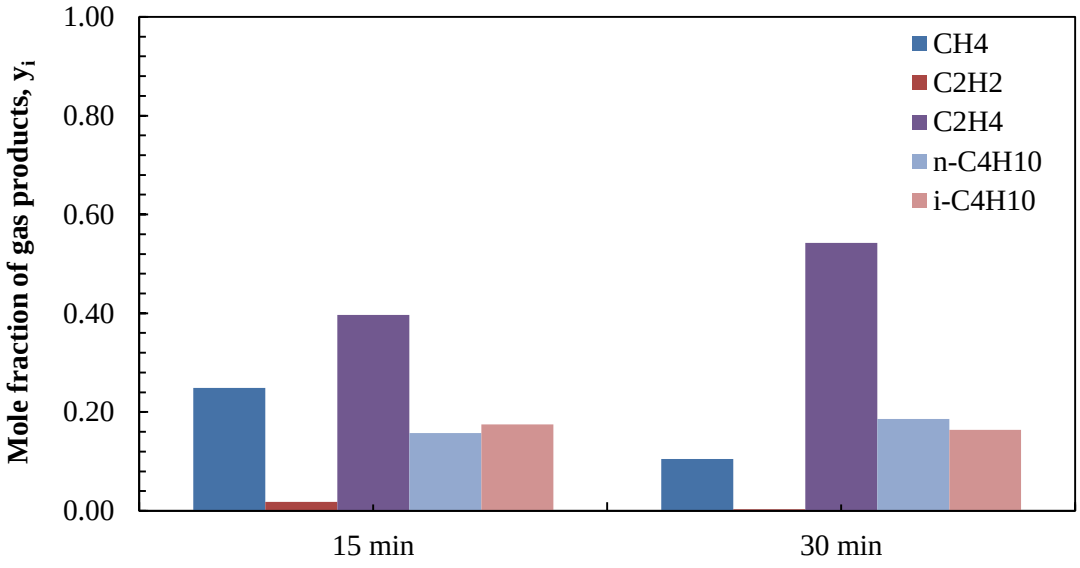

Figure 36. Mole fractions of gas products obtained from the catalytic thermal degradation of PS at 415 °C and different reaction times

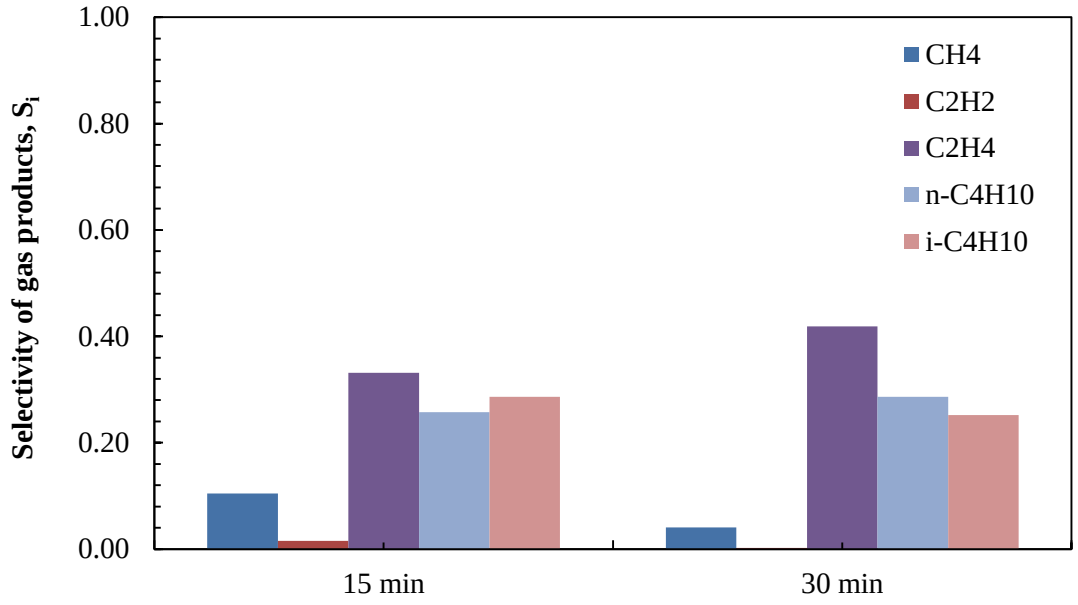

Figure 37. Selectivities of gas products obtained from the catalytic thermal degradation of PS at 415 °C and different reaction times

Figures 36 & 37 revealed that the gas products were composed of ethylene, methane and butane in the catalytic thermal decomposition reaction of polystyrene. When the reaction time increased to 30 min, the mole fraction and selectivity of ethylene increased while the mole fractions and selectivities of n-C_4H_{10} and i-C_4H_{10} remained almost constant. The amounts of methane and acetylene also decreased with an increase in reaction time. In the literature, the fractions of C_2 – C_4 hydrocarbons increased in the presence of commercial silica-alumina catalyst at 360 °C [56].

The comparison of the mole fractions and selectivities of the gas products which were obtained from the non-catalytic and catalytic thermal degradation reactions of polystyrene at 415 °C are given in Figures 38 & 39, respectively.

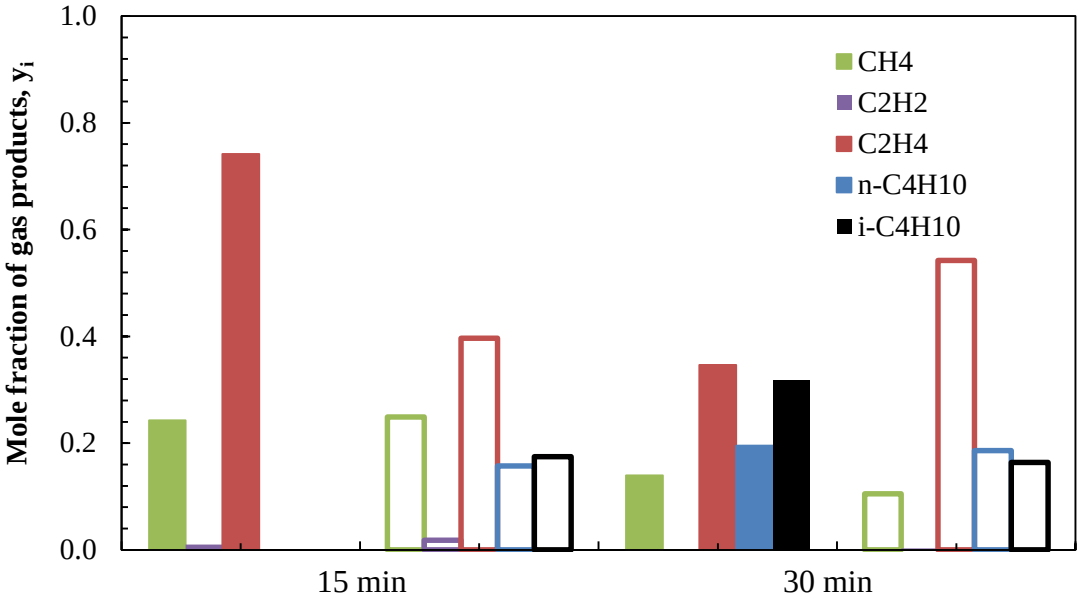

Figure 38. The comparison of mole fractions of gas products obtained from the non-catalytic and catalytic thermal degradation of PS at 415 °C (Filled: Pure PS; Blank: PS+SAPO-34)

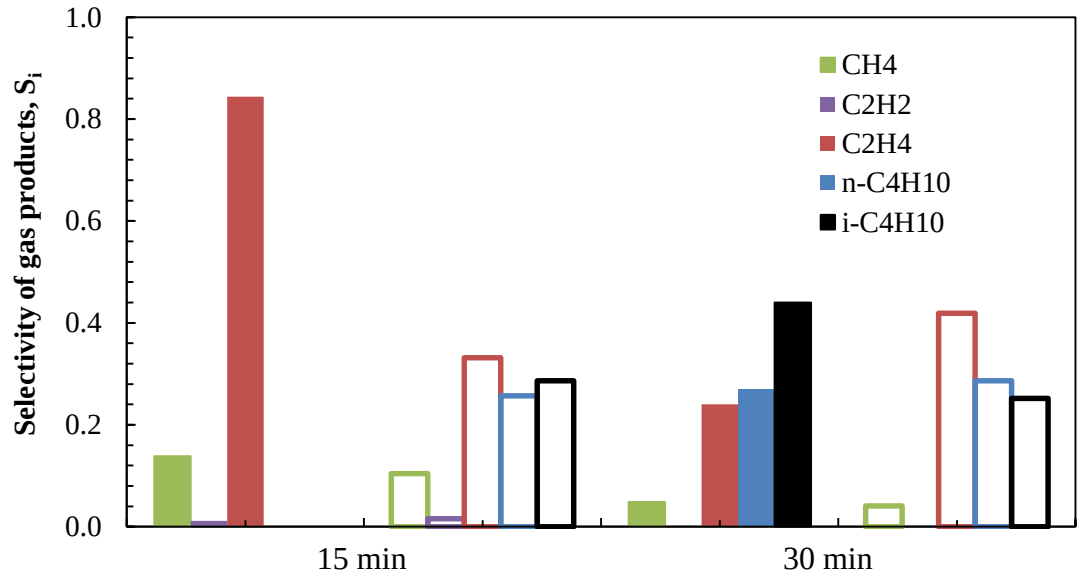

Figure 39. The comparison of selectivities of gas products obtained from the non-catalytic and catalytic thermal degradation of PS at 415 °C (Filled: Pure PS; Blank: PS+SAPO-34)

Figures 38 & 39 revealed that the formation of propene and propane wasn't observed in both the non-catalytic and catalytic thermal degradation of polystyrene. This was an expected result since polystyrene didn't comprise the propene structure. The fractions of methane and ethylene decreased while the amounts of n-butane and i-butane increased in the presence of SAPO-34 catalyst for 15 min reaction time. It was an expected result since the polymer degraded into lighter hydrocarbons in the presence of the catalyst. It was also observed from the figures that acetylene formed at lower reaction time. The fraction of acetylene also increased slightly when SAPO-34 was used. However, when the reaction time increased to 30 min, acetylene formation was not observed. This change might be due to acetylene conversion into other gaseous products. Consequently, SAPO-34 material was highly selective to ethylene and butane in degradation reactions of polystyrene compared to pure PS.

6.3.2.3. Liquid Analysis of Polystyrene Non-Catalytic Thermal Degradation

Liquid products were analyzed using GC. The calculated mole fraction & selectivity values of liquid products obtained from the thermal decomposition reaction of polystyrene are given in Appendix I.

The mole fraction and selectivity values of liquid products obtained from the thermal decomposition reaction of polystyrene at 415 °C for different reaction times are given in Figures 40 & 41, respectively.

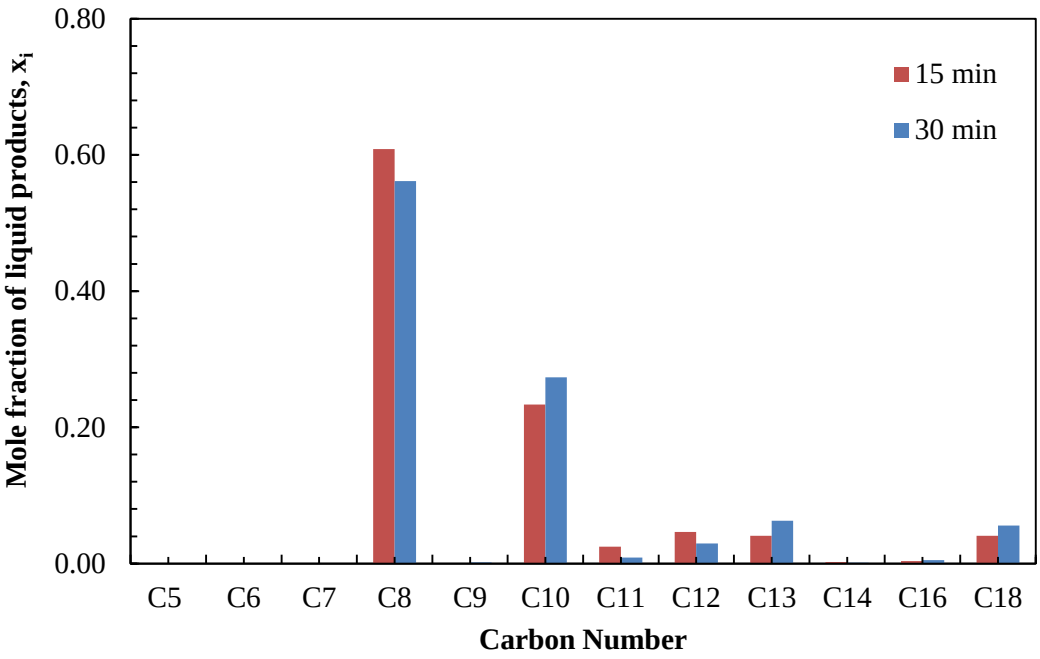

Figure 40. The variation of liquid product mole fractions from the non-catalytic thermal degradation of PS at 415 °C

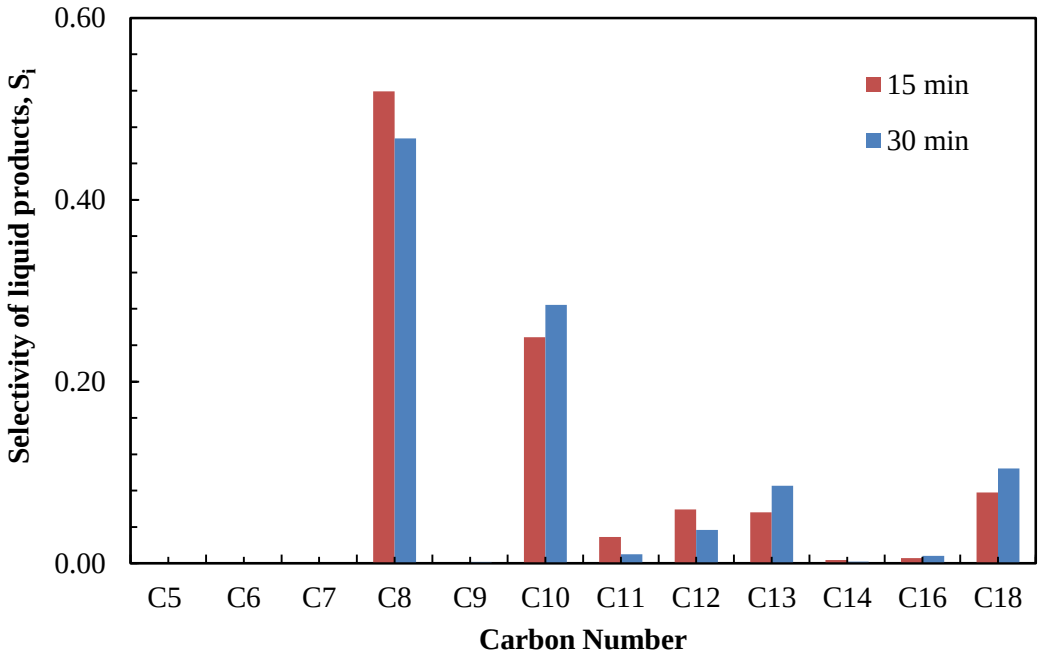

Figure 41. The variation of liquid product selectivities from the non-catalytic thermal degradation of PS at 415 °C

It was observed from Figures 40 & 41 that the majority of the liquid products were composed of C_8 hydrocarbons involving octane, ethylbenzene, m,p,o-xylene and styrene which was an expected result since polystyrene contains styrene monomers. Hydrocarbon groups of C_{10} - C_{18} were also observed. With an increase in reaction time from 15 min to 30 min, the fractions of $C_{10,}$ C_{13} and C_{18} hdyrocarbons increased while the amounts of C_8, C_{11} and C_{12} hydrocarbons decreased. In the literature, PS was degraded thermally at 360 °C and the liquid products obtained were mainly composed of C_9 and C_{17} hydrocarbons [56].

6.3.2.4. Liquid Analysis of Catalytic Thermal Degradation of Polystyrene

The catalytic thermal degradation reaction of polystyrene over SAPO-34 was carried out at 415 °C, different reaction times. The mole fraction and selectivity values of liquid products obtained from catalytic thermal degradation of polystyrene are tabulated in Appendix I.

The mole fraction & selectivity values of liquid products obtained from the catalytic thermal degradation of polystyrene at 415 °C for different reaction times are given in Figures 42 & 43, respectively.

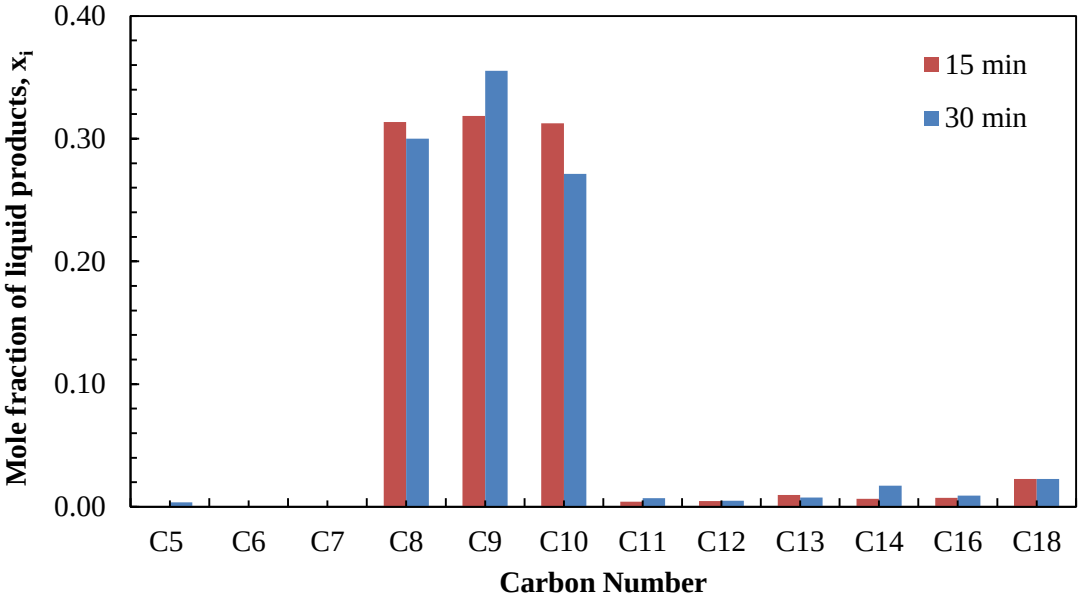

Figure 42. The variation of liquid product mole fractions from the catalytic thermal degradation of PS at 415 °C and different reaction times

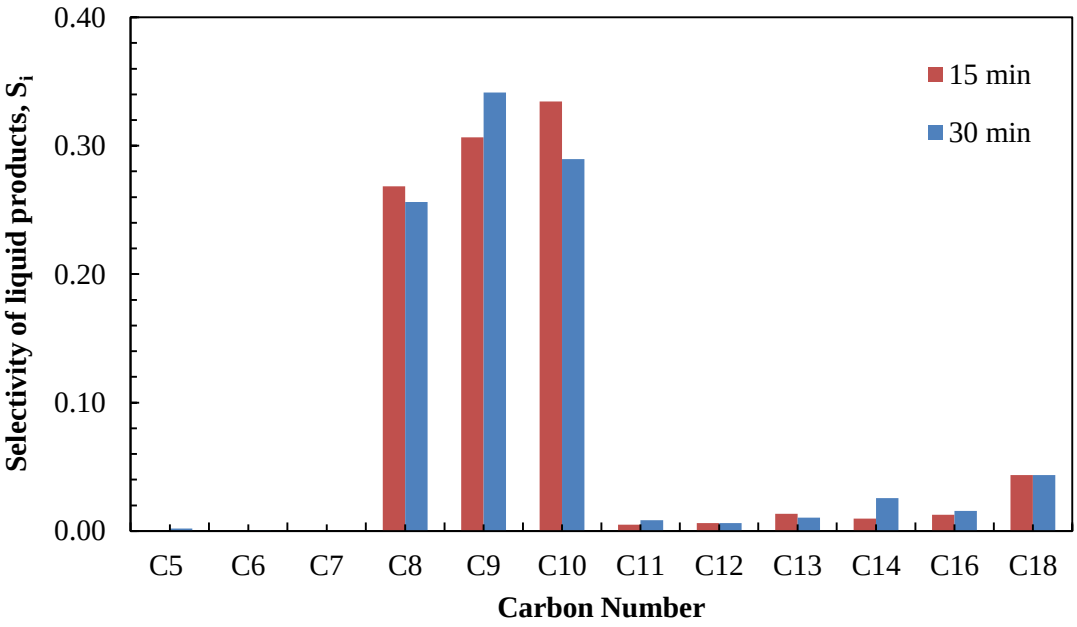

Figure 43. The variation of liquid product selectivities from the catalytic thermal degradation of PS at 415 °C and different reaction times

In the presence of SAPO-34, high selectivity to C_8, C_9, and C_{10} was observed. The majority of the liquid products were octane, ethylbenzene, m,p,o-xylene, styrene,

isopropyl benzene, n-nonane, n-propyl benzene, trimethylbenzene, tert-butyl benzene, n-decane, sec-butyl benzene, 4-isopropyl toluene, n-butyl benzene, and naphthalene. Due to conversion of heavier hydrocarbons to lighter hydrocarbons, hydrocarbons in the carbon number range of C_8 – C_{18} were formed. In a study of the catalytic degradation of PS over HNZ (natural clinoptilolite zeolite), HZSM-5 (hydrogen-type zeolite socony mobil-5), and SA (silica-alumina) at 400 ºC for 2 h, the main liquid products were in a carbon number range of C_7 – C_9. Styrene, ethylbenzene, toluene had the highest amounts [12]. However, in the presence of SAPO-34, the liquid products were mainly composed of C_8 – C_{10} hydrocarbon groups.

SAPO-34 was a proper catalyst for the conversion of polystyrene to lighter hydrocarbons which were C_8 – C_{10}. Value added chemicals could be recovered from the polystyrene waste under suitable conditions.

CHAPTER 7

CONCLUSIONS AND RECOMMENDATIONS

In this study, SAPO-34 material was synthesized hydrothermally to be used in the degradation reactions of polypropylene and polystyrene. The material was characterized using several techniques to understand the structural, physical and chemical properties.

The SAPO-34 catalyst was synthesized succesfully. The characteristic peaks of SAPO-34 were observed in the XRD pattern. SEM images revealed the cubic structure of the material. The average particle size of the material was 2.5 x 2.5 μm. Nitrogen adsorption analysis revealed that the synthesized material exhibited *Type 1* isotherm, which is the characteristic of microporous material. The surface area of SAPO-34 material was 308.5 m^2/g. Its average pore diameter was 1.35 nm. NMR spectra exhibited octahedrally and tetrahedrally coordinated aluminum atoms and tetrahedrally coordinated silicon atoms in the structure. The existence of Bronsted and Lewis acid sites in the synthesized catalyst was determined by DRIFTS analysis.

Thermogravimetric analysis showed that SAPO-34 decreased the degradation temperature and activation energy of polypropylene degradation reaction from 172 kJ/mol to 131±11 kJ/mol. The material also decreased the activation energy of polystyrene degradation reaction from 357±4 kJ/mol to 262±4 kJ/mol while it did not cause a significant change in the degradation temperature.

The non-catalytic and catalytic thermal decomposition reactions of polypropylene and polystyrene took place in the degradation reaction system and products were obtained at the end of the reactions for polypropylene. Solid residue and no liquid were observed at lower reaction temperatures. However, when the temperature increased, liquid formation was observed while the solid residue wasn't observed. In the degradation

reactions of polystyrene, no solid residue formed while liquid products were observed. In both reactions of PP & PS, gaseous products formed at all reaction temperature values. In the degradation of PP at 315 °C and 400 °C, the yield of the gaseous products increased due to the presence of SAPO-34. In the degradation reactions of PS, the presence of SAPO-34 didn't change the product yields.

The analysis of gaseous products revealed that the selectivities of C_2 and C_3 hydrocarbons were very high in the degradation reactions of polypropylene. At 315 °C, a little propene formed due to the presence of SAPO-34. The presence of SAPO-34 also promoted the formation of methane, propane and butane in addition to ethane, ethylene and propene at 400 °C for 15 min reaction time. With an increase in reaction time, acetylene formation was also observed in addition to methane, propane, butane, ethane, ethylene and propene in the presence of the catalyst. At 425 °C, the amounts of the gas products didn't change significantly. Similarly, they were almost same at 440 °C for 15 min reaction time. However, for 30 min reaction time, the amount of acetylene decreased significantly while the fraction of propene doubled.

In the non-catalytic and catalytic thermal decomposition reactions of polypropylene, liquid products were observed at 425 °C and 440 °C. At both reaction temperatures, the majority of the liquid products was composed of C_{10}. At 425 °C, the presence of SAPO-34 promoted the formation of C_5 in addition to $C_8 - C_{18}$ hydrocarbons for 15 min reaction time. In the presence of SAPO-34 catalyst, heavier hydrocarbons degraded to lighter hydrocarbons with an increase in temperature and the amounts of lighter hydrocarbons were higher than that of lighter hydrocarbons in the absence of catalyst for 30 min. However, the amounts of lighter hydrocarbons in the absence of catalyst was high compared to the catalytic degradation reaction at low reaction time.

In the thermal decomposition of polystyrene, the amount of ethylene was the highest at 415 °C for both reaction times. Butane formation was observed in addition to methane, acetylene, and ethylene in the presence of SAPO-34 for 15 min reaction time while it didn't form in the absence of the catalyst. Propene and propane did not form in the both the non-catalytic and catalytic degradation of PS.

In the non-catalytic thermal degradation of PS, the majority of the liquid products were composed of C_8 hydrocarbons. Also the products contained the hydrocarbon groups of C_{10}, C_{11}, C_{12}, C_{13} and C_{18}. When SAPO-34 was used, the mole fractions and selectivities of C_8, C_{12} and C_{13} hydrocarbons decreased while the mole fractions and selectivities of $C_9 - C_{10}$ and C_{14} & C_{16} increased. In another saying, a remarkable increase in the mole fraction and selectivity of C_9 hydrocarbons was observed due to the presence of SAPO-34. In the presence of SAPO-34, value added chemicals could be recovered from PS waste under suitable conditions.

According to the results, SAPO-34 material enhanced the production of gaseous hydrocarbons most for both PP & PS degradation reactions.

In the future studies, TPA or aluminum can be impregnated to the catalyst to enhance the effect of catalyst on the product distribution. Moreover, mesoporous SAPO-34 could be used in the degradation reactions to provide better permeability through the pores. Additionally, the degradation reaction of PS can be carried out at different reaction temperatures and times to observe the effect of the temperature & time on product distribution.

REFERENCES

[1] M. Biron, *Thermoplastics and Thermoplastic Composites: Technical Information for Plastics Users*. Burlington: Elsevier Ltd, 2007.

[2] S. Hulse, *Plastics Product Recycling*. Shropshire, UK: Rapra Technology Limited, 2000.

[3] J. Aguado and D. P. Serrano, *Feedstock Recycling of Plastic Wastes*. Cambridge, UK: MPG Books Ltd., 1999.

[4] J. Scheirs and W. Kaminsky, *Feedstock Recycling and Pyrolysis of Waste Plastics: Converting Waste Plastics Into Diesel and Other Fuels*. J. Wiley & Sons, 2006.

[5] D. Garcia, R. A., Serrano, D. P., Otero, "Catalytic cracking of HDPE over hybrid zeolitic-mesoporous materials," *J. Anal. Appl. Pyrol.*, vol. 74, pp. 379–386, 2005.

[6] J. D. Peterson, S. Vyazovkin, and C. a. Wight, "Kinetics of the Thermal and Thermo-Oxidative Degradation of Polystyrene, Polyethylene and Poly(propylene)," *Macromol. Chem. Phys.*, vol. 202, no. 6, pp. 775–784, Mar. 2001.

[7] Z. Nawaz, X. Tang, and F. Wei, "Hexene catalytic cracking over 30 % SAPO-34 catalyst for propylene maximization : Influence of reaction conditions and reaction pathway exploration," vol. 26, no. 04, pp. 705–712, 2009.

[8] S. Al O, J. Aguado, J. L. Sotelo, D. P. Serrano, J. A. Calles, and J. M. Escola, "Catalytic Conversion of Polyolefins into Liquid Fuels over MCM-41 : Comparison with ZSM-5 and Amorphous," vol. 3, no. 13, pp. 1225–1231, 1997.

[9] J. Aguado, D. P. Serrano, G. S. Miguel, J. M. Escola, and J. M. Rodríguez, "Catalytic activity of zeolitic and mesostructured catalysts in the cracking of pure and waste polyolefins," *J. Anal. Appl. Pyrolysis*, vol. 78, no. 1, pp. 153–161, Jan. 2007.

[10] G. Manos, A. Garforth, and J. Dwyer, "Catalytic Degradation of High-Density Polyethylene over Different Zeolitic Structures," *Ind. Eng. Chem. Res.*, vol. 39, pp. 1198 – 1202, 2000.

[11] J. H. Park, H. S. Heo, Y.-K. Park, K.-E. Jeong, H.-J. Chae, J. M. Sohn, J.-K. Jeon, and S.-S. Kim, "Catalytic degradation of high-density polyethylene over SAPO-34 synthesized with various templates," *Korean J. Chem. Eng.*, vol. 27, no. 6, pp. 1768–1772, Aug. 2010.

[12] S. Y. Lee, J. H. Yoon, J. R. Kim, and D. W. Park, "Catalytic degradation of polystyrene over natural clinoptilolite zeolite," *Polym. Degrad. Stab.*, vol. 74, no. 2, pp. 297–305, Jan. 2001.

[13] P. J. Flory, *Principles of Polymer Chemistry*. New York, USA: Cornell University Press., 1995.

[14] L. Sawyer, D. Grubb, and G. F. Meyers, *Polymer Microscopy*. New York, USA: Springer Science and Business Media, 2008.

[15] C. Maier and T. Calafut, *Polypropylene: The Definitive User's Guide and Databook*. New York, USA: William Andrew Inc., 1998.

[16] H. Karian, *Handbook of Polypropylene and Polypropylene Composites, Revised and Expanded*. Basel, Switzerland: Marcel Dekker Inc., 2009.

[17] http://en.wikipedia.org/wiki/Polypropylene (last accessed on September 2nd, 2014)

[18] V. R. Gowariker, N. V. Viswanathan, and J. Sreedhar, *Polymer Science*. New Delhi, India: Nisha Enterprises, 2005.

[19] J. R. Wünsch, *Polystyrene: Synthesis, Production and Applications*. Shropshire, UK: Rapra Technology Limited, 2000.

[20] E. Lokensgard, *Industrial Plastics: Theory and Applications*. New York, USA: Delmar, 2010.

[21] H. R. Kricheldorf, O. Nuyken, and G. Swift, *Handbook of Polymer Synthesis: Second Edition*. New York, USA: Marcel Dekker Inc., 2005.

[22] http://en.wikipedia.org/wiki/Polystyrene (last accessed on September 2nd, 2014)

[23] D. B. Malpass, *Introduction to Industrial Polyethylene: Properties, Catalysts, and Processes*. New Jersey, USA: John Wiley & Sons, 2010.

[24] A. Peacock, *Handbook of Polyethylene: Structures: Properties, and Applications*. Basel, Switzerland: Marcel Dekker Inc., 2000.

[25] C. Vasile and M. Pascu, *Practical Guide to Polyethylene*. Shropshire, UK: Rapra Technology Limited, 2005.

[26] J. Leadbitter, J. A. Day, and J. L. Ryan, *PVC: Compounds, Processing and Applications*. Shropshire, UK: Rapra Technology Limited, 1994.

[27] S. Patrick, *Practical Guide to Polyvinyl Chloride*. Shropshire, UK: Rapra Technology Limited, 2005.

[28] http://en.wikipedia.org/wiki/Polyvinyl_chloride (last accessed on September 2nd, 2014)

[29] http://parasailin.blogspot.com.tr (last accessed on September 2nd, 2014)

[30] O. Olabisi and K. Adewale, *Handbook of Thermoplastics*. New York, USA: Marcel Dekker Inc., 1997.

[31] http://en.wikipedia.org/wiki/Polyethylene_terephthalate (last accessed on September 2nd, 2014)

[32] M. R. Jan, J. Shah, and H. Gulab, "Catalytic degradation of waste high-density polyethylene into fuel products using BaCO3 as a catalyst," *Fuel Process. Technol.*, vol. 91, no. 11, pp. 1428–1437, Nov. 2010.

[33] A. A. Garforth, S. Ali, J. Hernández-Martínez, and A. Akah, "Feedstock recycling of polymer wastes," *Curr. Opin. Solid State Mater. Sci.*, vol. 8, no. 6, pp. 419–425, Dec. 2004.

[34] I. C. Neves, G. Botelho, A. V. Machado, and P. Rebelo, "The effect of acidity behaviour of Y zeolites on the catalytic degradation of polyethylene," *Eur. Polym. J.*, vol. 42, no. 7, pp. 1541–1547, Jul. 2006.

[35] J. Halász, Z. Kónya, Z. T. Faragó, and K. Siegert, "Degradation of pure and waste polyolefins and PVC in the presence of modified porous catalysts," *Stud. Surf. Sci. Catal.*, vol. 174, pp. 1021–1026, 2008.

[36] R. Singhal, C. Singhal, and S. Upadhyayula, "Thermal-catalytic degradation of polyethylene over silicoaluminophosphate molecular sieves—A thermogravimetric study," *J. Anal. Appl. Pyrolysis*, vol. 89, no. 2, pp. 313–317, Nov. 2010.

[37] K. Pielichowski and J. Njuguna, *Thermal Degradation of Polymeric Materials*. Shropshire, UK: Rapra Technology Limited, 2005.

[38] N. S. Akpanudoh, K. Gobin, and G. Manos, "Catalytic degradation of plastic waste to liquid fuel over commercial cracking catalysts," *J. Mol. Catal. A Chem.*, vol. 235, no. 1–2, pp. 67–73, Jul. 2005.

[39] D. W. Park, E. Y. Hwang, J. R. Kim, J. K. Choi, Y. A. Kim, and H. C. Woo, "Catalytic degradation of polyethylene over solid acid catalysts," *Polym. Degrad. Stab.*, vol. 65, pp. 193–198, 1999.

[40] D. Pant, "A new role of alumina in polyethylene degradation: A step towards commercial polyethylene recycling," *J. Sci. Ind. Res.*, vol. 64, pp. 967–972, 2005.

[41] D. Wang, P. Tian, M. Yang, S. Xu, D. Fan, X. Su, Y. Yang, C. Wang, and Z. Liu, "Synthesis of SAPO-34 with alkanolamines as novel templates and their application for CO2 separation," *Microporous Mesoporous Mater.*, vol. 194, pp. 8–14, Aug. 2014.

[42] G. Liu, P. Tian, J. Li, D. Zhang, F. Zhou, and Z. Liu, "Synthesis, characterization and catalytic properties of SAPO-34 synthesized using diethylamine as a template," *Microporous Mesoporous Mater.*, vol. 111, no. 1–3, pp. 143–149, Apr. 2008.

[43] E. M. Flanigen, J. C. Jansen, and H. van Bekkum, "Synthesis of AlPO4 – based molecular sieves," in *Introduction to Zeolite Science and Practice*, Amsterdam, Netherlands: Elsevier B.V., 1991.

[44] S. Kulprathipanja, *Zeolites in Industrial Separation and Catalysis*. Weinheim, Germany: Wiley-VCH, 2010.

[45] A. Nakatsuka, H. Okada, K. Fujiwara, N. Nakayama, and T. Mizota, "Crystallographic configurations of water molecules and exchangeable cations in a hydrated natural CHA-zeolite (chabazite)," *Microporous Mesoporous Mater.*, vol. 102, no. 1–3, pp. 188–195, May 2007.

[46] N. Najafi, S. Askari, and R. Halladj, "Hydrothermal synthesis of nanosized SAPO-34 molecular sieves by different combinations of multi templates," *Powder Technol.*, vol. 254, pp. 324–330, Mar. 2014.

[47] A. K. Singh, R. Yadav, and A. Sakthivel, “Synthesis, characterization, and catalytic application of mesoporous SAPO-34 (MESO-SAPO-34) molecular sieves,” *Microporous Mesoporous Mater.*, vol. 181, pp. 166–174, Nov. 2013.

[48] P. Wang, D. Yang, J. Hu, J. Xu, and G. Lu, “Synthesis of SAPO-34 with small and tunable crystallite size by two-step hydrothermal crystallization and its catalytic performance for MTO reaction,” *Catal. Today*, vol. 212, pp. 62.e1–62.e8, Sep. 2013.

[49] J.-Y. Kim, J. Kim, S.-T. Yang, and W.-S. Ahn, “Mesoporous SAPO-34 with amine-grafting for CO2 capture,” *Fuel*, vol. 108, pp. 515–520, Jun. 2013.

[50] H. Demir, “Dimethyl Ether (DME) Synthesis Using Mesoporous SAPO-34 Like Catalytic Materials,” Middle East Technical University, 2011.

[51] Z. Obalı, N. A. Sezgi, and T. Doğu, “Catalytic degradation of polypropylene over alumina loaded mesoporous catalysts,” *Chem. Eng. J.*, vol. 207–208, pp. 421–425, Oct. 2012.

[52] Z. Obalı, N. A. Sezgi, and T. Doğu, “The synthesis and characterization of aluminum loaded SBA-type materials as catalyst for polypropylene degradation reaction,” *Chem. Eng. J.*, vol. 176–177, pp. 202–210, Dec. 2011.

[53] Z. Obali, N. A. Sezgi, and T. Doğu, “Performance of Acidic Mcm-Like Aluminosilicate Catalysts in Pyrolysis of Polypropylene,” *Chem. Eng. Commun.*, vol. 196, no. 1–2, pp. 116–130, Oct. 2008.

[54] B. Aydemir, N. A. Sezgi, and T. Doğu, “Synthesis of TPA Impregnated SBA-15 Catalysts and Their Performance in Polyethylene Degradation Reaction,” *AIChE J.*, vol. 58, no. 8, pp. 2466–2472, 2012.

[55] J. . Kim, Y. . Kim, J. . Yoon, D. . Park, and H. . Woo, “Catalytic degradation of polypropylene: effect of dealumination of clinoptilolite catalyst,” *Polym. Degrad. Stab.*, vol. 75, no. 2, pp. 287–294, Jan. 2002.

[56] K. Murata, M. Brebu, and Y. Sakata, “The effect of silica–alumina catalysts on degradation of polyolefins by a continuous flow reactor,” *J. Anal. Appl. Pyrolysis*, vol. 89, no. 1, pp. 30–38, Sep. 2010.

[57] S.-J. Chiu and Y.-S. Wu, “A comparative study on thermal and catalytic degradation of polybutylene terephthalate,” *J. Anal. Appl. Pyrolysis*, vol. 86, no. 1, pp. 22–27, Sep. 2009.

[58] S. Chaianansutcharit, R. Katsutath, A. Chaisuwan, T. Bhaskar, A. Nigo, A. Muto, and Y. Sakata, "Catalytic degradation of polyolefins over hexagonal mesoporous silica: Effect of aluminum addition," *J. Anal. Appl. Pyrolysis*, vol. 80, no. 2, pp. 360–368, Oct. 2007.

[59] C. Hammond, *The Basics of Crystallography and Diffraction*. Oxford, UK: Oxford University Press, 2009.

[60] A. R. West, *Solid State Chemistry and Its Applications*. Oxford, UK: John Wiley & Sons, 1990.

[61] A. Khursheed, *Scanning Electron Microscope Optics and Spectrometers*. London, UK: World Scientific Publishing Co. Pte. Ltd., 2011.

[62] C. E. Lyman, *Scanning Electron Microscopy, X-Ray Microanalysis, and Analytical Electron Microscopy*. New York, USA: Plenum Publishing Co., 1990.

[63] Z. Obalı, "Synthesis of Aluminum Incorporated Mesoporous Catalysts for Pyrolysis of Polypropylene," Middle East Technical University, 2010.

[64] A. M. Prakash and S. Unnikrishnan, "Synthesis of SAPO-34 High Silicon lncorporation in the Presence of Morpholine as Template," *J. CHem. Soc. Faraday Trans.*, vol. 90, no. 15, pp. 2291–2296, 1994.

[65] E. M. Lok, B.M., Messina, C.A., Patton, R.L., Gajek, R.T., Cannan, T.R., Flanigen, "Crystalline Silicoaluminophosphates," US Patent 4,440,871, 1984.

[66] International Centre for Diffraction Data, "Selected Powder Diffraction Data for Education & Training : Search Manual and Data Cards," *Data, International Centre for Diffraction*. PA, The Centre – Swartmore, 1988.

[67] J. Rouquerol, F. Rouquerol, and K. S. W. Sing, *Adsorption by Powders and Porous Solids: Principles, Methodology and Applications*. London, UK: Academic Press, 1999.

[68] Z. M. Yan, J. Q. Zhuang, L. Xu, X. W. Han, and Z. M. Liu, "Direct Observation of Various Al Sites in SAPO-34 by 27 Al Multiquantum (MQ) Magic Angle Spinning (MAS) NMR," vol. 14, no. 1, pp. 87–90, 2003.

[69] A. Buchholz, W. Wang, A. Arnold, M. Xu, and M. Hunger, “Successive steps of hydration and dehydration of silicoaluminophosphates H-SAPO-34 and H-SAPO-37 investigated by in situ CF MAS NMR spectroscopy,” *Microporous Mesoporous Mater.*, vol. 57, no. 2, pp. 157–168, Jan. 2003.

[70] J. Tan, Z. Liu, X. Bao, X. Liu, X. Han, C. He, and R. Zhai, “Crystallization and Si incorporation mechanisms of SAPO-34,” *Microporous Mesoporous Mater.*, vol. 53, no. 1–3, pp. 97–108, Jun. 2002.

[71] G. Liu, P. Tian, and Z. Liu, “Synthesis of SAPO-34 Molecular Sieves Templated with Diethylamine and Their Properties Compared with Other Templates,” *Chinese J. Catal.*, vol. 33, no. 1, pp. 174–182, Jan. 2012.

[72] G. F. Froment, “Effects of Particle Size and Modified SAPO-34 on Conversion of Methanol to Light Olefins and Dimethyl Ether Michael G . Abraha , Xianchun Wu , and Rayford G . Anthony Kinetics , Catalysis and Reaction Engineering Laboratory Department of Chemical Engineer,” pp. 211–218, 2001.

[73] L. Wang, J. R. Gaudet, W. Li, and D. Weng, “Migration of Cu species in Cu/SAPO-34 during hydrothermal aging,” *J. Catal.*, vol. 306, pp. 68–77, Oct. 2013.

[74] B. Aydemir, “Synthesis of Mesoporous Catalysts and Their Performance in Pyrolysis of Polyethylene,” Middle East Technical University, 2010.

[75] C. S. Jou, “Obtaining the Kinetic Parameters from Thermogravimetry Using a Modified Coats and Redfern Technique,” no. 1971, pp. 1037–1040, 1987.

[76] J. G. A. P. Filho, E. C. Graciliano, A. O. S. Silva, M. J. B. Souza, and A. S. Araujo, “Thermo gravimetric kinetics of polypropylene degradation on ZSM-12 and ZSM-5 catalysts,” *Catal. Today*, vol. 107–108, pp. 507 – 512, 2005.

[77] V. Karmore and G. Madras, “Kinetics for thermal degradation of polystyrene in presence of p-toluene sulfonic acid,” *Adv. Environ. Res.*, vol. 7, no. 1, pp. 117 – 121, 2002.

[78] J.-S. Kim, W.-Y. Lee, S.-B. Lee, S.-B. Kim, and M.-J. Choi, “Degradation of polystyrene waste over base promoted Fe catalysts,” *Catal. Today*, vol. 87, no. 1–4, pp. 59 – 68, 2003.

[79] D. L. Burdick and W. L. Leffler, *Petrochemicals in Nontechnical Language*, 4th editio. United States of America: Pennwell, 2010.

[80] D. Houshmand, B. Roozbehani, and A. Badakhshan, "Thermal and Catalytic Degradation of Polystyrene with a Novel Catalyst," no. 1, pp. 234–238, 2013.

[81] A. Karaduman, E. H. Simsek, B. Cicek, and A. Y. Bilgesu, "Thermal degradation of polystyrene wastes in various solvents," *J. Anal. Appl. Pyrolysis*, vol. 62, pp. 273 – 280, 2002.

[82] A. W. Coats and J. P. Redfern, "Kinetic parameters from Thermogravimetric data," *Nature*, vol. 201, pp. 68 – 69, 1964.

APPENDIX A

XRD DATA AND PATTERNS OF MATERIALS

The XRD patterns of the synthesized SAPO-34 materials are given in Figures A.1 – A.4. XRD patterns of SAPO-34 materials which were pure and used in the degradation reaction of PP and PS are given in Figures A.5 and A.6, respectively. X-ray powder diffraction data of SAPO-34, SiO_2, $AlPO_4$, α-Al_2O_3 SiO, and $Al(PO_3)_3$ are given in Tables A.1 – A.7.

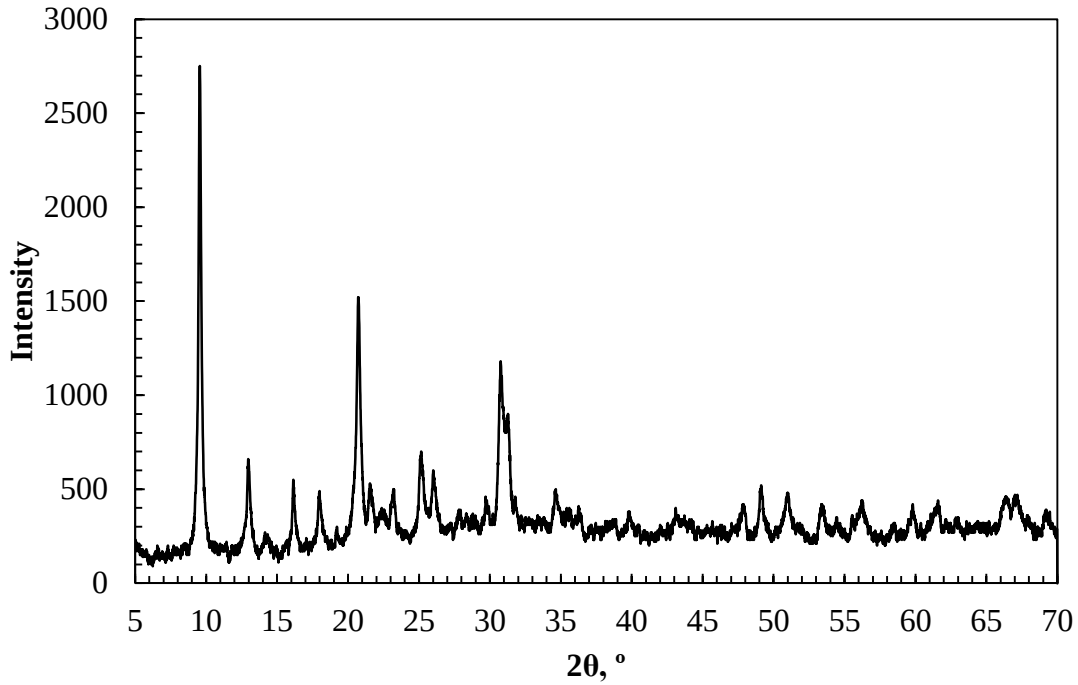

Figure A. 1. XRD pattern of synthesized SAPO-34 #2

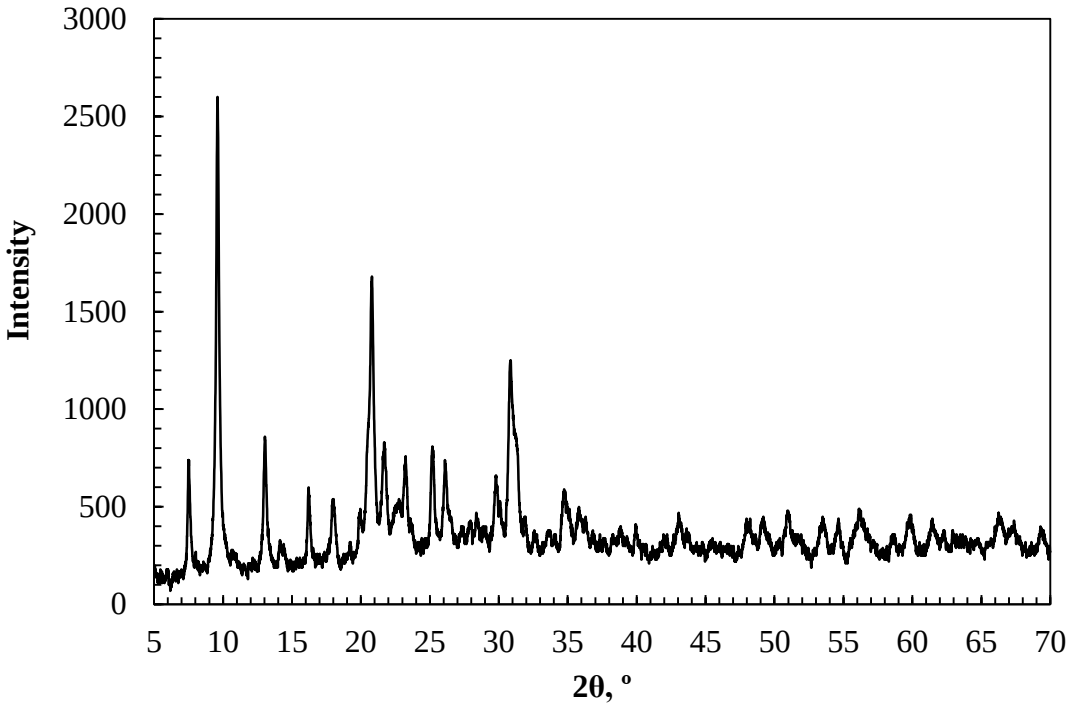

Figure A. 2. XRD pattern of synthesized SAPO-34 #3

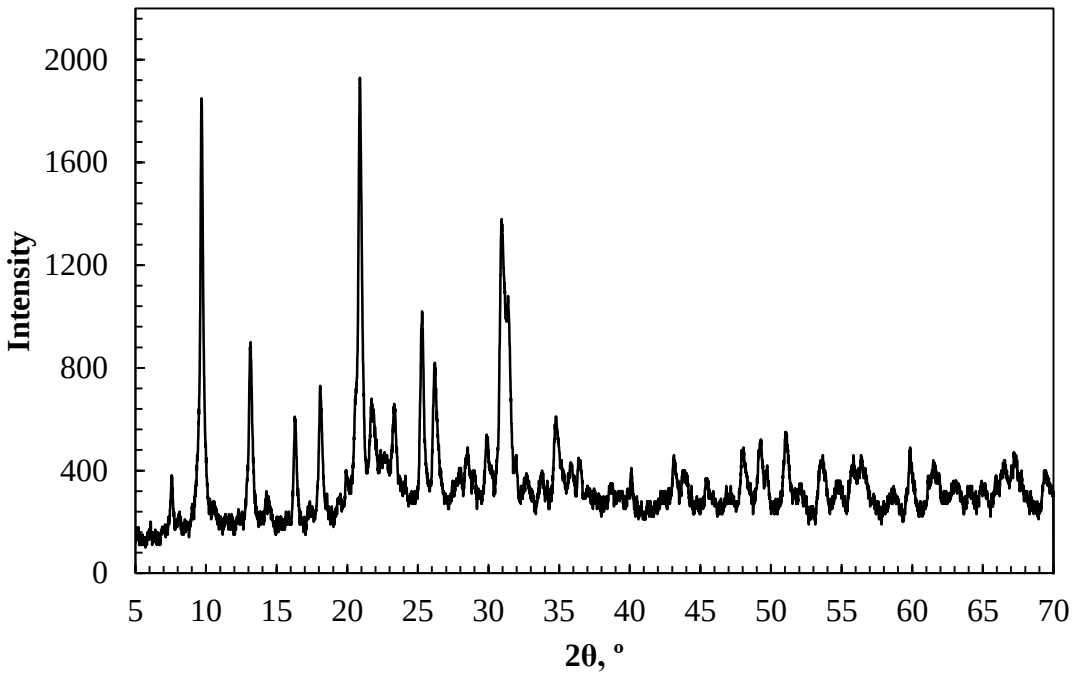

Figure A. 3. XRD pattern of synthesized SAPO-34 #4

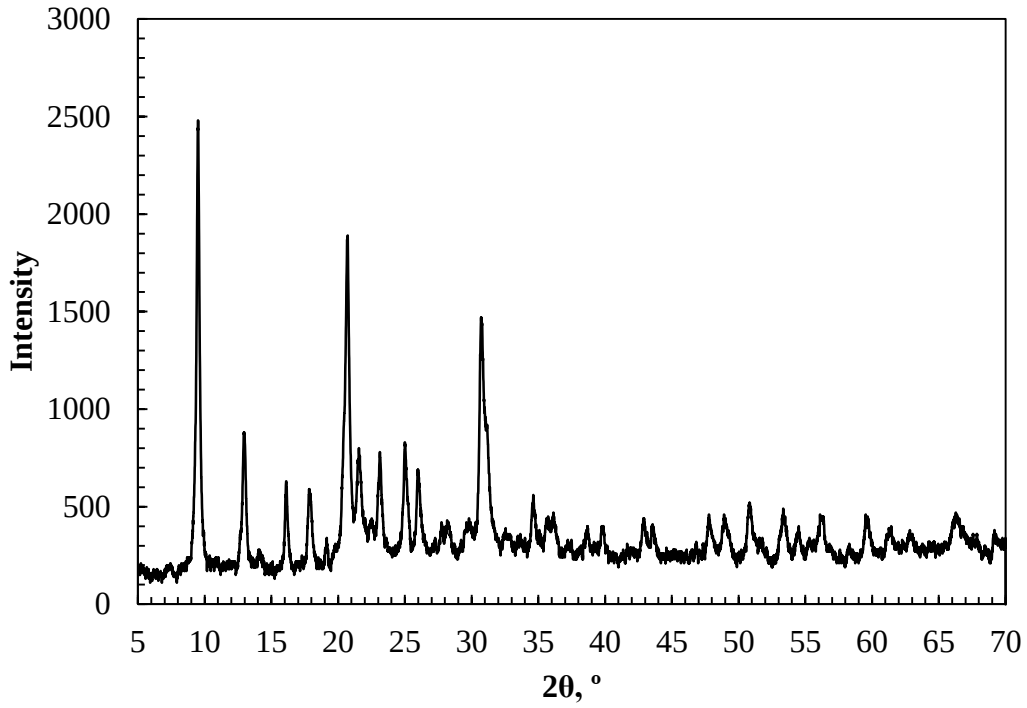

Figure A. 4. XRD pattern of synthesized SAPO-34 #5

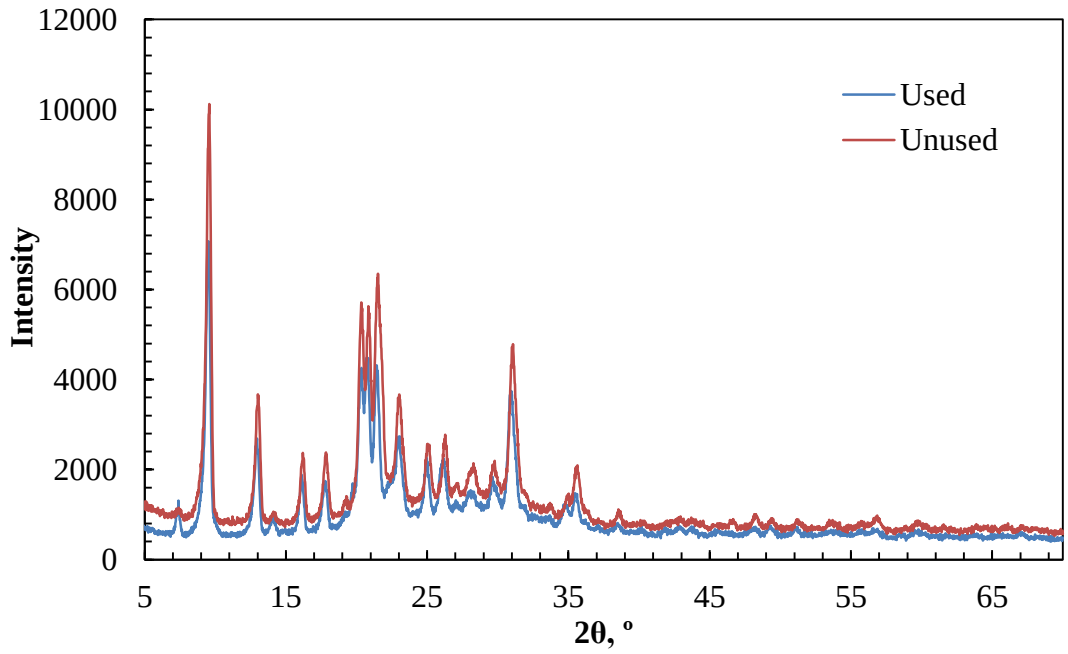

Figure A. 5. XRD patterns of SAPO-34 materials which were unused and used in the degradation reaction of PP at 440 ºC for 30 min

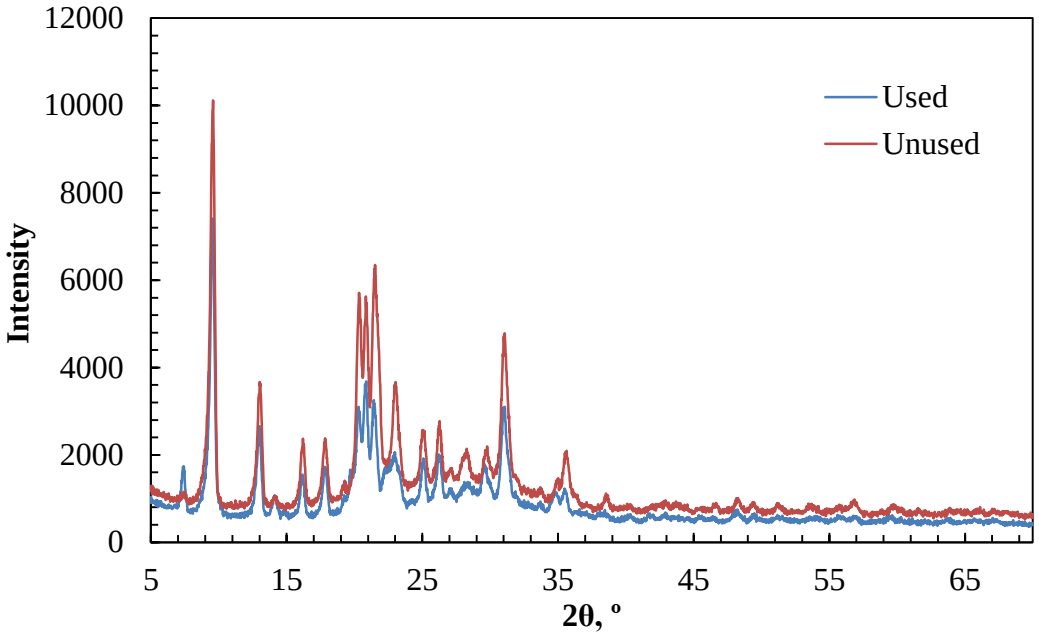

Figure A. 6. XRD patterns of SAPO-34 materials which were unused and used in the degradation reaction of PS at 415 ºC for 30 min

Table A. 1. X-ray powder diffraction data of SAPO-34 [65]

d (Å)	2θ (°)	100*(I/I$_o$)
9.36-9.17	9.45-9.65	81-100
6.92-6.78	12.8-13.05	8-20
6.35-6.24	13.95-14.2	8-23
5.54-5.47	16.0-16.2	25-54
4.97-4.89	17.85-18.15	11-76
4.67	19.0	0-2
4.32-4.25	20.55-20.9	44-100
4.03-3.95	22.05-22.5	0-5
3.87-3.84	23.0-23.15	2-10
3.57-3.51	24.95-25.4	12-87
3.45-3.43	25.8-26.0	14-26
3.243-3.220	27.5-27.7	1-4
3.181-3.143	28.05-28.4	1-12
3.058-3.018	29.2-29.6	3-9
2.931-2.912	30.5-30.7	19-75
2.880-2.849	31.05-31.4	15-28
2.780-2.763	32.2-32.4	1-5
2.683-2.648	33.4-33.85	0-6
2.611-2.589	34.35-34.65	4-15
2.495-2.462	36.0-36.5	2-11
2.321-2.315	38.8-38.9	0-2
2.276-2.270	39.6-39.7	2-4
2.099-2.080	43.1-43.5	3-6
1.918-1.907	47.4-47.7	2-6
1.866-1.852	48.8-49.2	4-7
1.828-1.809	49.9-50.45	0-2
1.802-1.781	50.65-51.3	1-8
1.728-1.720	53.0-53.25	2-7
1.691-1.678	54.25-54.7	0-4
1.650-1.645	55.7-55.9	2-5

Table A. 2. XRD data of SiO_2 [66]

d (Å)	2θ (°)	100*(I/I_o)
4.05	21.9272	100
2.485	36.1136	20
2.841	31.4618	13
3.135	28.4457	11
1.87	48.6483	7
2.465	36.4169	5
2.118	42.6513	5
1.929	47.0689	5
1.612	57.0866	5
1.494	62.0701	5
3.53	25.2068	4
2.019	44.8533	3
1.69	54.2289	3
1.6	57.5546	3
1.533	60.3239	3
1.431	65.1305	3
1.419	65.7505	3
1.398	66.8666	3
1.365	68.7054	3
1.352	69.4602	3
1.333	70.5964	3
1.299	72.7341	3
1.281	73.9244	3
1.223	78.0713	3
1.21	79.0731	3
1.206	79.3872	3
2.34	38.4364	1
1.73	52.8763	1
1.634	56.249	1
1.233	77.3197	1
1.188	80.8359	1
1.183	81.249	1
1.757	52.0023	<1
1.571	58.7197	<1
1.567	58.8843	<1
1.379	67.9121	<1
1.346	69.8147	<1
1.242	76.657	<1

Table A. 3. XRD data of $AlPO_4$ [66]

d (Å)	2θ (°)	100*(I/I_0)
4.077	21.78	100
2.506	35.8	20
3.162	28.2	10
2.867	31.17	10
1.949	46.56	7
2.491	36.02	5
2.135	42.3	5
1.888	48.15	5
1.625	56.59	5
1.5074	61.46	5
3.553	25.04	3
3.539	25.14	3
3.496	25.46	3
2.038	44.41	3
1.77	51.59	3
1.749	52.26	3
1.707	53.65	3
1.6163	56.92	3
1.5823	58.26	3
1.5452	59.8	3
1.4431	64.52	3
1.4341	64.97	3
1.3789	67.92	3
1.3474	69.73	3
1.3104	72	3
1.2913	73.24	3
5.012	17.68	1
1.651	55.62	1
1.4101	66.22	1
1.363	68.82	1
1.3582	69.1	1
1.2333	77.3	1
1.2151	78.68	1
1.1936	80.38	1
1.1866	80.95	1
1.779	51.31	<1
1.2443	76.49	<1
1.1977	80.05	<1
1.1794	81.55	<1

Table A. 4. XRD data of α-Al_2O_3 [66]

d (Å)	2θ (°)	100*(I/I_o)
2.085	43.36	100
2.552	35.13	90
1.601	57.52	80
3.479	25.58	75
1.374	68.19	50
1.74	52.55	45
2.379	37.78	40
1.404	66.54	30
0.8303	136.15	22
1.239	76.88	16
1.0426	95.25	14
0.9076	116.13	14
0.797	150.23	14
0.7931	152.43	13
0.9976	101.09	12
0.858	127.72	12
0.8072	145.19	11
1.51	61.34	8
1.2343	77.22	8
1.1898	80.69	8
1.0988	89.01	8
1.0781	91.2	8
0.8991	117.89	8
0.7988	149.27	7
1.514	61.16	6
1.147	84.37	6
1.1255	86.37	6
1.546	59.76	4
1.276	74.26	4
1.1246	86.46	4
1.0831	90.66	4
0.9819	103.34	4
0.9345	111.02	4
0.9178	114.12	4
0.9052	116.62	4
0.8804	122.06	4
0.8502	129.91	4
0.846	131.14	4
0.8137	142.38	4
1.964	46.18	2
1.337	70.35	2
1.1382	85.18	2
1.0175	98.4	2

Table A.4. (continued) XRD data of α-Al_2O_3 [66]

d (Å)	2θ (°)	100*(I/I_o)
0.8698	124.64	2
2.165	41.68	<1
1.16	83.21	<1
0.9857	102.78	<1
0.9431	109.52	<1
0.9413	109.83	<1
0.8884	120.23	<1

Table A. 5. XRD data of SiO [66]

d (Å)	2θ (°)	100*(I/I_o)
3.18	28.06	100
1.93	47.09	100
1.64	56.08	80
1.25	76.16	50
1.11	87.98	50
1.36	69.06	20
1.05	94.48	20
0.96	106.84	20
0.92	113.85	20
0.86	127.38	20
0.83	136.5	20
0.79	154.76	20
2.7	33.18	10
2.52	35.63	10
1.54	60.08	10
1.32	71.47	10
0.89	120.04	5
0.84	133.2	5

Table A. 6. XRD data of $Al(PO_3)_3$ [66]

d (Å)	2θ (°)	100*(I/I₀)
4.34	20.45	100
3.432	25.94	60
3.67	24.23	55
2.927	30.51	45
3.07	29.06	30
2.692	33.25	30
5.61	15.78	25
2.354	38.2	20
4.85	18.28	18
2.227	40.47	18
1.869	48.68	18
1.5963	57.7	18
2.507	35.79	14
1.743	52.45	14
1.6648	55.12	14
2.171	41.56	12
1.6179	56.86	12
1.4986	61.86	12
1.4473	64.31	12
1.981	45.76	10
1.4803	62.71	10
1.3092	72.08	10
1.941	46.76	8
1.4161	65.9	8
2.801	31.92	6
2.118	42.65	6
1.903	47.75	6
1.6412	55.98	6
1.387	67.47	6
1.3462	69.8	6
1.4013	66.69	4
2.024	44.74	2
1.835	49.64	2
1.69	54.23	2
1.5549	59.39	2
1.5349	60.24	2
1.373	68.25	2
1.3594	69.03	2
1.3333	70.58	2

Table A. 7. XRD data of the synthesized SAPO-34#1 material

d (Å)	2θ (°)	100*(I/I₀)
9.421	9.63	100
6.964	13.04	22
6.397	14.2	5
5.598	16.24	11
5.027	18.1	12
4.726	19.26	4
4.363	20.88	49
4.129	22.08	20
3.935	23.18	17
3.627	25.18	17
3.502	26.09	12
3.287	27.83	5
3.221	28.41	7
3.076	29.78	6
2.983	30.73	33
2.947	31.11	22
2.818	32.57	4
2.735	33.59	5
2.646	34.75	7
2.543	36.2	7
2.372	38.91	4
2.317	39.87	5
2.147	43.18	7
1.951	47.74	5
1.898	49.17	10
1.873	49.87	2
1.839	50.86	6
1.757	53.4	7
1.722	54.56	4
1.692	55.62	2

APPENDIX B

SEM & EDS RESULTS OF THE SYNTHESIZED MATERIAL

EDS spectra of the synthesized materials are given in Figures B.1 – B.4.

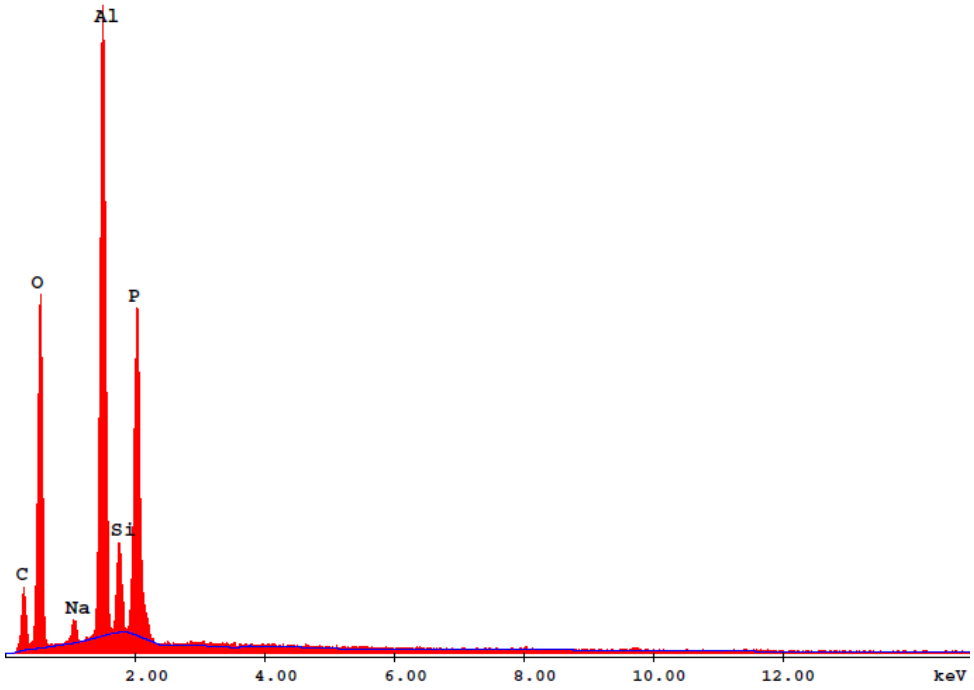

Figure B. 1. EDS spectrum of the synthesized SAPO-34#2 material

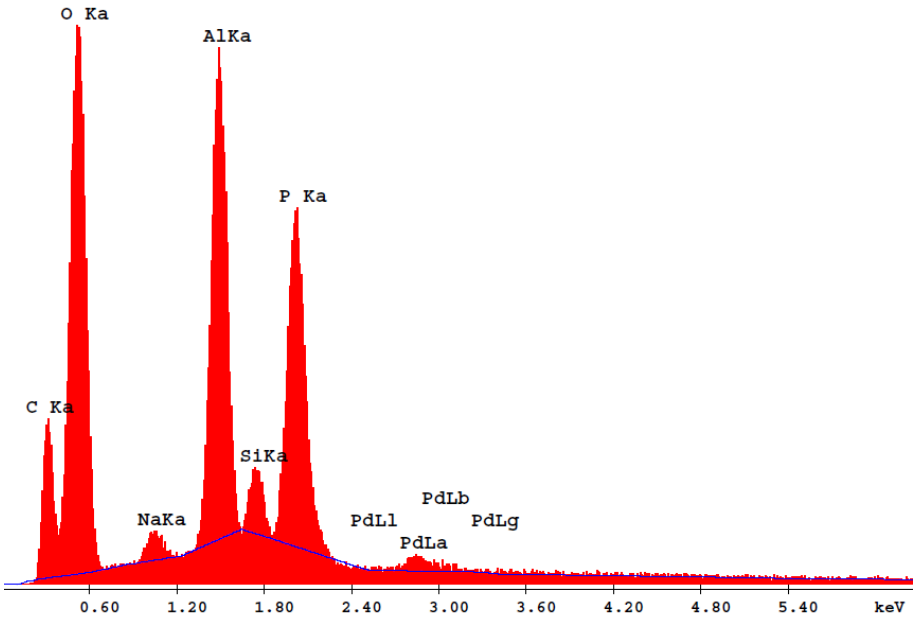

Figure B. 2. EDS spectrum of the synthesized SAPO-34#3 material

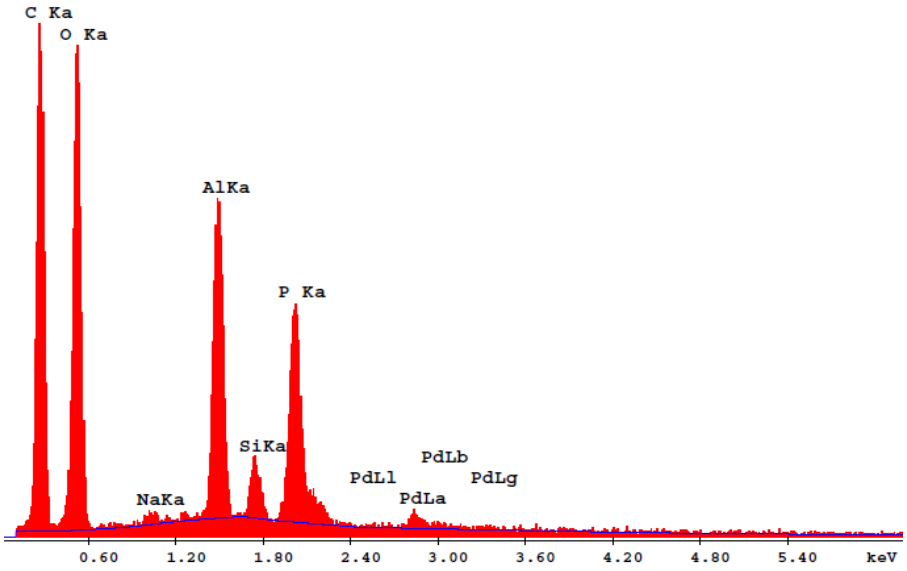

Figure B. 3. EDS spectrum of the synthesized SAPO-34#4 material

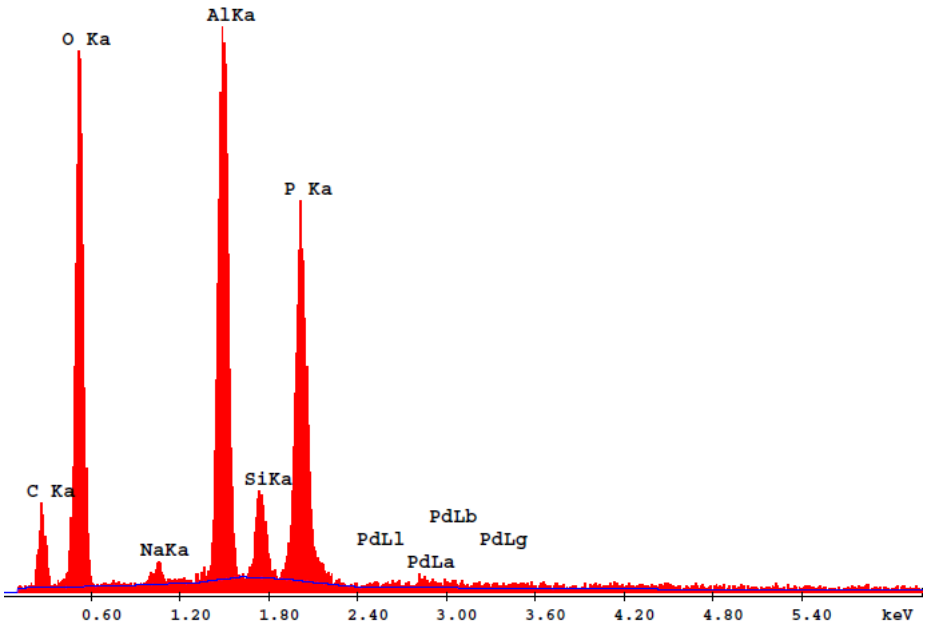

Figure B. 4. EDS spectrum of the synthesized SAPO-34#4 material

APPENDIX C

CALCULATION OF ACTIVATION ENERGIES FOR POLYPROPYLENE & POLYSTYRENE DEGRADATION REACTIONS

The kinetic parameters such as activation energy, reaction order, pre-exponential factor for both polypropylene and polystyrene degradation reactions were calculated using TGA data. In order to find the activation energies, *Coats and Redfern Method (1964)* [82] was used.

The reaction taking place in the degradation reaction is given below:

$aA_{(s)} \rightarrow bB_{(s)} + cC_{(l)} + dD_{(g)}$

The weight loss during the reaction can be expressed by using an Arrehenius-type reaction equation:

$$\frac{d\alpha}{dt} = k_{avr} * (1 - a)^n \quad \text{(C.1)}$$

Here α is the fraction of A decomposed at time *t*, *n* is the overall reaction order and k_{avr} is the rate constant. α can be defined as:

$$a = \frac{w_0 - w_t}{w_0 - w_\infty} \quad \text{(C.2)}$$

where w_0, w_t, w_∞ are the initial weight of the sample, weight at time t, and final weight values, respectively.

The rate constant, k_{avr}, can be described in terms of Arrhenius equation:

$$k_{avr} = A * exp^{-E_A/(R*T)} \quad \text{(C.3)}$$

where A and E_A are the pre-exponential factor and activation energy of the reaction, respectively.

The temperature value at any time can be written as:

$T = T_0 + q*t$ (C.4)

Here q is the heating rate, t is time and T_0 is the initial temperature.

By inserting the Eqns. C. 3 & C.4 into the Eqn. C.1 and rearranging it, Eqn. C.5 is obtained:

$$\frac{da}{(1-a)^n} = \frac{A}{q} * e^{-\left(\frac{E_A}{R*T}\right)} * dT \quad \text{(C.5)}$$

The boundary conditions for Eqn. C.5 are:

$T = T_0, \quad \alpha = 0$

$T = T, \quad \alpha = \alpha$ (C.6)

Eqn. C.5 is integrated using the boundary conditions which are given in Eqn. C.6:

$$\frac{1-(1-a)^{(1-n)}}{(1-n)*T^2} = \frac{A*R}{q*E_A}\left[\left(1 - \frac{2*R*T}{E_A}\right)\right] * \exp\left(\frac{E_A}{R*T}\right) \quad \textit{(for } n \neq 1\textit{)} \quad \text{(C.7)}$$

This expression can be further simplified by assuming that $(2*R*T)/E_A << 1$ and by taking natural logarithm of both sides, Eqns. C.8 & C.9 are used for estimating the kinetic parameters from TGA data:

$$ln\frac{1-(1-\alpha)^{(1-n)}}{(1-n)*T^2} = \ln\left[\frac{A*R}{q*E_A}\right] - \frac{E_A}{R*T} \quad \textit{(for } n \neq 1\textit{)} \quad \text{(C.8)}$$

Integration of Eqn. C.5 for the first order reaction (n=1) gives:

$$\ln\left(\frac{-ln(1-\alpha)}{T^2}\right) = \ln\left[\frac{A*R}{q*E_A}\right] - \frac{E_A}{R*T} \quad \textit{(for } n = 1\textit{)} \quad \text{(C.9)}$$

By plotting the right-hand and left-hand sides of the Eqn. C.9 as a function of 1/T, activation energy (E_A) and pre-exponential factor can be found from the slope and the intercept of the trendline. The plots for a first order reaction and a second order reaction for the degradation reaction of polypropylene are given in Figure C.1. In order to find the reaction order, the correlation coefficients should be calculated. The plot with the

highest coefficient value, the reaction order and activation energy value were calculated. Thereby, since the R^2 value of the first order degradation reaction of polypropylene is greater than the value for the second order, it is accepted that the order of the polypropylene degradation reaction is “1”.

Same calculations were done to find the activation energy and pre-exponential factor values of the polystyrene degradation reaction. The plots for a first order reaction and a second order reaction for the degradation reaction of polystyrene are given in Figure C.2. Since the R^2 value of the first order degradation reaction of polystyrene is greater than that of the second order, it is accepted that the order of the polystyrene degradation reaction is “1”.

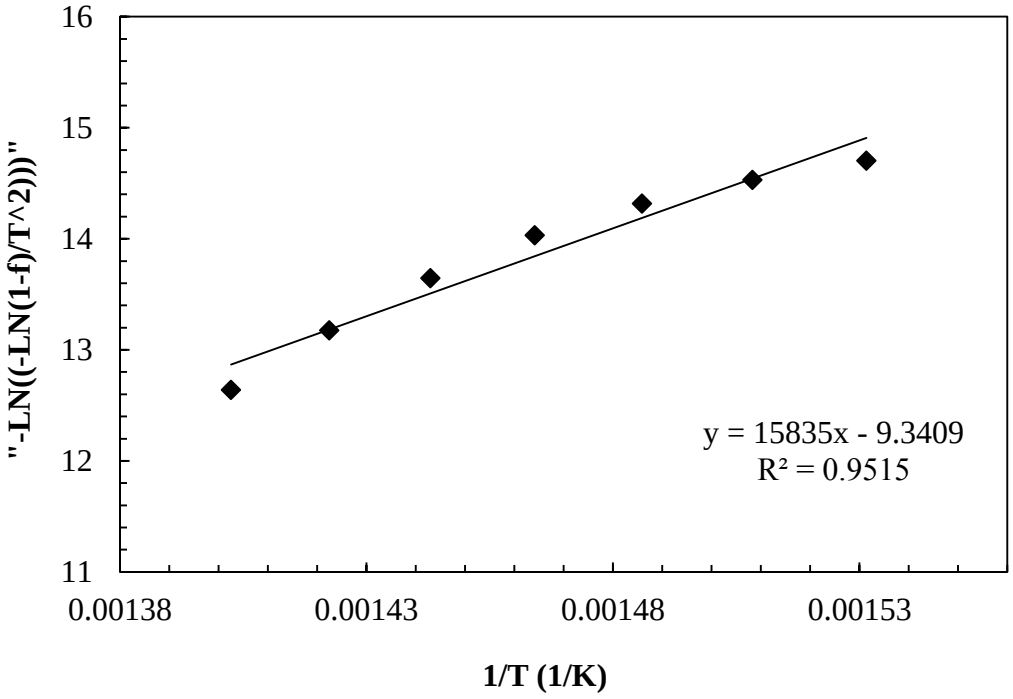

(a)

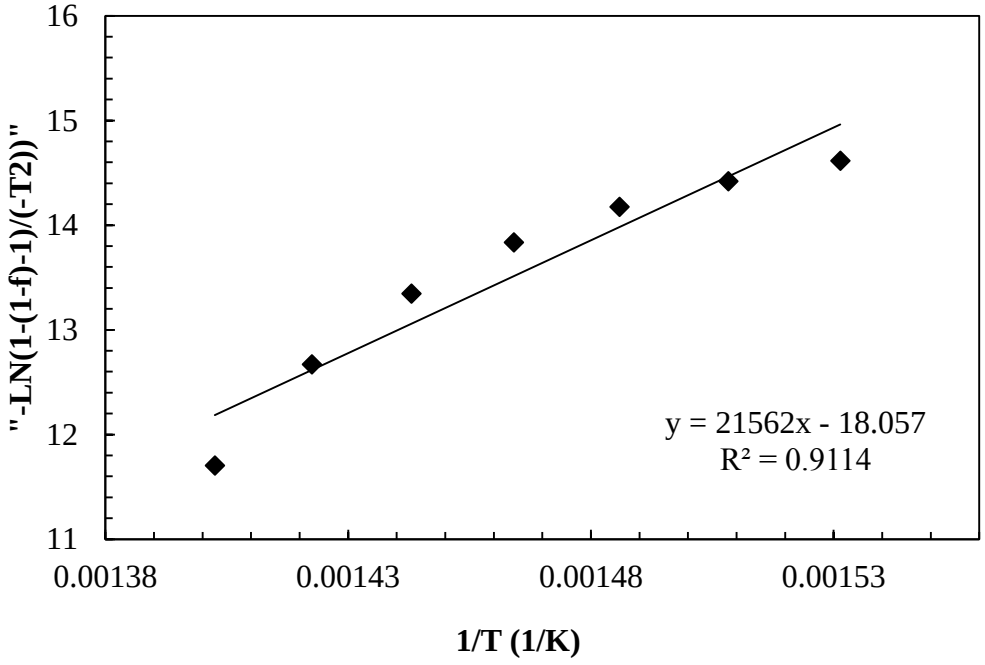

(b)

Figure C. 1. Determination of the polypropylene degradation reaction order for n = 1 assumption (a) and n = 2 assumption (b)

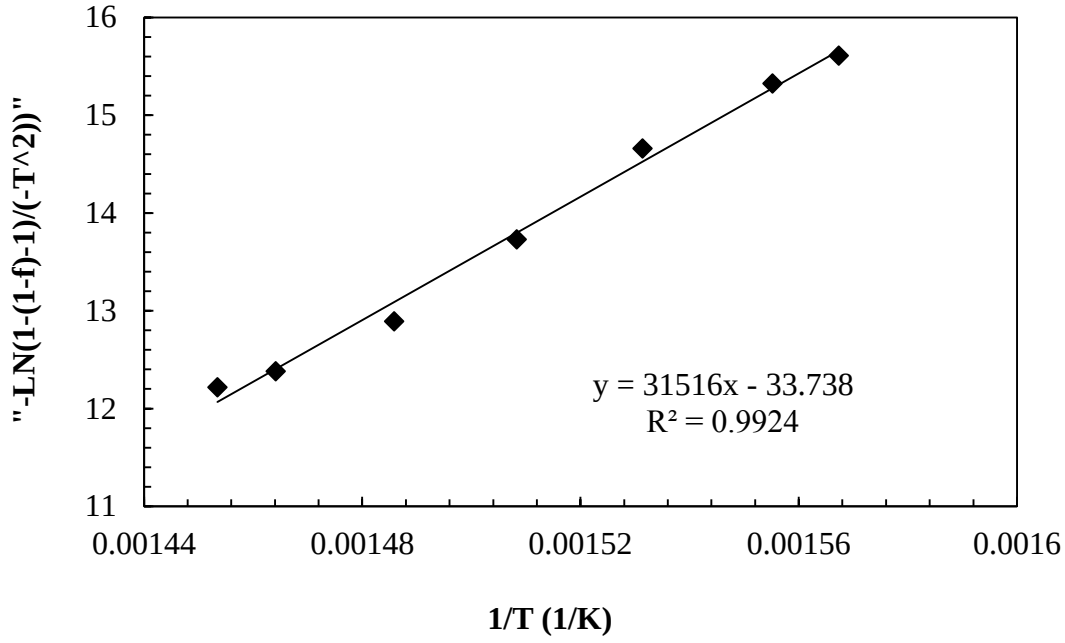

(a)

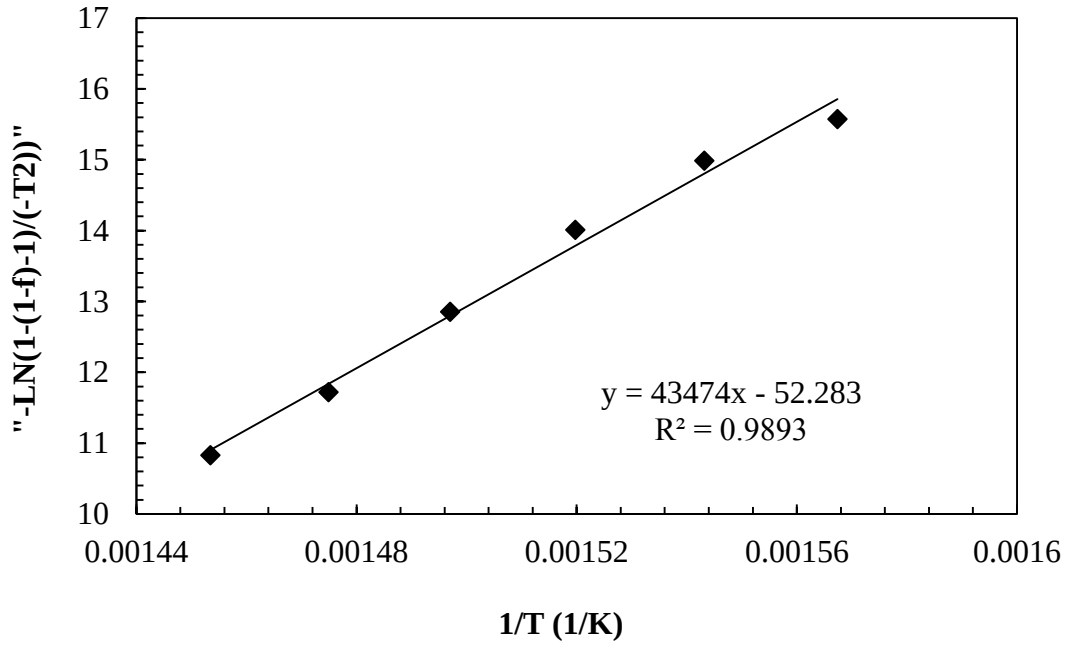

(b)

Figure C. 2. Determination of the polystyrene degradation reaction order for n = 1 assumption (a) and n = 2 assumption (b)

Activation energy values of both PP and PS degradation reactions were calculated using the TGA data obtained from 3 TGA degradation experiments (Table C.1).

Table C. 1. Activation Energy values calculated using 3 TGA degradation experiment data

	Activation Energy, kJ/mol		
	RUN I	**RUN II**	**RUN III**
PP+SAPO-34	131	121	142
PS+SAPO-34	262	265	269
PS	357	352	360

The standard deviations were calculated using Eqn. C.10.

$$\sigma = \sqrt{\frac{1}{N}\sum_{i=1}^{N}(x_i - \mu)^2} \qquad \text{(C.10)}$$

where σ is the standard deviation, N is the number of variables, μ is the average value of the variables, x denotes the expectation value.

For the degradation reactions of PP+SAPO-34, PS+SAPO-34 and pure PS, the standard deviations were found to be 11, 4 and 4, respectively.

The activation energies and pre-exponential factors for pure polystyrene, and catalyst-polypropylene and catalyst-polystyrene mixtures are given in Table C.2.

Table C. 2. Activation energy and pre-exponential factor values for the non-catalytic and catalytic degradation reactions of polypropylene & polystyrene

Sample ID	Activation Energy, kJ/mol	Pre-exponential Factor, K^2/sec
SAPO-34/PP = 1/2	131±11	$4.92*10^{10}$
Pure PS	357±4	$1.40*10^{29}$
SAPO-34/PS =1/2	262±4	$3.86*10^{21}$

APPENDIX D

RESULTS OF DEGRADATION REACTIONS

The amounts of gaseous & liquid products and solid residue from the degradation reactions of PS & PP are given in Tables D.1 & D.2, respectively.

Table D. 1. The amounts of gaseous & liquid products and solid residue from the degradation reactions of PS

Sample	Reaction Temperature, (°C)	Reaction Time, min	Gas, (g)	Liquid, (g)	Solid residue, (g)
PS	415	15	0.76	0.24	0.00
		30	0.69	0.31	0.00
PS+SAPO-34	415	15	0.77	0.23	0.00
		30	0.66	0.34	0.00

Table D. 2. The amounts of gaseous & liquid products and solid residue from the degradation reactions of PP

Sample	Reaction Temperature, (°C)	Reaction Time, min	Gas, (g)	Liquid, (g)	Solid residue, (g)
PP	315	15	0.24	0.00	0.76
		30	0.24	0.00	0.76
	400	15	0.42	0.00	0.58
		30	0.98	0.00	0.02
	425	15	0.86	0.14	0.00
		30	0.78	0.22	0.00
	440	15	0.86	0.14	0.00
		30	0.87	0.13	0.00
PP+SAPO-34	315	15	0.46	0.00	0.54
		30	0.80	0.00	0.20
	400	15	0.63	0.00	0.37
		30	1.00	0.00	0.00
	425	15	0.63	0.37	0.00
		30	0.78	0.22	0.00
	440	15	0.85	0.15	0.00
		30	0.76	0.24	0.00

TGA plots of PP and PS degradation reactions are given in Figure D.1 & D.2, respectively.

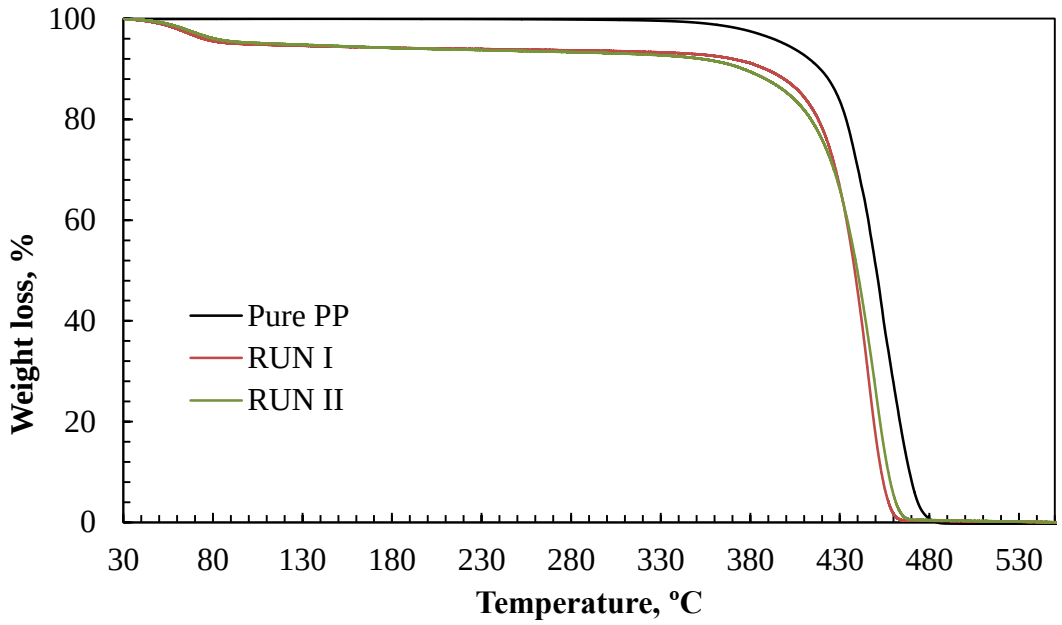

Figure D. 1. TGA plots of PP degradation reaction (SAPO-34/PP = 1/2)

(Reproducibility experiments)

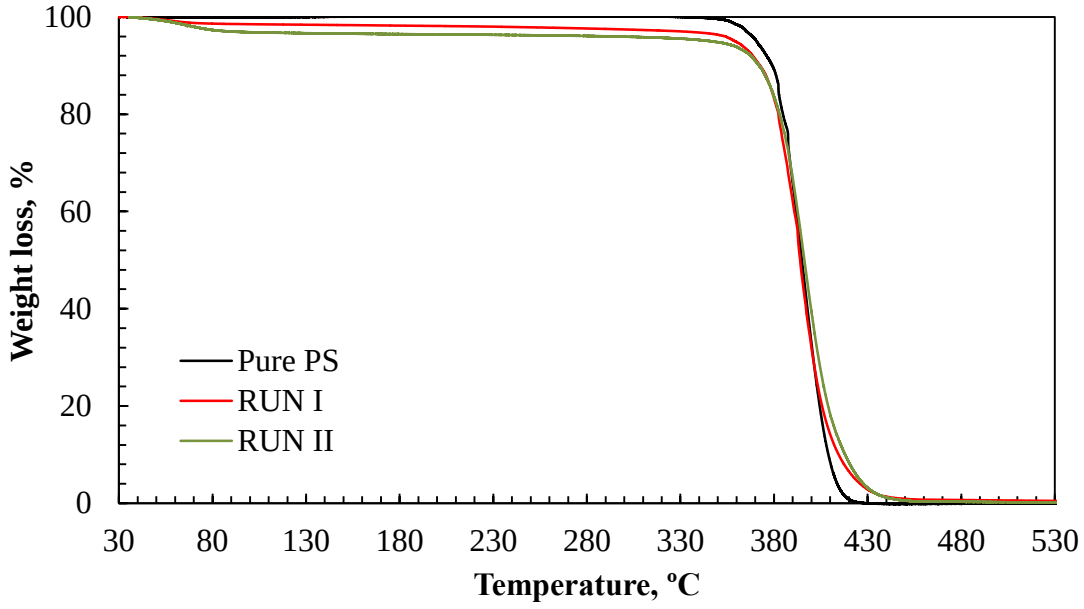

Figure D. 2. TGA plots of PS degradation reaction (SAPO-34/PP = 1/2)

(Reproducibility experiments)

TGA plots of the used SAPO-34 catalyst in PP & PS degradation reactions are given in Figures D3 & D4, respectively.

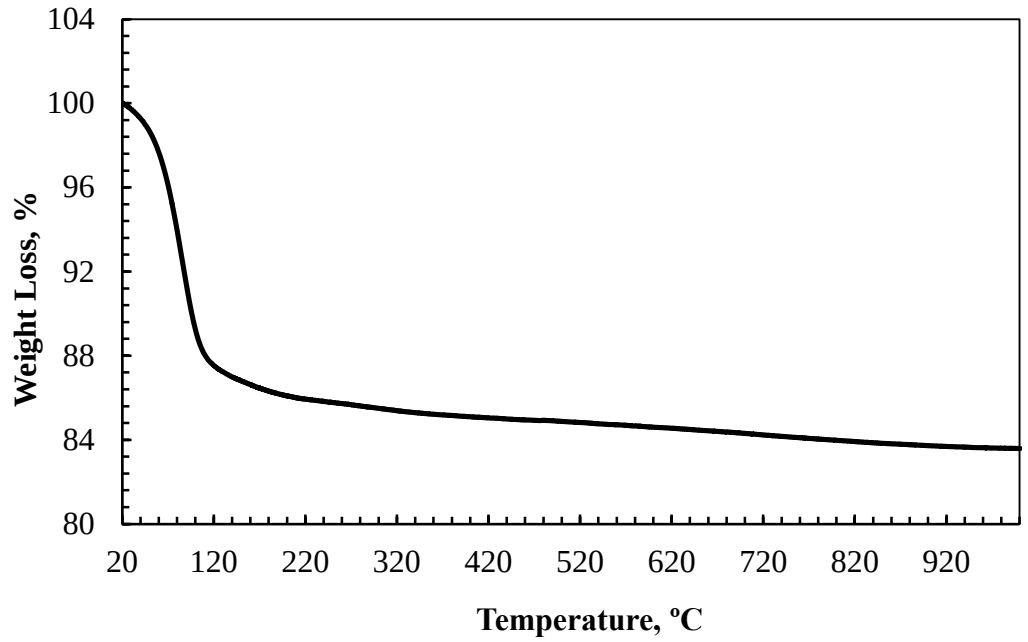

Figure D. 3. TGA plot of the used SAPO-34 catalyst in the degradation reactions of PP (440 ºC; 30 min)

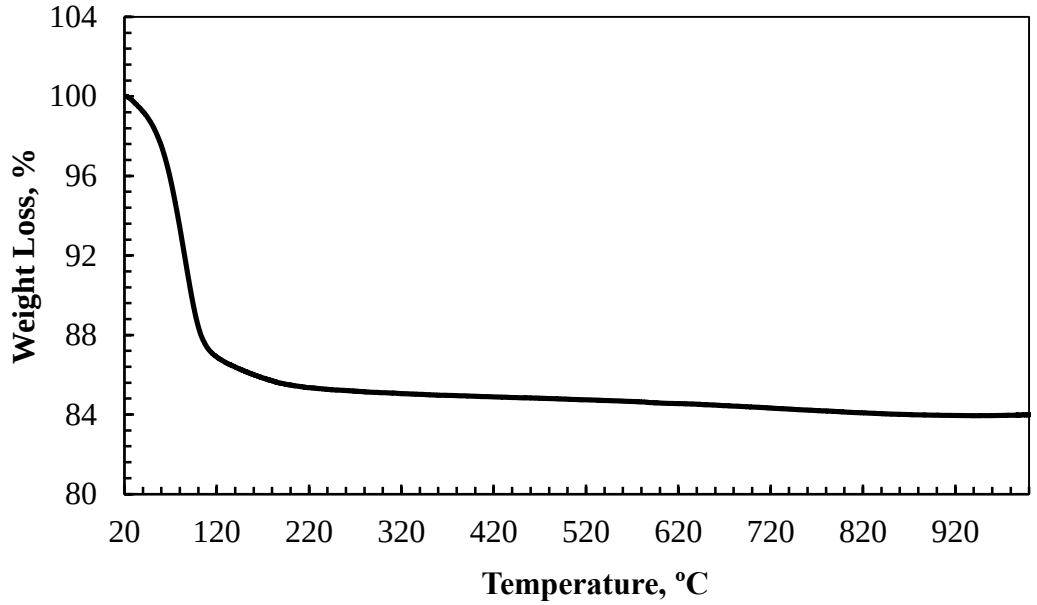

Figure D. 4. TGA plot of the used SAPO-34 catalyst in the degradation reactions of PS (415 ºC; 30 min)

APPENDIX E

CALCULATION OF GASEOUS PRODUCT CALIBRATION FACTORS USING GAS CHROMATOGRAPHY

Calibration factors were calculated with the help of calibration experiments. The aim of finding these factors is to determine the moles of the gaseous products which were obtained from the degradation experiment. The calibration experiments were performed using the following gas mixtures (Table E.1). The content of these mixtures is given in Table E.1. From these experiments, calibration factors and retention times of the products were determined. The calibration gas mixtures were injected to the GC six times.

Table E. 1. The calibration gas mixtures

Gas Mixture 1		Gas Mixture 2	
Gas ID	**Mole (%)**	**Gas ID**	**Mole (%)**
CO	1	CH_4	1
CO_2	1	C_2H_6	1
CH_4	1	C_3H_6	1
C_2H_6	1	C_3H_8	1
C_2H_4	1	C_4H_{10}	1
C_2H_2	1	N_2	95
N_2	94		

E.1. Sample Calculation for Determination of Gaseous Product Calibration Factors

The gas mixture used in the calibration was composed of;

A: CH_4 D: C_2H_6 G: n-C_4H_{10}

B: C_2H_2 E: C_3H_6 H: i-C_4H_{10}

C: C_2H_4 F: C_3H_8

The total amount of gas products was calculated using gas mixture 2 from Equation E.1:

(N_2 free basis calculation)

$$n_{Total} = A_A*\beta_A + A_D*\beta_D + A_E*\beta_E + A_F*\beta_F + A_G*\beta_G + A_H*\beta_H \quad \text{(E.1)}$$

where;

A_i: The area of i^{th} component

β: The calibration factor of i^{th} component

Also the mole fraction of the compound i in the gas mixture was calculated using Equation E.2:

$$y_i = \frac{n_i}{n_{Total}} = \frac{A_i*\beta_i}{A_A*\beta_A+A_D*\beta_D+A_E*\beta_E+A_F*\beta_F+A_G*\beta_G+A_H*\beta_H} \quad \text{(E.2)}$$

where;

y_i: The mole fraction of i^{th} component

n_i: The mole of i^{th} component

The ratio of CH_4 mole fraction to the mole fraction of compound i is given in Equation E.3:

$$\frac{y_A}{y_i} = \frac{n_A}{n_i} = \frac{A_A * \beta_A}{A_i * \beta_i} \quad \text{(E.3)}$$

The calibration factor of methane, CH_4, is assigned as 1.0 since methane is common in both calibration mixtures. From Equation C.3, β_i was calculated for each component since the areas of i^{th} and A^{th} components are known. The calibration factors obtained from these calculations and retention areas are given in Table E.2.

Table E. 2. Retention times, average areas & calibration factors of gaseous products

Gas ID	Retention time, min	$A_{Average}$, mVolt.sec	Calibration factor, β
CH_4	0.52	19.34	1.00
C_2H_2	1.57	29.80	0.44
C_2H_4	3.06	47.72	0.41
C_2H_6	1.9	29.70	0.65
C_3H_6	6.33	32.78	0.59
C_3H_8	7.13	33.62	0.58
n-C_4H_{10}	28.66	32.14	0.60
i-C_4H_{10}	26.1	32.14	0.60

APPENDIX F

CALCULATION OF MOLE & WEIGHT FRACTIONS & SELECTIVITIES FOR GAS PRODUCTS

Mole & weight fractions of compound i were calculated from Equation F.1 and Equation F.2, respectively.

$$y_i = \frac{n_i}{n_{total}} = \frac{A_i \beta_i}{A_A \beta_A + A_B \beta_B + A_C \beta_C + A_D \beta_D + A_E \beta_E + A_F \beta_F + A_G \beta_G + A_H \beta_H} \quad \text{(F.1)}$$

$$w_i = \frac{m_i}{m_{total}} = \frac{y_i MW_i}{y_A MW_A + y_B MW_B + y_C MW_C + y_D MW_D + y_E MW_E + y_F MW_F + y_G MW_G + y_H MW_H} \quad \text{(F.2)}$$

Components in the mixture are given below:

A: CH_4 D: C_2H_6 G: n-C_4H_{10}

B: C_2H_2 E: C_3H_6 H: i-C_4H_{10}

C: C_2H_4 F: C_3H_8

In order to find the selectivity of component i, carbon balance was done (F.3):

$$S_A = \frac{n_A}{n_A + 2n_B + 2n_C + 2n_D + 3n_E + 3n_F + 4n_G + 4n_H} \quad \text{(F.3)}$$

F.1. Sample calculation for CH_4 component:

Area values of peaks, calibration factors and moles of gas products of polypropylene degradation experiment at 440 °C for 30 min without catalyst are given in Table F.1. Using these values, mole & weight fractions and selectivity of CH_4 component were calculated.

Table F. 1. Area of peaks, calibration factors and moles of gas products of polypropylene degradation experiment (T: 440 C, t: 30 min, pure PP)

Compound	Area (mV*sec)	Calibration Factor, β	Mole, n
CH_4	5.800	1.00	5.800
C_2H_2	1.813	0.44	0.798
C_2H_6	29.623	0.65	19.255
C_2H_4	40.533	0.41	16.619
C_3H_6	19.750	0.59	11.653
C_3H_8	4.188	0.58	2.429
n-C_4H_{10}	4.348	0.60	2.609
i-C_4H_{10}	5.235	0.60	3.141

The mole fraction of methane was calculated using Eqn. F.1:

$$y_A = \frac{n_A}{n_{total}} = \frac{5.8}{5.8 + 0.798 + 19.29 + 16.427 + 11.653 + 2.409 + 2.617 + 3.150}$$

$$= 0.0931$$

The weight fraction of methane was calculated using Eqn. F.2:

$$w_A = \frac{m_A}{m_{total}}$$

$$= \frac{0.0931 * 16}{0.0933 * 16 + 0.0129 * 26 + 0.2645 * 28 + 0.3119 * 30 + 0.1872 * 42 + 0.0387 * 44 + 0.0419 * 58 + 0.0508 * 58}$$

$$= 0.0446$$

The selectivity of methane was calculated using Eqn. F.3:

$$S_A = \frac{5.8}{5.8 + 2 * 0.798 + 2 * 16.427 + 2 * 19.29 + 3 * 11.653 + 3 * 2.409 + 4 * 2.617 + 4 * 3.15}$$

$$= 0.04$$

APPENDIX G

MOLE & WEIGHT FRACTIONS AND SELECTIVITY VALUES OF GAS PRODUCTS

Mole & weight fractions and selectivities of gas products obtained from the non-catalytic and catalytic thermal degradation experiments of polypropylene and polystyrene are tabulated in Tables G.1–G.16 and Tables G.17–G.20, respectively.

Table G. 1. Mole and weight fractions and selectivities obtained from the analysis of the gas products (pure PP, 315 °C, 15 min)

Compound	Mole fraction, y_i	Weight fraction, w_i	Selectivity, S_i
CH_4	0.0000	0.0000	0.0000
C_2H_2	0.0000	0.0000	0.0000
C_2H_6	0.0000	0.0000	0.0000
C_2H_4	1.0000	1.0000	1.0000
C_3H_6	0.0000	0.0000	0.0000
C_3H_8	0.0000	0.0000	0.0000
n-C_4H_{10}	0.0000	0.0000	0.0000
i-C_4H_{10}	0.0000	0.0000	0.0000

Table G. 2. Mole and weight fractions and selectivities obtained from the analysis of the gas products (pure PP, 315 °C, 30 min)

Compound	Mole fraction, y_i	Weight fraction, w_i	Selectivity, S_i
CH_4	0.0000	0.0000	0.0000
C_2H_2	0.0000	0.0000	0.0000
C_2H_6	0.0000	0.0000	0.0000
C_2H_4	1.0000	1.0000	1.0000
C_3H_6	0.0000	0.0000	0.0000
C_3H_8	0.0000	0.0000	0.0000
n-C_4H_{10}	0.0000	0.0000	0.0000
i-C_4H_{10}	0.0000	0.0000	0.0000

Table G. 3. Mole and weight fractions and selectivities obtained from the analysis of the gas products (pure PP, 400 °C, 15 min)

Compound	Mole fraction, y_i	Weight fraction, w_i	Selectivity, S_i
CH_4	0.0000	0.0000	0.0000
C_2H_2	0.0000	0.0000	0.0000
C_2H_6	0.0675	0.0570	0.0612
C_2H_4	0.7255	0.6603	0.6574
C_3H_6	0.2070	0.2827	0.2814
C_3H_8	0.0000	0.0000	0.0000
n-C_4H_{10}	0.0000	0.0000	0.0000
i-C_4H_{10}	0.0000	0.0000	0.0000

Table G. 4. Mole and weight fractions and selectivities obtained from the analysis of the gas products (pure PP, 400 °C, 30 min)

Compound	Mole fraction, y_i	Weight fraction, w_i	Selectivity, S_i
CH_4	0.0000	0.0000	0.0000
C_2H_2	0.0000	0.0000	0.0000
C_2H_6	0.0585	0.0478	0.0513
C_2H_4	0.6621	0.5835	0.5814
C_3H_6	0.2794	0.3686	0.3673
C_3H_8	0.0000	0.0000	0.0000
n-C_4H_{10}	0.0000	0.0000	0.0000
i-C_4H_{10}	0.0000	0.0000	0.0000

Table G. 5. Mole and weight fractions and selectivities obtained from the analysis of the gas products (pure PP, 425 °C, 15 min)

Compound	Mole fraction, y_i	Weight fraction, w_i	Selectivity, S_i
CH_4	0.1229	0.0568	0.0501
C_2H_2	0.0036	0.0031	0.0029
C_2H_6	0.1055	0.0791	0.0858
C_2H_4	0.2539	0.2049	0.2063
C_3H_6	0.4194	0.5080	0.5113
C_3H_8	0.0258	0.0329	0.0315
n-C_4H_{10}	0.0103	0.0173	0.0168
i-C_4H_{10}	0.0587	0.0979	0.0954

Table G. 6. Mole and weight fractions and selectivities obtained from the analysis of the gas products (pure PP, 425 °C, 30 min)

Compound	Mole fraction, y_i	Weight fraction, w_i	Selectivity, S_i
CH_4	0.1307	0.0579	0.0518
C_2H_2	0.0454	0.0327	0.0360
C_2H_6	0.1123	0.0932	0.0890
C_2H_4	0.1703	0.1320	0.1350
C_3H_6	0.3331	0.3873	0.3962
C_3H_8	0.0970	0.1182	0.1154
n-C_4H_{10}	0.0495	0.0795	0.0785
i-C_4H_{10}	0.0618	0.0992	0.0980

Table G. 7. Mole and weight fractions and selectivities obtained from the analysis of the gas products (pure PP, 440 °C, 15 min)

Compound	Mole fraction, y_i	Weight fraction, w_i	Selectivity, S_i
CH_4	0.0683	0.0301	0.0209
C_2H_2	0.0119	0.0098	0.0386
C_2H_6	0.0969	0.0695	0.1186
C_2H_4	0.2905	0.2232	0.3186
C_3H_6	0.3815	0.4413	0.2992
C_3H_8	0.0347	0.0415	0.0504
n-C_4H_{10}	0.0612	0.0971	0.0873
i-C_4H_{10}	0.0551	0.0876	0.0852

Table G. 8. Mole and weight fractions and selectivities obtained from the analysis of the gas products (pure PP, 440 °C, 30 min)

Compound	Mole fraction, y_i	Weight fraction, w_i	Selectivity, S_i
CH_4	0.0921	0.0440	0.0398
C_2H_2	0.0129	0.0100	0.0111
C_2H_6	0.3119	0.2792	0.2689
C_2H_4	0.2645	0.2210	0.2281
C_3H_6	0.1872	0.2346	0.2422
C_3H_8	0.0387	0.0507	0.0500
n-C_4H_{10}	0.0419	0.0725	0.0723
i-C_4H_{10}	0.0508	0.0879	0.0876

Table G. 9. Mole and weight fractions and selectivities obtained from the analysis of the gas products (PP+SAPO-34, 315 °C, 15 min)

Compound	Mole fraction, y_i	Weight fraction, w_i	Selectivity, S_i
CH_4	0.0000	0.0000	0.0000
C_2H_2	0.0000	0.0000	0.0000
C_2H_6	0.0000	0.0000	0.0000
C_2H_4	0.9910	0.9865	0.9865
C_3H_6	0.0090	0.0135	0.0135
C_3H_8	0.0000	0.0000	0.0000
n-C_4H_{10}	0.0000	0.0000	0.0000
i-C_4H_{10}	0.0000	0.0000	0.0000

Table G. 10. Mole and weight fractions and selectivities obtained from the analysis of the gas products (PP+SAPO-34, 315 °C, 30 min)

Compound	Mole fraction, y_i	Weight fraction, w_i	Selectivity, S_i
CH_4	0.0000	0.0000	0.0000
C_2H_2	0.0000	0.0000	0.0000
C_2H_6	0.0000	0.0000	0.0000
C_2H_4	0.9994	0.9992	0.9992
C_3H_6	0.0006	0.0008	0.0008
C_3H_8	0.0000	0.0000	0.0000
n-C_4H_{10}	0.0000	0.0000	0.0000
i-C_4H_{10}	0.0000	0.0000	0.0000

Table G. 11. Mole and weight fractions and selectivities obtained from the analysis of the gas products (PP+SAPO-34, 400 °C, 15 min)

Compound	Mole fraction, y_i	Weight fraction, w_i	Selectivity, S_i
CH_4	0.0470	0.0259	0.0227
C_2H_2	0.0000	0.0000	0.0000
C_2H_6	0.0171	0.0153	0.0165
C_2H_4	0.8547	0.8232	0.8273
C_3H_6	0.0383	0.0553	0.0556
C_3H_8	0.0111	0.0168	0.0161
n-C_4H_{10}	0.0246	0.0490	0.0476
i-C_4H_{10}	0.0073	0.0146	0.0141

Table G. 12. Mole and weight fractions and selectivities obtained from the analysis of the gas products (PP+SAPO-34, 400 °C, 30 min)

Compound	Mole fraction, y_i	Weight fraction, w_i	Selectivity, S_i
CH_4	0.1358	0.0791	0.0701
C_2H_2	0.0119	0.0094	0.0103
C_2H_6	0.0884	0.0789	0.0745
C_2H_4	0.4697	0.4033	0.4134
C_3H_6	0.0876	0.1120	0.1144
C_3H_8	0.0143	0.0190	0.0184
n-C_4H_{10}	0.0357	0.0635	0.0628
i-C_4H_{10}	0.0429	0.0763	0.0756

Table G. 13. Mole and weight fractions and selectivities obtained from the analysis of the gas products (PP+SAPO-34, 425 °C, 15 min)

Compound	Mole fraction, y_i	Weight fraction, w_i	Selectivity, S_i
CH_4	0.1259	0.0628	0.0560
C_2H_2	0.0175	0.0142	0.0155
C_2H_6	0.1175	0.1094	0.1040
C_2H_4	0.3640	0.3174	0.3234
C_3H_6	0.3036	0.3950	0.4025
C_3H_8	0.0631	0.0861	0.0838
n-C_4H_{10}	0.0037	0.0066	0.0065
i-C_4H_{10}	0.0047	0.0084	0.0083

Table G. 14. Mole and weight fractions and selectivities obtained from the analysis of the gas products (PP+SAPO-34, 425 °C, 30 min)

Compound	Mole fraction, y_i	Weight fraction, w_i	Selectivity, S_i
CH_4	0.1527	0.0225	0.0201
C_2H_2	0.0495	0.0334	0.0367
C_2H_6	0.1465	0.1150	0.1095
C_2H_4	0.1577	0.1159	0.1183
C_3H_6	0.3665	0.4043	0.4124
C_3H_8	0.0936	0.1077	0.1049
n-C_4H_{10}	0.0474	0.0715	0.0705
i-C_4H_{10}	0.0861	0.1296	0.1277

Table G. 15. Mole and weight fractions and selectivities obtained from the analysis of the gas products (PP+SAPO-34, 440 °C, 15 min)

Compound	Mole fraction, y_i	Weight fraction, w_i	Selectivity, S_i
CH_4	0.1108	0.0512	0.0457
C_2H_2	0.0288	0.0212	0.0233
C_2H_6	0.0928	0.0804	0.0766
C_2H_4	0.3424	0.2783	0.2840
C_3H_6	0.2546	0.3083	0.3146
C_3H_8	0.0591	0.0760	0.0740
n-C_4H_{10}	0.0624	0.1041	0.1026
i-C_4H_{10}	0.0492	0.0806	0.0793

Table G. 16. Mole and weight fractions and selectivities obtained from the analysis of the gas products (PP+SAPO-34, 440 °C, 30 min)

Compound	Mole fraction, y_i	Weight fraction, w_i	Selectivity, S_i
CH_4	0.1191	0.0537	0.0479
C_2H_2	0.0055	0.0040	0.0044
C_2H_6	0.0577	0.0489	0.0465
C_2H_4	0.2956	0.2336	0.2378
C_3H_6	0.3850	0.4552	0.4632
C_3H_8	0.0491	0.0607	0.0590
n-C_4H_{10}	0.0457	0.0747	0.0734
i-C_4H_{10}	0.0423	0.0691	0.0679

Table G. 17. Mole and weight fractions and selectivities obtained from the analysis of the gas products (Pure PS, 415 °C, 15 min)

Compound	Mole fraction, y_i	Weight fraction, w_i	Selectivity, S_i
CH_4	0.2430	0.1552	0.1386
C_2H_2	0.0100	0.0120	0.0115
C_2H_6	0.0055	0.0057	0.0063
C_2H_4	0.7415	0.8270	0.8437
C_3H_6	0.0000	0.0000	0.0000
C_3H_8	0.0000	0.0000	0.0000
n-C_4H_{10}	0.0000	0.0000	0.0000
i-C_4H_{10}	0.0000	0.0000	0.0000

Table G. 18. Mole and weight fractions and selectivities obtained from the analysis of the gas products (Pure PS, 415 °C, 30 min)

Compound	Mole fraction, y_i	Weight fraction, w_i	Selectivity, S_i
CH_4	0.1396	0.0536	0.0484
C_2H_2	0.0010	0.0007	0.0007
C_2H_6	0.0000	0.0000	0.0000
C_2H_4	0.3464	0.2327	0.2402
C_3H_6	0.0000	0.0000	0.0000
C_3H_8	0.0000	0.0000	0.0000
n-C_4H_{10}	0.1954	0.2717	0.2708
i-C_4H_{10}	0.3177	0.4413	0.4399

Table G. 19. Mole and weight fractions and selectivities obtained from the analysis of the gas products (PS+SAPO-34, 415 °C, 15 min)

Compound	Mole fraction, y_i	Weight fraction, w_i	Selectivity, S_i
CH_4	0.2489	0.1150	0.1043
C_2H_2	0.0182	0.0158	0.0153
C_2H_6	0.0000	0.0000	0.0000
C_2H_4	0.3967	0.3203	0.3317
C_3H_6	0.0000	0.0000	0.0000
C_3H_8	0.0000	0.0052	0.0052
n-C_4H_{10}	0.1574	0.2571	0.2571
i-C_4H_{10}	0.1749	0.2865	0.2865

Table G. 20. Mole and weight fractions and selectivities obtained from the analysis of the gas products (PS+SAPO-34, 415 °C, 30 min)

Compound	Mole fraction, y_i	Weight fraction, w_i	Selectivity, S_i
CH_4	0.1048	0.0451	0.0404
C_2H_2	0.0031	0.0025	0.0024
C_2H_6	0.0000	0.0000	0.0000
C_2H_4	0.5425	0.4084	0.4187
C_3H_6	0.0000	0.0000	0.0000
C_3H_8	0.0000	0.0000	0.0000
n-C_4H_{10}	0.1858	0.2894	0.2865
i-C_4H_{10}	0.1639	0.2546	0.2521

APPENDIX H

CALCULATION OF CALIBRATION FACTORS OF LIQUID PRODUCTS

In order to analyze the liquid products which were obtained from the non-catalytic and catalytic thermal degradation reactions of polypropylene and polystyrene, calibration experiments were carried out. Using the results of these experiments, calibration factor and retention time for each liquid product were found. Five different paraffin mixtures were used for the calibration. The contents of the mixtures are given in Tables H.1 – H.5.

Table H. 1. First paraffin mixture used in calibration

Liquid ID	Wt. (mg)	Liquid ID	Wt. (mg)
C_5H_{12}	50.5	$C_{10}H_{22}$	50.5
C_6H_{14}	50.5	$C_{11}H_{24}$	50.5
C_7H_{16}	50.5	$C_{12}H_{26}$	50.5
C_8H_{18}	50.5	$C_{13}H_{28}$	50.5
C_9H_{20}	50.5	$C_{14}H_{30}$	50.5

Table H. 2. Second paraffin mixture used in calibration

Liquid ID	Conc. (mg/L)
Benzene (C_6H_6)	100
Toluene (C_7H_8)	100
Ethylbenzene (C_8H_{10})	100
m-xylene ($C_6H_4(CH_3)_2$)	100
p-xylene ($C_6H_4(CH_3)_2$)	100
Styrene ($C_6H_5CH=CH_2$)	100
o-xylene ($C_6H_4(CH_3)_2$)	100

Table H. 3. Third paraffin mixture used in calibration

Liquid ID	Conc. (mg/L)
Benzene (C_6H_6)	200
Toluene (C_7H_8)	200
Ethylbenzene (C_8H_{10})	200
m-xylene ($C_6H_4(CH_3)_2$)	200
p-xylene ($C_6H_4(CH_3)_2$)	200
Styrene ($C_6H_5CH=CH_2$)	200
o-xylene ($C_6H_4(CH_3)_2$)	200
Isopropyl benzene (C_9H_{12})	200
n-Propyl benzene (C_9H_{12})	200
1,3,5-Trimethylbenzene (C_9H_{12})	200
1,2,4-Trimethylbenzene (C_9H_{12})	200
tert-Butyl benzene ($C_{10}H_{14}$)	200
sec-Butyl benzene ($C_{10}H_{14}$)	200
4-Isopropyltoluene ($C_{10}H_{14}$)	200
n-butyl benzene ($C_{10}H_{14}$)	200
Naphthalene ($C_{10}H_8$)	200

Table H. 4. Fourth paraffin mixture used in calibration

Liquid ID	Weight (%)
n-Hexane ($C_6H_{14)}$	50
Benzene (C_6H_6)	50

Table H. 5. Fifth paraffin mixture used in calibration

Liquid ID	Weight (%)
n-Hexane ($C_6H_{14)}$	50
Cyclohexane (C_6H_{12})	50

H.1. Calibration factor calculations

The procedure for calculation of the calibration factor is given for the first mixture. Nomenclature of the components is given below:

C_5H_{12} :	A	C_8H_{18} :	D	$C_{11}H_{24}$:	G
C_6H_{14} :	B	C_9H_{20} :	E	$C_{12}H_{26}$:	H
C_7H_{16} :	C	$C_{10}H_{22}$:	F	$C_{13}H_{28}$:	I

Total amount of liquid products in the first mixture was calculated using Equation H.1.:

$$\mathbf{n_{Total}} = A_A*\beta_A + A_B*\beta_B + A_C*\beta_C + A_D*\beta_D + A_E*\beta_E + A_F*\beta_F + A_G*\beta_G + A_H*\beta_H + A_I*\beta_I \quad \text{(H.1)}$$

The mole fractions of the liquid compounds were calculated using Equation H.2:

$$x_i = \frac{n_i}{n_{Total}} = \frac{A_i * \beta_i}{A_A * \beta_A + A_B * \beta_B + A_C * \beta_C + A_D * \beta_D + A_E * \beta_E + A_F * \beta_F * A_G * \beta_G + A_H * \beta_H + A_I * \beta_I} \quad \text{(H.2)}$$

The ratio of the mole fraction of compound A to the mole fraction of compound i is given in Equation H.3:

$$\frac{x_A}{x_i} = \frac{n_A}{n_i} = \frac{A_A*\beta_A}{A_i*\beta_i} \quad \text{(H.3)}$$

Volume fractions of the compounds can be calculated using Equation H.4, if necessary:

$$z_A = x_A * \frac{M*W_A}{\rho_A} \quad \text{(H.4)}$$

In the calibration calculations, the calibration factor of n-hexane (β_B) was arbitrarily assigned as 1.0. Using the Eqn. H.3, the calibration factor of the component i, β_i, was calculated since the other parameters were already known. Calibration factors of components in the other mixtures were calculated by using the values obtained from the first calibration mixture. Calculated calibration factors and retention times of the liquid compounds are tabulated in Table H.6.

Table H. 6. Calibration factors and retention times of the liquid compounds

Liquid ID	Retention Time, min	Calibration Factor, β
n-Pentane (C_5H_{12})	3.48	3.49
n-Hexane (C_6H_{14})	4.14	1.00
Cyclohexane (C_6H_{12})	7.27	0.43
Benzene (C_6H_6)	7.38	0.72
n-Heptane (C_7H_{16})	8.14	0.97
Toluene (C_7H_8)	11.315	0.72
n-Octane (C_8H_{18})	12.21	0.93
Ethylbenzene (C_8H_{10})	17.23	0.50
m-xylene ($C_6H_4(CH_3)_2$)	18.17	0.74
p-xylene ($C_6H_4(CH_3)_2$)	18.17	0.74
Styrene ($C_6H_5CH=CH_2$)	19.415	0.69
o-xylene ($C_6H_4(CH_3)_2$)	19.79	0.55
Isopropyl benzene (C_9H_{12})	20.485	0.93
n-Nonane (C_9H_{12})	21.42	0.72
n-Propyl benzene (C_9H_{12})	22.125	0.49
1,3,5-Trimethylbenzene (C_9H_{12})	22.68	0.70
1,2,4-Trimethylbenzene (C_9H_{12})	22.915	1.85
tert-Butyl benzene ($C_{10}H_{14}$)	23.66	0.67
n-Decane ($C_{10}H_{22}$)	24.95	0.73
sec-Butyl benzene ($C_{10}H_{14}$)	27.93	1.91
n-Undecane ($C_{11}H_{24}$)	28.09	0.50
4-Isopropyltoluene ($C_{10}H_{14}$)	28.175	1.50
n-Dodecane ($C_{12}H_{26}$)	30.97	0.30
n-Tridecane ($C_{13}H_{28}$)	33.85	0.34
n-butyl benzene ($C_{10}H_{14}$)	33.97	0.76
n-Tetradecane ($C_{14}H_{30}$)	38.31	0.28
Naphthalene ($C_{10}H_8$)	49.44	3.44
n-Hexadecane ($C_{16}H_{34}$)	51.22	0.70
n-Octadecane ($C_{18}H_{38}$)	69.40	1.44

APPENDIX I

MOLE FRACTIONS, WEIGHT FRACTIONS AND SELECTIVITIES OF LIQUID PRODUCTS

Mole fractions and selectivities of liquid products obtained from the non-catalytic and catalytic thermal degradation experiments of polypropylene and polystyrene are tabulated in Tables I.1 – I.8 and Tables I.9 – I.12, respectively.

Table I. 1. Mole fractions & selectivities obtained from the analysis of the liquid products (Pure PP, 425 °C, 15 min)

Liquid ID	Mole fraction, x_i	Selectivity, S_i
n-Pentane (C_5H_{12})	0.00000	0.00000
n-Hexane (C_6H_{14})	0.00000	0.00000
Cyclohexane (C_6H_{12})	0.00000	0.00000
Benzene (C_6H_6)	0.00000	0.00000
n-Heptane (C_7H_{16})	0.00000	0.00000
Toluene (C_7H_8)	0.00000	0.00000
n-Octane (C_8H_{18})	0.00000	0.00000
Ethylbenzene (C_8H_{10})	0.03627	0.02750
m-xylene ($C_6H_4(CH_3)_2$)	0.00208	0.00158
p-xylene ($C_6H_4(CH_3)_2$)	0.00208	0.00158
Styrene ($C_6H_5CH=CH_2$)	0.00274	0.00207
o-xylene ($C_6H_4(CH_3)_2$)	0.00532	0.00402
Isopropyl benzene (C_9H_{12})	0.00000	0.00000
n-Nonane (C_9H_{12})	0.00000	0.00000
n-Propyl benzene (C_9H_{12})	0.00000	0.00000
1,3,5-Trimethylbenzene (C_9H_{12})	0.03598	0.03061
1,2,4-Trimethylbenzene (C_9H_{12})	0.03651	0.03113
tert-Butyl benzene ($C_{10}H_{14}$)	0.05144	0.04875
n-Decane ($C_{10}H_{22}$)	0.14665	0.13908
sec-Butyl benzene ($C_{10}H_{14}$)	0.25991	0.24634
n-Undecane ($C_{11}H_{24}$)	0.02074	0.02164
4-Isopropyltoluene ($C_{10}H_{14}$)	0.00486	0.00462
n-Dodecane ($C_{12}H_{26}$)	0.01012	0.01151
n-Tridecane ($C_{13}H_{28}$)	0.04689	0.05754
n-butyl benzene ($C_{10}H_{14}$)	0.04664	0.04420
n-Tetradecane ($C_{14}H_{30}$)	0.00496	0.00659
Naphthalene ($C_{10}H_8$)	0.21768	0.20647
n-Hexadecane ($C_{16}H_{34}$)	0.01690	0.02566
n-Octadecane ($C_{18}H_{38}$)	0.05224	0.08912

Table I. 2. Mole fractions & selectivities obtained from the analysis of the liquid products (Pure PP, 425 °C, 30 min)

Liquid ID	Mole fraction, x_i	Selectivity, S_i
n-Pentane (C5H12)	0.00427	0.00200
n-Hexane (C6H14)	0.00029	0.00016
Cyclohexane (C6H12)	0.00000	0.00000
Benzene (C6H6)	0.00000	0.00000
n-Heptane (C7H16)	0.00000	0.00000
Toluene (C7H8)	0.00000	0.00000
n-Octane (C8H18)	0.00000	0.00000
Ethylbenzene (C8H10)	0.04138	0.03115
m-xylene (C6H4(CH3)2)	0.00422	0.00318
p-xylene (C6H4(CH3)2)	0.00443	0.00334
Styrene (C6H5CH=CH2)	0.00533	0.00401
o-xylene (C6H4(CH3)2)	0.01084	0.00817
Isopropyl benzene (C9H12)	0.00000	0.00000
n-Nonane (C9H12)	0.00000	0.00000
n-Propyl benzene (C9H12)	0.00306	0.00259
1,3,5-Trimethylbenzene (C9H12)	0.05033	0.04262
1,2,4-Trimethylbenzene (C9H12)	0.04814	0.04076
tert-Butyl benzene (C10H14)	0.04643	0.04370
n-Decane (C10H22)	0.12229	0.11507
sec-Butyl benzene (C10H14)	0.21741	0.20457
n-Undecane (C11H24)	0.01970	0.02039
4-Isopropyltoluene (C10H14)	0.00322	0.00303
n-Dodecane (C12H26)	0.00883	0.00997
n-Tridecane (C13H28)	0.08258	0.10103
n-butyl benzene (C10H14)	0.05935	0.05584
n-Tetradecane (C14H30)	0.00439	0.00579
Naphthalene (C10H8)	0.18537	0.17442
n-Hexadecane (C16H34)	0.02167	0.03265
n-Octadecane (C18H38)	0.05645	0.09558

Table I. 3. Mole fractions & selectivities obtained from the analysis of the liquid products (PP+SAPO-34, 425 °C, 15 min)

Liquid ID	Mole fraction, x_i	Selectivity, S_i
n-Pentane (C_5H_{12})	0.00768	0.00356
n-Hexane (C_6H_{14})	0.00000	0.00000
Cyclohexane (C_6H_{12})	0.00000	0.00000
Benzene (C_6H_6)	0.00000	0.00000
n-Heptane (C_7H_{16})	0.00000	0.00000
Toluene (C_7H_8)	0.00000	0.00000
n-Octane (C_8H_{18})	0.00634	0.00478
Ethylbenzene (C_8H_{10})	0.00000	0.00000
m-xylene ($C_6H_4(CH_3)_2$)	0.00273	0.00205
p-xylene ($C_6H_4(CH_3)_2$)	0.00273	0.00205
Styrene ($C_6H_5CH=CH_2$)	0.00188	0.00142
o-xylene ($C_6H_4(CH_3)_2$)	0.00259	0.00196
Isopropyl benzene (C_9H_{12})	0.00006	0.00005
n-Nonane (C_9H_{12})	0.00720	0.00610
n-Propyl benzene (C_9H_{12})	0.00108	0.00091
1,3,5-Trimethylbenzene (C_9H_{12})	0.00000	0.00000
1,2,4-Trimethylbenzene (C_9H_{12})	0.01518	0.01173
tert-Butyl benzene ($C_{10}H_{14}$)	0.00794	0.00732
n-Decane ($C_{10}H_{22}$)	0.10453	0.09430
sec-Butyl benzene ($C_{10}H_{14}$)	0.12587	0.11376
n-Undecane ($C_{11}H_{24}$)	0.02773	0.02838
4-Isopropyltoluene ($C_{10}H_{14}$)	0.08809	0.07944
n-Dodecane ($C_{12}H_{26}$)	0.04213	0.04458
n-Tridecane ($C_{13}H_{28}$)	0.05286	0.06199
n-butyl benzene ($C_{10}H_{14}$)	0.13515	0.12192
n-Tetradecane ($C_{14}H_{30}$)	0.01770	0.02294
Naphthalene ($C_{10}H_8$)	0.23542	0.21236
n-Hexadecane ($C_{16}H_{34}$)	0.01901	0.02738
n-Octadecane ($C_{18}H_{38}$)	0.09611	0.15104

Table I. 4. Mole fractions & selectivities obtained from the analysis of the liquid products (PP+SAPO-34, 425 °C, 30 min)

Liquid ID	Mole fraction, x_i	Selectivity, S_i
n-Pentane (C_5H_{12})	0.00859	0.00403
n-Hexane (C_6H_{14})	0.00770	0.00433
Cyclohexane (C_6H_{12})	0.00119	0.00067
Benzene (C_6H_6)	0.00000	0.00000
n-Heptane (C_7H_{16})	0.00127	0.00084
Toluene (C_7H_8)	0.00213	0.00140
n-Octane (C_8H_{18})	0.00443	0.00332
Ethylbenzene (C_8H_{10})	0.00241	0.00180
m-xylene ($C_6H_4(CH_3)_2$)	0.00806	0.00604
p-xylene ($C_6H_4(CH_3)_2$)	0.00806	0.00604
Styrene ($C_6H_5CH=CH_2$)	0.00937	0.00703
o-xylene ($C_6H_4(CH_3)_2$)	0.00870	0.00653
Isopropyl benzene (C_9H_{12})	0.00378	0.00319
n-Nonane (C_9H_{12})	0.02103	0.01775
n-Propyl benzene (C_9H_{12})	0.01632	0.01378
1,3,5-Trimethylbenzene (C_9H_{12})	0.01547	0.01305
1,2,4-Trimethylbenzene (C_9H_{12})	0.04152	0.03504
tert-Butyl benzene ($C_{10}H_{14}$)	0.00113	0.00106
n-Decane ($C_{10}H_{22}$)	0.06038	0.05662
sec-Butyl benzene ($C_{10}H_{14}$)	0.14294	0.13406
n-Undecane ($C_{11}H_{24}$)	0.09438	0.09737
4-Isopropyltoluene ($C_{10}H_{14}$)	0.02773	0.02601
n-Dodecane ($C_{12}H_{26}$)	0.06513	0.07329
n-Tridecane ($C_{13}H_{28}$)	0.03351	0.04085
n-butyl benzene ($C_{10}H_{14}$)	0.04258	0.03993
n-Tetradecane ($C_{14}H_{30}$)	0.02435	0.03196
Naphthalene ($C_{10}H_8$)	0.28066	0.26321
n-Hexadecane ($C_{16}H_{34}$)	0.01415	0.02123
n-Octadecane ($C_{18}H_{38}$)	0.05304	0.08954

Table I. 5. Mole fractions & selectivities obtained from the analysis of the liquid products (Pure PP, 440 °C, 15 min)

Liquid ID	Mole fraction, x_i	Selectivity, S_i
n-Pentane (C_5H_{12})	0.02725	0.01285
n-Hexane (C_6H_{14})	0.03215	0.01819
Cyclohexane (C_6H_{12})	0.00000	0.00000
Benzene (C_6H_6)	0.03500	0.01980
n-Heptane (C_7H_{16})	0.03999	0.02640
Toluene (C_7H_8)	0.00444	0.00293
n-Octane (C_8H_{18})	0.00000	0.00000
Ethylbenzene (C_8H_{10})	0.00679	0.00512
m-xylene ($C_6H_4(CH_3)_2$)	0.01641	0.01238
p-xylene ($C_6H_4(CH_3)_2$)	0.01641	0.01238
Styrene ($C_6H_5CH=CH_2$)	0.01837	0.01386
o-xylene ($C_6H_4(CH_3)_2$)	0.02167	0.01635
Isopropyl benzene (C_9H_{12})	0.04219	0.03581
n-Nonane (C_9H_{12})	0.00488	0.00414
n-Propyl benzene (C_9H_{12})	0.00096	0.00081
1,3,5-Trimethylbenzene (C_9H_{12})	0.00159	0.00135
1,2,4-Trimethylbenzene (C_9H_{12})	0.00423	0.00359
tert-Butyl benzene ($C_{10}H_{14}$)	0.00000	0.00000
n-Decane ($C_{10}H_{22}$)	0.01048	0.00989
sec-Butyl benzene ($C_{10}H_{14}$)	0.05360	0.05054
n-Undecane ($C_{11}H_{24}$)	0.01834	0.01903
4-Isopropyltoluene ($C_{10}H_{14}$)	0.00000	0.00000
n-Dodecane ($C_{12}H_{26}$)	0.01899	0.02149
n-Tridecane ($C_{13}H_{28}$)	0.05308	0.06507
n-butyl benzene ($C_{10}H_{14}$)	0.15571	0.14684
n-Tetradecane ($C_{14}H_{30}$)	0.01837	0.02425
Naphthalene ($C_{10}H_8$)	0.25529	0.24074
n-Hexadecane ($C_{16}H_{34}$)	0.04205	0.06345
n-Octadecane ($C_{18}H_{38}$)	0.10176	0.17273

Table I. 6. Mole fractions & selectivities obtained from the analysis of the liquid products (Pure PP, 440 °C, 30 min)

Liquid ID	Mole fraction, x_i	Selectivity, S_i
n-Pentane (C5H12)	0.04294	0.02057
n-Hexane (C6H14)	0.05881	0.03235
Cyclohexane (C6H12)	0.00000	0.00000
Benzene (C6H6)	0.00000	0.00000
n-Heptane (C7H16)	0.02533	0.01705
Toluene (C7H8)	0.01578	0.01063
n-Octane (C8H18)	0.00510	0.00245
Ethylbenzene (C8H10)	0.00512	0.00378
m-xylene (C6H4(CH3)2)	0.01722	0.01262
p-xylene (C6H4(CH3)2)	0.01722	0.01262
Styrene (C6H5CH=CH2)	0.00636	0.00478
o-xylene (C6H4(CH3)2)	0.01476	0.01082
Isopropyl benzene (C9H12)	0.03586	0.03105
n-Nonane (C9H12)	0.05012	0.04339
n-Propyl benzene (C9H12)	0.01100	0.00953
1,3,5-Trimethylbenzene (C9H12)	0.00242	0.00209
1,2,4-Trimethylbenzene (C9H12)	0.00465	0.00403
tert-Butyl benzene (C10H14)	0.00000	0.00000
n-Decane (C10H22)	0.02970	0.02756
sec-Butyl benzene (C10H14)	0.00000	0.00000
n-Undecane (C11H24)	0.01500	0.01528
4-Isopropyltoluene (C10H14)	0.00000	0.00000
n-Dodecane (C12H26)	0.01962	0.02187
n-Tridecane (C13H28)	0.05759	0.06938
n-butyl benzene (C10H14)	0.14871	0.13775
n-Tetradecane (C14H30)	0.02293	0.02977
Naphthalene (C10H8)	0.22671	0.21002
n-Hexadecane (C16H34)	0.06145	0.09273
n-Octadecane (C18H38)	0.10561	0.17641

Table I. 7. Mole fractions & selectivities obtained from the analysis of the liquid products (PP+SAPO-34, 440 °C, 15 min)

Liquid ID	Mole fraction, x_i	Selectivity, S_i
n-Pentane (C_5H_{12})	0.02486	0.01196
n-Hexane (C_6H_{14})	0.02010	0.01036
Cyclohexane (C_6H_{12})	0.00000	0.00000
Benzene (C_6H_6)	0.03411	0.01793
n-Heptane (C_7H_{16})	0.00614	0.00414
Toluene (C_7H_8)	0.01087	0.00673
n-Octane (C_8H_{18})	0.00000	0.00000
Ethylbenzene (C_8H_{10})	0.00041	0.00030
m-xylene ($C_6H_4(CH_3)_2$)	0.00966	0.00697
p-xylene ($C_6H_4(CH_3)_2$)	0.00966	0.00697
Styrene ($C_6H_5CH=CH_2$)	0.00729	0.00543
o-xylene ($C_6H_4(CH_3)_2$)	0.00464	0.00352
Isopropyl benzene (C_9H_{12})	0.00592	0.00485
n-Nonane (C_9H_{12})	0.00653	0.00552
n-Propyl benzene (C_9H_{12})	0.00339	0.00294
1,3,5-Trimethylbenzene (C_9H_{12})	0.00364	0.00315
1,2,4-Trimethylbenzene (C_9H_{12})	0.00980	0.00849
tert-Butyl benzene ($C_{10}H_{14}$)	0.00699	0.00673
n-Decane ($C_{10}H_{22}$)	0.06695	0.06014
sec-Butyl benzene ($C_{10}H_{14}$)	0.13106	0.11671
n-Undecane ($C_{11}H_{24}$)	0.08591	0.08090
4-Isopropyltoluene ($C_{10}H_{14}$)	0.00832	0.00801
n-Dodecane ($C_{12}H_{26}$)	0.03285	0.03601
n-Tridecane ($C_{13}H_{28}$)	0.06487	0.07346
n-butyl benzene ($C_{10}H_{14}$)	0.04464	0.03921
n-Tetradecane ($C_{14}H_{30}$)	0.03563	0.04386
Naphthalene ($C_{10}H_8$)	0.18350	0.16133
n-Hexadecane ($C_{16}H_{34}$)	0.06080	0.08350
n-Octadecane ($C_{18}H_{38}$)	0.12146	0.19089

Table I. 8. Mole fractions & selectivities obtained from the analysis of the liquid products (PP+SAPO-34, 440 °C, 30 min)

Liquid ID	Mole fraction, x_i	Selectivity, S_i
n-Pentane (C_5H_{12})	0.09699	0.05116
n-Hexane (C_6H_{14})	0.08806	0.05573
Cyclohexane (C_6H_{12})	0.01198	0.00758
Benzene (C_6H_6)	0.04049	0.02563
n-Heptane (C_7H_{16})	0.06126	0.04523
Toluene (C_7H_8)	0.01165	0.00860
n-Octane (C_8H_{18})	0.01017	0.00858
Ethylbenzene (C_8H_{10})	0.00715	0.00603
m-xylene ($C_6H_4(CH_3)_2$)	0.01203	0.01016
p-xylene ($C_6H_4(CH_3)_2$)	0.01203	0.01016
Styrene ($C_6H_5CH=CH_2$)	0.01668	0.01407
o-xylene ($C_6H_4(CH_3)_2$)	0.00972	0.00820
Isopropyl benzene (C_9H_{12})	0.06053	0.05746
n-Nonane (C_9H_{12})	0.03337	0.03168
n-Propyl benzene (C_9H_{12})	0.01682	0.01597
1,3,5-Trimethylbenzene (C_9H_{12})	0.00300	0.00285
1,2,4-Trimethylbenzene (C_9H_{12})	0.00672	0.00638
tert-Butyl benzene ($C_{10}H_{14}$)	0.00367	0.00387
n-Decane ($C_{10}H_{22}$)	0.01953	0.02060
sec-Butyl benzene ($C_{10}H_{14}$)	0.04073	0.04296
n-Undecane ($C_{11}H_{24}$)	0.04101	0.04758
4-Isopropyltoluene ($C_{10}H_{14}$)	0.04094	0.04318
n-Dodecane ($C_{12}H_{26}$)	0.03815	0.04829
n-Tridecane ($C_{13}H_{28}$)	0.03446	0.04725
n-butyl benzene ($C_{10}H_{14}$)	0.02472	0.02608
n-Tetradecane ($C_{14}H_{30}$)	0.02089	0.03085
Naphthalene ($C_{10}H_8$)	0.14429	0.15220
n-Hexadecane ($C_{16}H_{34}$)	0.02282	0.03852
n-Octadecane ($C_{18}H_{38}$)	0.07012	0.13313

Table I. 9. Mole fractions & selectivities obtained from the analysis of the liquid products (Pure PS, 415 °C, 15 min)

Liquid ID	Mole fraction, x_i	Selectivity, S_i
n-Pentane (C_5H_{12})	0.00000	0.00000
n-Hexane (C_6H_{14})	0.00000	0.00000
Cyclohexane (C_6H_{12})	0.00000	0.00000
Benzene (C_6H_6)	0.00000	0.00000
n-Heptane (C_7H_{16})	0.00000	0.00000
Toluene (C_7H_8)	0.00000	0.00000
n-Octane (C_8H_{18})	0.00000	0.00000
Ethylbenzene (C_8H_{10})	0.00000	0.00000
m-xylene ($C_6H_4(CH_3)_2$)	0.16236	0.13851
p-xylene ($C_6H_4(CH_3)_2$)	0.36707	0.31316
Styrene ($C_6H_5CH=CH_2$)	0.03445	0.02939
o-xylene ($C_6H_4(CH_3)_2$)	0.04471	0.03814
Isopropyl benzene (C_9H_{12})	0.00000	0.00000
n-Nonane (C_9H_{12})	0.00000	0.00000
n-Propyl benzene (C_9H_{12})	0.00000	0.00000
1,3,5-Trimethylbenzene (C_9H_{12})	0.00000	0.00000
1,2,4-Trimethylbenzene (C_9H_{12})	0.00000	0.00000
tert-Butyl benzene ($C_{10}H_{14}$)	0.01908	0.02035
n-Decane ($C_{10}H_{22}$)	0.02539	0.02707
sec-Butyl benzene ($C_{10}H_{14}$)	0.04044	0.04312
n-Undecane ($C_{11}H_{24}$)	0.02478	0.02906
4-Isopropyltoluene ($C_{10}H_{14}$)	0.04229	0.04510
n-Dodecane ($C_{12}H_{26}$)	0.04645	0.05944
n-Tridecane ($C_{13}H_{28}$)	0.04051	0.05616
n-butyl benzene ($C_{10}H_{14}$)	0.01987	0.02119
n-Tetradecane ($C_{14}H_{30}$)	0.00239	0.00357
Naphthalene ($C_{10}H_8$)	0.08617	0.09189
n-Hexadecane ($C_{16}H_{34}$)	0.00348	0.00594
n-Octadecane ($C_{18}H_{38}$)	0.04058	0.07790

Table I. 10. Mole fractions & selectivities obtained from the analysis of the liquid products (Pure PS, 415 °C, 30 min)

Liquid ID	Mole fraction, x_i	Selectivity, S_i
Ethylbenzene (C_8H_{10})	0.00182	0.00160
m-xylene ($C_6H_4(CH_3)_2$)	0.27411	0.23981
p-xylene ($C_6H_4(CH_3)_2$)	0.27411	0.23981
Styrene ($C_6H_5CH=CH_2$)	0.03581	0.03133
o-xylene ($C_6H_4(CH_3)_2$)	0.02258	0.01976
1,2,4-Trimethylbenzene (C_9H_{12})	0.00177	0.00175
tert-Butyl benzene ($C_{10}H_{14}$)	0.01055	0.01154
n-Decane ($C_{10}H_{22}$)	0.10330	0.11297
sec-Butyl benzene ($C_{10}H_{14}$)	0.03195	0.03494
n-Undecane ($C_{11}H_{24}$)	0.00958	0.01153
4-Isopropyltoluene ($C_{10}H_{14}$)	0.01971	0.02156
n-Dodecane ($C_{12}H_{26}$)	0.01892	0.02483
n-Tridecane ($C_{13}H_{28}$)	0.03803	0.05407
n-butyl benzene ($C_{10}H_{14}$)	0.02537	0.02775
n-Tetradecane ($C_{14}H_{30}$)	0.00132	0.00202
Naphthalene ($C_{10}H_8$)	0.10522	0.11507
n-Hexadecane ($C_{16}H_{34}$)	0.00535	0.00936
n-Octadecane ($C_{18}H_{38}$)	0.02048	0.04032

Table I. 11. Mole fractions & selectivities obtained from the analysis of the liquid products (PS+SAPO-34, 415 °C, 15 min)

Liquid ID	Mole fraction, x_i	Selectivity, S_i
n-Pentane (C_5H_{12})	0.00000	0.00000
n-Hexane (C_6H_{14})	0.00000	0.00000
Cyclohexane (C_6H_{12})	0.00000	0.00000
Benzene (C_6H_6)	0.00000	0.00000
n-Heptane (C_7H_{16})	0.00000	0.00000
Toluene (C_7H_8)	0.00000	0.00000
n-Octane (C_8H_{18})	0.00000	0.00000
Ethylbenzene (C_8H_{10})	0.00168	0.00144
m-xylene ($C_6H_4(CH_3)_2$)	0.04380	0.03749
p-xylene ($C_6H_4(CH_3)_2$)	0.04380	0.03749
Styrene ($C_6H_5CH=CH_2$)	0.18777	0.16069
o-xylene ($C_6H_4(CH_3)_2$)	0.03663	0.03135
Isopropyl benzene (C_9H_{12})	0.00000	0.00000
n-Nonane (C_9H_{12})	0.00000	0.00000
n-Propyl benzene (C_9H_{12})	0.02636	0.02538
1,3,5-Trimethylbenzene (C_9H_{12})	0.08250	0.07943
1,2,4-Trimethylbenzene (C_9H_{12})	0.20962	0.20181
tert-Butyl benzene ($C_{10}H_{14}$)	0.00000	0.00000
n-Decane ($C_{10}H_{22}$)	0.04923	0.05266
sec-Butyl benzene ($C_{10}H_{14}$)	0.03479	0.03722
n-Undecane ($C_{11}H_{24}$)	0.00424	0.00499
4-Isopropyltoluene ($C_{10}H_{14}$)	0.10175	0.10885
n-Dodecane ($C_{12}H_{26}$)	0.00472	0.00606
n-Tridecane ($C_{13}H_{28}$)	0.00972	0.01352
n-butyl benzene ($C_{10}H_{14}$)	0.08482	0.09073
n-Tetradecane ($C_{14}H_{30}$)	0.00645	0.00965
Naphthalene ($C_{10}H_8$)	0.04206	0.04499
n-Hexadecane ($C_{16}H_{34}$)	0.00739	0.01264
n-Octadecane ($C_{18}H_{38}$)	0.02265	0.04362

Table I. 12. Mole fractions & selectivities obtained from the analysis of the liquid products (PS+SAPO-34, 415 °C, 30 min)

Liquid ID	Mole fraction, x_i	Selectivity, S_i
n-Pentane (C_5H_{12})	0.00375	0.00200
n-Hexane (C_6H_{14})	0.00063	0.00040
Ethylbenzene (C_8H_{10})	0.00143	0.00122
m-xylene ($C_6H_4(CH_3)_2$)	0.03457	0.02952
p-xylene ($C_6H_4(CH_3)_2$)	0.03457	0.02952
Styrene ($C_6H_5CH=CH_2$)	0.19494	0.16647
o-xylene ($C_6H_4(CH_3)_2$)	0.03464	0.02958
n-Propyl benzene (C_9H_{12})	0.03094	0.02972
1,3,5-Trimethylbenzene (C_9H_{12})	0.08124	0.07805
1,2,4-Trimethylbenzene (C_9H_{12})	0.24320	0.23364
tert-Butyl benzene ($C_{10}H_{14}$)	0.00079	0.00084
n-Decane ($C_{10}H_{22}$)	0.05066	0.05407
sec-Butyl benzene ($C_{10}H_{14}$)	0.04227	0.04512
n-Undecane ($C_{11}H_{24}$)	0.00715	0.00839
4-Isopropyltoluene ($C_{10}H_{14}$)	0.04243	0.04529
n-Dodecane ($C_{12}H_{26}$)	0.00489	0.00626
n-Tridecane ($C_{13}H_{28}$)	0.00754	0.01046
n-butyl benzene ($C_{10}H_{14}$)	0.08615	0.09196
n-Tetradecane ($C_{14}H_{30}$)	0.01716	0.02565
Naphthalene ($C_{10}H_8$)	0.04911	0.05242
n-Hexadecane ($C_{16}H_{34}$)	0.00921	0.01572
n-Octadecane ($C_{18}H_{38}$)	0.02274	0.04369